

الجمهورية الجزائرية الديمقراطية الشعبية
People's Democratic Republic of Algeria
وزارة التعليم العالي و البحث العلمي
Ministry of Higher Education and Scientific Research

University of Mohamed Khider - Biskra

Faculty of Science and Technology

Department: Electrical Engineering

Ref /.../G.E/2018



جامعة محمد خيضر بسكرة

كلية العلوم و التكنولوجيا

قسم: الهندسة الكهربائية

المرجع: Ref/.../G.E/2018

Thesis for the degree of

Doctor in Sciences

Speciality: Electrical Engineering

Option: Electronic

**Contribution to the Rapid Acquisition of Signals
for UWB Communication Systems**

by:

GHENDIR Said

Publicly presented on 03/07/2018

Committee Members:

Pr. BENAKCHA Abdelhamid	Professor	Chairman	University of Biskra
Pr. MIMI Malika	Professor	Examiner	University of Mostaganem
Pr. BAARIR Zine-eddine	Professor	Examiner	University of Biskra
Dr. LAKHDA Nacereddine	Lecturer "A"	Examiner	University of El-Oued
Dr. ABED Djamel	Lecturer "A"	Examiner	University of 8 mai 1945 Guelma
Dr. SBAA Salim	Lecturer "A"	Supervisor	University of Biskra

الجمهورية الجزائرية الديمقراطية الشعبية
People's Democratic Republic of Algeria
وزارة التعليم العالي و البحث العلمي
Ministry of Higher Education and Scientific Research

Université Mohamed Khider – Biskra

Faculté des Sciences et de la Technologie

Département: Génie Electrique

Ref /.../G.E/2018



جامعة محمد خيضر بسكرة

كلية العلوم و التكنولوجيا

قسم: الهندسة الكهربائية

المرجع: Ref/.../G.E/2018.

Thèse présentée en vue de l'obtention du diplôme de

Doctorat en Sciences

Spécialité: Génie électrique

Option: Electronique

**Contribution à l'Acquisition Rapide de Signaux
pour les Systèmes de Communication UWB**

Présentée par :

GHENDIR Said

Soutenue publiquement le 03/07/2018

Devant le jury composé de :

Pr. BENAKCHA Abdelhamid	Professeur	Président	Université de Biskra
Pr. MIMI Malika	Professeur	Examineur	Université de Mostaganem
Pr. BAARIR Zine-eddine	Professeur	Examineur	Université de Biskra
Dr. LAKHDAR Nacereddine	Maitre de Conférence "A"	Examineur	Université de El-Oued
Dr. ABED Djamel	Maitre de Conférence "A"	Examineur	Université de 8 mai 1945 Guelma
Dr. SBAA Salim	Maitre de Conférence "A"	Rapporteur	Université de Biskra

Acknowledgments

First of all, I thank Allah, who helped me to carry out this work by his power and guidance.

I would like to thank all those who contributed to the smooth running of this thesis. To those who supported me during these years.

I would like to express my gratitude for my supervisor Dr. Salim SBAA. His guidance, tutelage, encouragement, various advices, and his constructive criticisms have been instrumental in the accomplishment of this dissertation. Also to thank his attention, sympathy, availability during all these years that have qualified me to improve my scientific capabilities. All my gratitude to you Dr Salim.

I also thank Dr. Ali AL-SHERBAZ who I was under his tutelage in England during 18 months at the University of Northampton. This work could not have been as what it is now without his guidance, patience and interesting remarks. Many thanks to him for inviting me and his support to me.

I thank Pr. Abdelmalik TALEB AHMED for his help, support, and many thanks to him for letting the doors of his laboratory opened to me all the time at the University of Valenciennes in France.

I would like to express my gratitude to all the committee members who do me the great honour to accept examining my thesis, and I thank them very much for being members in the present thesis.

Abstract

Ultra Wide-band is a promising technology for future short-range wireless communications with high data rate. In generally, one of the biggest difficult tasks for researchers today is the acquisition task of signals, where they are looking through different tools for getting a good quality of transmission; the phenomenon of multipath always stands up in the front as the first problem to be faced. When we talk about the Ultra Wide Band (UWB) signals, the problem becomes more complicated due to ultrashort impulses duration used by this kind of signals that causes the generation of paths by huge numbers.

In this thesis, to address the task mentioned above, the study is subdivided into two aspects. The first one is the UWB channel estimation that we have done to have information about the amplitudes and the delays of the paths. For this purpose, a maximum likelihood method is used to find the amplitudes and the delays estimate using two estimation contexts: Data Aided (DA) and Non-Data-Aided (NDA). In the second aspect, various parameters affecting the acquisition of signals are evaluated. Furthermore, several contributions in the framework of a new strategy based on an Intelligent Controlling System (ICS) are done and detailed in this thesis for the first once.

This system is characterised by its flexibility through two techniques, one that allows to users to communicate even with different M-ary PPM levels at the same time. Another technique that gives the flexibility for dealing with the phenomenon of multipath, where this latter is combated through manipulating the modulation's levels via the ICS to achieve a rapid acquisition of UWB signals.

Keywords: ICS, ML, M-ary PPM, TH-UWB, UWB signal acquisition

Résumé

L'Ultra Large Band (ULB) est une nouvelle technologie émergente pour les futures communications sans fil à courte portée qui présente un débit de transmission très élevé. La tâche de l'acquisition de signaux ULB est connue dans le domaine de communication qu'une des plus grandes tâches difficiles pour les chercheurs aujourd'hui, car ils essaient par différents outils de chercher comment mener à bien cette acquisition à la bonne qualité de transmission afin d'augmenter les performances du system ULB. Quand les signaux ULB sont adoptés, le phénomène des multi-trajets (trajets-multiples) s'élève toujours au front comme problème laborieux à l'égard de la tâche de l'acquisition, où le problème dans ce cas devient plus compliqué en raison de la durée des impulsions ultra courtes utilisées par ce type de signaux qui provoque la génération de multi-trajets d'une manière très dense.

Dans cette thèse, pour faire face à la tâche susmentionnée, cette étude est subdivisée en deux aspects. Le premier est l'estimation du canal ULB qui est faite afin d'avoir les paramètres du canal et comment ce dernier se comporte-t-il avec les signaux. Dans ce but, une méthode basée sur le maximum de vraisemblance a été utilisée pour obtenir les amplitudes et les retards estimés en deux contexte d'estimation: une estimation supervisé (Data Aided, DA) et une estimation autodidacte (Non Data-Aided, NDA). Le deuxième aspect est l'acquisition de signaux ULB en utilisant l'estimation du canal qui est citée-avant pour compenser les effets du canal et corriger les signaux reçus. Dans ce dernier aspect, différents paramètres affectant l'acquisition de signaux sont évalués. En plus, plusieurs nouveautés et contributions dans le cadre d'une nouvelle stratégie basée sur un système de contrôle intelligent (Intelligent Controlling System, ICS) sont faites et détaillées dans cette thèse pour la première fois. Ce système d'acquisition est caractérisé par sa flexibilité à travers deux techniques, une qui permet aux utilisateurs de communiquer avec différents niveaux M-aire PPM en même temps, et l'autre technique qui permet la flexibilité en termes d'interaction avec le phénomène de multi-trajets, où ce phénomène est confronté en manipulant les différents niveaux de modulations via le (ICS) pour obtenir une acquisition rapide de signaux UWB.

Mots Clés : ICS, ML, M-ary PPM, ULB, acquisition signaux ULB

ملخص

التكنولوجيا التي تعتمد على الإشارات ذات النطاقات الواسعة (إ.ن.و) هي تكنولوجيا ناشئة وواعدة بالنسبة لمستقبل الاتصالات اللاسلكية قصيرة المدى والتي تقدم سرعة إرسال معلومات عالية جدا. ومن المعروف في مجال الاتصالات أن واحدة من أكبر المهام الصعبة للباحثين اليوم هو كيفية التقاط إشارات في وجود ظاهرة المسارات المتعددة لنفس الإشارة.

في هذه الأطروحة، نحن نسعى للتعامل مع إشارات ذات النطاق الواسع (إ.ن.و) وذلك ببساطة عن طريق:

أولا تقييم قناة الإرسال للحصول على معلومات عن كيفية تفاعلها مع الإشارات المرسله وذلك بتقييم سعات وتأخيرات المسارات المتعددة للإشارة المرسله .

ثانيا إستعادة وإلتقاط الإشارات ذات (إ.ن.و، UWB) المرسله باستخدام تقديرات القناة للتخلص من تأثيرات القناة ولتصحيح الإشارات المستقبلية. و بالإضافة إلى ذلك، فإننا قمنا في هذه الأطروحة باقتراح العديد من الطرق والمساهمات الجديدة في إطار إستراتيجية جديدة تقوم على نظام التحكم الذكي (نظام التحكم الذكي، ICS) والذي تم اقتراحه و تفصيله حصرا في هذه الأطروحة. ويتميز هذا النظام الجديد بمرونته من خلال اثنين من التقنيات، الأولى تتيح للمستخدمين الاتصال بتضمينات المختلفة في نفس الوقت (ت.إ.ن. PPM) والتقنية الثانية تمكن من التعامل بمرونة مع ظاهرة المسارات متعددة، حيث التقنية المقترحة تواجه هذه الظاهرة عن طريق إدارة التضمينات المختلفة عبر ICS من أجل إلتقاط واستقبال سريعين لإشارات (ن.و)

كلمات مفتاحية: تقييم قناة ، نظام مراقبة ذكي، إ.ن.و، تضمين ت.إ.ن

Contents

<i>Acknowledgments</i>	<i>i</i>
<i>Abstract</i>	<i>ii</i>
<i>Résumé</i>	<i>iii</i>
<i>List of Figures</i>	<i>viii</i>
<i>List of Acronyms</i>	<i>x</i>
<i>List of Symbols</i>	<i>xiii</i>

INTRODUCTION	2
Problematic issue and challenges	2
Objective to achieve	3
Contributions and novelties	3
Thesis outline.....	4

CHAPTER I: UWB COMMUNICATION SYSTEM

I.1 Overview	7
I.2 What is Ultra Wideband?	8
I.2.1 Principle	8
I.2.2 UWB and Shannon theorem.....	9
I.3 UWB standards	9
I.4 UWB technology and other technologies.....	10
I.5 Panorama of cohabitation.....	11
I.6 Frequency mask and UWB impulse.....	11
I.7 Impulse waveform.....	12
I.8 Applications of UWB.....	14
I.8.1 Imaging Systems	15
I.8.2 Embedded radar equipment.....	16
I.8.3 Communication and measurement devices	16
I.9 Advantages and Disadvantages	17
I.9.1 Advantages	17
I.9.2 Disadvantages	18
I.10 TH-UWB communication system.....	18
I.11 Impulse Radio IR-UWB.....	19
I.12 TH-UWB signal structure	20
I.12.1 PPM Modulation (Pulse Position Modulation).....	21
I.12.2 M-Ary PPM Modulation	23
I.12.3 TH-UWB signal form.....	23
I.13 TH-C effect on the transmitted signal spectrum.....	24
I.14 Summary	27

CHAPTER II: MODELLING OF UWB MULTIPATH CHANNEL

II.1 Overview.....	29
II.2 IEEE 802.15.3a Channel model (Model 3a).....	30
II.2.1 Presentation.....	30
II.2.2 Modeling of multipath channel.....	31
II.2.3 Evaluation of modelling.....	37
II.3 Critique of modelling.....	38
II.4 Simulation of IEEE 802.15.3a Channel.....	38
II.5 Summary.....	41

CHAPTER III: UWB CHANNEL ESTIMATION AND ACQUISITION OF SIGNALS

III.1 Overview	43
III.2 TH-PPM UWB Signal Format	44
III.3 Working principle of rake receiver.....	47
III.3.1 A-Rake Receiver (All Rake).....	50
III.3.2 P-Rake receiver (Partial Rake)	50
III.3.3 S-Rake receiver (Selection Rake).....	51
III.4 UWB channel estimation.....	51
III.4.1 Data-Aided Channel estimation	52
III.4.2 Non-Data Aided channel estimation.....	55
III.5 TH-UWB system description	57
III.6 Organization of the transmitted data	57
III.7 Simulation results	58
III.7.1 Simulation parameters	58
III.7.2 Channel estimation error	60
III.7.3 Influence of the estimation context	61
III.7.4 Influence of the data rate	64
III.7.5 Influence of the multiple-access.....	66
III.7.6 Influence of the estimation sequence length.....	68
III.7.7 Influence of the modulation factor	69
III.7.8 Influence of the paths number	69
III.7.9 Influence of the receiver type	70
III.8 Summary.....	72

CHAPTER IV: A NEW STRATEGY FOR THE RAPID ACQUISITION OF SIGNALS

IV.1 Overview	74
IV.2 Suggested strategy description	75
IV.3 M-ary PPM time hopping scheme.....	77
IV.4 Proposed multi-hands Rake Receiver	79
IV.5 Performance analysis.....	82
IV.6 Simulation results	88

IV.7 Summary	92
CONCLUSIONS AND FUTURE WORKS	93
Appendices	97
Appendix A: UWB Technology	98
A.1 Comparative table of short-range wireless technologies	98
A.2 Some Applications for UWB and Marketed Products.....	99
Appendix B: IEEE 802.15.3a Channel Standard.....	102
B1. Multipath channel characteristics and modeling parameters	102
B2. Illustration of multipath channel characteristics	103
Appendix C: Relevant Publications and International Communications	105
Bibliography.....	107

List of Figures

CHAPTER I:

Fig I.1 The spectrum of UWB signals and other signals	8
Fig I.2 Organization of IEEE 802.15	9
Fig I.3 Summary diagram represents the data rates versus the range.....	10
Fig I.4 Different systems coexisting with UWB	11
Fig I.5 Transmitted power limits imposed by the FCC for UWB signals	12
Fig I.6 The impulses derived from the Gaussian.....	13
Fig I.7.a GPR can detect multiple targets up to 10m.....	15
Fig I.7.b Example of GPR that detects two targets at a distance of 5m	15
Fig I.8 UWB radar for collision detection	16
Fig I.9 Typical domestic use of UWB systems	17
Fig I.10 Example of a UWB system in multi-users case.....	19
Fig I.11 Block diagram of an IR-UWB transmitter.....	20
Fig I.12 TH-UWB signal structure for PPM modulation	21
Fig I.13 Two states "0" and "1" modulated in PPM for two users	22
Fig I.14 M-Ary PPM Modulation (M=4)	23
Fig I.15 TH-UWB signal for three users	24
Fig I.16 Sequence of regular monocycles impulses	25
Fig. I.17 Sequence of irregular monocycles impulses.....	26

CHAPTER II:

Fig II.1 Illustration of the propagation mechanisms.....	31
Fig II.2 Main multipath mechanisms.....	32
Fig II.3 Synoptic illustration of the impulse response of a UWB multipath channel	33
Fig II.4 The energy attenuation versus the delays	35
Fig II.5 Illustration des caractéristiques du profil de puissance	37
Fig II.6 100 realizations generated by the Model CM1.....	39
Fig II.7 Some typical impulse responses for Models CM1, CM2, CM3, CM4	40

CHAPTER III:

Fig III.1 Blocks diagram of the TH-UWB transmission link	45
Fig III.2 Illustration for a TH-UWB signal with PPM modulation.....	47
Fig III.3 General structure of the rake receiver	48
Fig III.4 Demodulating a symbol with the PPM modulation	49
Fig III.5 Detailed diagram of the rake receiver for a single user.....	49
Fig III.6 The paths taken into account by A-Rake	50
Fig III.7 The paths taken into account by P-Rake	50
Fig III.8 The paths taken into account by S-Rake	51

Fig III.9 Sufficient statistics	53
Fig III.10 Block diagram of UWB transmission link	57
Fig III.11 Organization of the transmitted data	58
Fig III.12 MSE versus SNR.....	59
Fig III.13 a) One realization generated for CM2, b) Its corresponding estimated channel.....	60
Fig III.14 BER performance for DA and NDA estimation	61
Fig III.15 BER versus SNR for PPM modulation using DA and NDA estimation.....	63
Fig III.16 MSE of the channel estimation (for CM1 in this case) versus data rate	64
Fig. III.17 BER evaluations for the model CM1	65
Fig III.18 MSE of the estimated model CM1 based on the number of users	66
Fig III.19 BER evaluations for the model CM1	67
Fig III.20 BER versus the estimation sequence length.....	68
Fig III.21 BER versus modulation factor δ , SNR = 20dB	68
Fig III.22 Influence of the paths number on BER evaluations	69
Fig III.23 BER evaluation versus SNR for A-Rake, S-Rake and P-Rake	70

CHAPTER IV:

Fig IV.1 Proposed global block diagram for the flexible UWB transmission technique	76
Fig IV.2 Structure of M-ary PPM Time Hopping scheme	78
Fig IV.3 The proposed multi-hands Rake receiver.....	81
Fig.IV.4 BER evaluation versus E_b/N_0 for the new UWB system	89

List of Acronyms

AWGN	: Additive White Gaussian Noise
A-RAKE	: All RAKE
BER	: Bit Error Rate
BPSK	: Binary Phase Shift Keying
CDMA	: Code Division Multiple Access Accès
CM	: Channel Model
CSI	: Channel State Information
DA	: Data Aided
dB	: Decibel
dBm	: Decibel-milliwatts
DS-CDMA	: Direct Sequence – CDMA
DS-UWB	: Direct Sequence - Ultra Wide Band
EIRP	: Equivalent Isotropically Radiated Power
FCC	: Federal Communications Commission
FC	: Frequency Hopping
Freq	: Frequency
GHz	: Gigahertz
GPR	: Ground Penetrating Radar
GPS	: Global Positioning System

GSM	: Global System for Mobile Communications
ICS	: Intelligent Controlling System
IEEE	: Institute of Electrical and Electronics Engineers
IFI	: Inter Frame Interference
i.i.d	: independent and identically distributed
INTERP	: Interpolation
IR	: Impulse Radio
ISFI	: Inter-Symbol/Frame Interference
ISI	: Inter Symbol Interference
ISM	: Industrial, Scientific and Medical
Kbps	: kilobits per second
LOS	: Line of Sight
MAC	: Medium Access Control
MAI	: Multiple Access Interference
Mbps	: Megabits per second
MB-OFDM	: Multi-Band-Orthogonal Frequency Division Multiplexing
ML	: Maximum Likelihood
MMSE	: Minimum Mean Square Error
MRC	: Maximum Ratio Combining
MSC	: Mean Square Cross-correlation
MUI	: Multi-User Interference
mW	: milliWatt
NDA	: Non-Data Aided

NLOS	: Non Line Of Sight
ns	: Nanosecond
OFDM	: Orthogonal Frequency Division Multiplexing
OOK	: On-Off keying
OPPM	: Orthogonal Pulse Position Modulation
PCS	: Personal Communications Service
pdf	: probability density function
PAM	: Pulse Amplitude Modulation
PPM	: Pulse Position Modulation
P-RAKE	: Partial RAKE
Prob	: Probability
RMS	: Root Mean Square
SNR	: Signal to Noise Ratio
S-RAKE	: Selective RAKE
SV	: Saleh-Valenzuela
THC	: Time Hopping Code
TR	: Time-Reversal
UWB	: Ultra Wide Band
RV	: Random Variable
WLAN	: Wireless Area Network
WPAN	: Wireless Personal Area Network

List of Symbols

\tilde{a}_k	: Received symbol from the k^{th} path
$a^n(i)$: i^{th} transmitted symbol for a desired user n
A	: Desired signal component
B	: Signal bandwidth
$b(.)$: Block of an information symbol
$\beta_{k,l}$: Fading associated with k^{th} path of the ℓ^{th} packet
$\tilde{c}^n(j)$: Time hopping code for the J^{th} frame associated with the user n
c	: Time code specific to the concerned frame
C	: Channel capacity
Δ	: Time difference between the different paths and the different time slots
δ	: Modulation factor
$\delta(.)$: Dirac impulse
δ_{i-a}	: Kronecker delta
$\text{Erf}(.)$: Gauss error function
E_b	: Energy of an information symbol block
E^n	: Signal energy associated with the user n
E_w^n	: Impulse energy from user n
$E[.]$: Expected value
E_b/N_o	: Signal/Noise
\exp	: exponential
ε	: Normalization factor
f_c	: Central frequency.
f_H	: High frequency
f_L	: Low frequency

φ	: Received energy
G	: Gain of multipath
$h(\cdot)$: Channel impulse response
$J(\cdot)$: Sufficient statistic for M symbols
K	: Number of paths per packet
L	: Number of packets
L_c	: Total number of rake fingers
\log_a	: Logarithm to the base a
M	: Modulation order
m	: meter
$m(\cdot)$: Template signal
μ	: Mean value
N_o	: Noise energy
N_u	: Number of users
n	: Desired user
$n(\cdot)$: Additive noise component
n_1	: Fading of each packet
n_2	: Fading of each path
N	: Additive white Gaussian noise component
N_b	: Number of bits
N_c	: Number of chips
N_f	: Number of frames
NP	: Number of multipath components
$p_{k,l}$: Random inversions of impulses due to reflections
$P(\cdot)$: Probability density function
P_c	: Conditional probability of correct decision
\bar{P}_c	: Conditional probability of correct decision

Q	: Multiplication factor
ξ_ℓ	: Fading associated with ℓ^{th} packet
ρ	: Spreading radio
R_s	: Symbol rate
$R_w(.)$: Autocorrelation function of the pulse waveform
$r(.)$: Received signal
R_d	: Data Rate
$s(.)$: Received signal
<i>Sync</i>	: Synchronization
T_c	: Chip duration
T_f	: Frame duration
$\{T_l\}$: Arrival time of the 1 st path of the l^{th} packet
t_p	: Impulse width
T_s	: Symbol duration
T_w	: Impulse duration
<i>Var</i>	: Variance
$w(.)$: Gaussian impulse
w'	: First derivative of the Gaussian impulse
w''	: Second derivative of the Gaussian impulse
Ω_0	: Average energy of the first path of the first packet
X	: global "shadowing" effect
$z(.)$: Sufficient statistics
Z_a	: Desired energy quantity resulted from the a^{th} time slot
$Z_{\bar{a}}$: Undesired energy quantity resulted from the a^{th} time slot
Λ	: Arrival rate of a packet
λ	: Arrival rate of a path within a given packet
$\bar{\tau} = \tau_m$: Mean delay

τ_{rms}	: Standard deviation of delay
$\{\tau_{k,l}\}$: Delay of the k^{th} component of paths of the l^{th} packet
$\{\alpha_{k,l}\}$: Attenuation coefficient of k^{th} component of paths of the l^{th} packet
Γ	: Decay factor of a packet
γ	: Decay factor of a path
σ_{ISFI}	: Standard deviation of the Inter-Symbol/Frame Interference
σ_1	: Standard deviation of lognormal fading characterising a packet
σ_2	: Standard deviation of lognormal fading characterising a path
σ_x	: Standard deviation of lognormal characterising the global "shadowing"
\otimes	: Convolution operation
3a, 4a	: IEEE's working groups

Introduction

Introduction

The Ultra-Wide Band technology is used since the mid-1960s in radar applications. However, she experienced spectacular growth since 2002. Ultra-Wide Band is a radio technology that can be used for short-range communication systems with low power consumption at short ranges and high bandwidth communication. Thus, UWB technologies are being developed as an emerging wireless technology for high-speed wireless personal area networks and being considered for several technologies due to their attractive features.

The Federal Communications Commission (FCC), which is a US regulatory organ has authorised such as free use of the frequency band [3.1-10.6 GHz] for wireless communications. Quickly, UWB technology, after that appeared as the solution to be able to reach the speed of Gbits/sec. This data rate is an incredible rate in the current wireless, i.e., more than a billion of binary information per second, but also a solution to be able to offer new services by integrating with the transmission some features such as functions of detection and localization. In parallel to the regulatory aspects that are going on today around the world, strong activity of development and standardization brings together many actors, both in industry and academia, this to launch this promising technology. Since no technical constraint has been imposed, all solutions can be considered and the challenges to be solved are therefore extremely numerous and present at all technical levels (signal processing, components, antennas, acquisition of signals).

Problematic issue and challenges

Among the biggest problem faced by the UWB technology is the acquisition of signals and how these signals should be received in good conditions; where the multipath phenomenon has primordial effects on transmitted signals due to UWB channel characteristics. Furthermore, reaching high data rate is required in this technology, this matter might complicate the situation through making the acquisition of signals difficult to achieve and imposing the risk of Inter-Symbol Interference (ISI) and Inter-frame Interference (IFI), in this way, many problems could be gathered simultaneously. However, the multipath effects remain the significant challenge that should be confronted because the

UWB signals use ultra-short impulses, where the more the impulses are very short the more the multipath will have harmful effects.

Primarily this issue is justified because the multipath phenomenon has a strong impact on the UWB communications and there is persistent need to consider their influences.

Given numerous studies and publications (we will mention them along the three last chapters) on various topics related to UWB technology, we address in this thesis a new solution for the cited challenge to combat the multipath phenomenon based on different new ideas.

Objective to achieve

In this work, our objective is to seek and propose an intelligent technique to deal with the multipath to have a rapid acquisition as possible as we can without affecting the communication quality. For this reason, some steps and sub-objectives should be done and addressed in this work to carry out our final objective. Firstly, the multipath channel needs to be estimated to have an idea about how the signals will be affected. Secondly, some modifications on the communication system from the transmitter to the receiver will be set up to adapt it with the proposed solution.

This thesis will have an overview of all different blocks of the TH-UWB transmission link from the transmitter to the receiver, passing through a detailed study of the UWB communication system, channel modeling, channel estimation, and signals acquisition.

Contributions and novelties

Many significant contributions and novelties in this work are brought within the framework of some publications and international communications cited in (Appendix C) and some results that have not published yet. Thereby, the contributions and novelties making up this thesis can be summarized in the following points:

- 1- Evaluation of the TH-UWB system performances under the influence of different parameters such as (length of the estimation sequence, modulation factor, ...)
- 2- Establishing a new flexible transmission technique allowing the user to transmit data by different modulation level during the transmission.

- 3- Proposing a modified rake receiver named multi-hands receiver to achieve our strategy.
- 4- Proposing an intelligent controlling system (ICS) in order to confront the UWB multipath channel.
- 5- Developing of a new mathematical model according to the proposed strategy.

Thesis outline

The first chapter has two faces; one is more general and less technical, where it is more oriented towards regulatory and standardization aspects and gives a global overview summarizing current researches topics. This chapter, gives some concepts related to the UWB, principles, applications and challenges of UWB technology about other existing technologies, citing the frequency mask imposed by the FCC, and the impulse supported to construct the UWB signals. The second face focuses on technical aspects more than theoretical sides by going over the technique of Time Hopping code UWB (TH-UWB), the UWB signal form, the M-ary PPM modulation that are adopted, how to differentiate between users using the THC-UWB technique and the effects of this technique on the transmitted signal spectrum.

In the second chapter, the properties of the UWB channel models and the appropriate modeling are discussed, explaining the IEEE 802.15.3a standard of the UWB propagation channel, and plotting the impulse response for different scenarios.

The third chapter discusses a detailed description of the RAKE receiver that is used in this work, mentioning its characteristics and performance. Then, the channel estimation operation (amplitudes and delays estimates) is processed and done basing on the Maximum-likelihood (ML) approach, through which we will exploit the multiple paths of the UWB channel to improve the performance of the system. Finally, simulations results and interpretations about the influence of several parameters on the estimation and quality of transmission are evaluated (estimation context, transmission data rate, multi-users, rake receiver type, and so on).

The latest chapter offers the philosophy of the suggested strategy in details by addressing the usefulness of the M-ary PPM time hopping scheme and the modified rake receiver (named multi-hands rake receiver). Furthermore, this part explains the utility of the intelligent controlling technique and gives a detailed study of the performance analysis of all the system, with deriving an approximate analytical formula for the error probability of decision, where some performance evaluations are assessed and discussed.

Finally, some concluding elements and future works are given in the last part to wrap up this dissertation.

At this stage, the challenge presented in the thesis is justified, the UWB topic is defined, and the objective and scope of the work are explained. Also significant contributions to be shown later are clearly highlighted.

Chapter I

UWB Communication Systems

Chapter I

UWB communication systems

I.1 Overview

Many studies related to the ultra-short pulses began before the sixties [1], but the UWB term was only introduced around 1989 by the department of defense of the United States. The first patent for the application of ultra wide band communications is due to G.Ross in 1973 [2]. Until 1994, many works have been funded by the US government but under the guise of confidentiality. Since then, the study of transmission systems based on transmitting impulses in both the industrial and academic world has been the subject of numerous publications [3] [4]. The first article describing this solution for telecommunications, known as Impulse Radio (IR) that is due to P.Withington and L.Fullerton [5] in 1992. This article was followed by academic work started by Scholtz [6] in 1993, and it was not until 1997 that the UWB term appears in the title of an article on the IR [7]. Since then, the two appellations coexist according to the authors.

The FCC regulation has adopted in May 2000 a regulatory proposal notice (Notice of Proposed Rule Making). This regulation allows the emission of signals called "UWB" (Ultra Wide Band) in the frequency band [3, 1 GHz - 10 GHz 6] for telecommunications, with a very low level of power (-41, 3 dBm / MHz) [8]. Following to the FCC, The IEEE established two working groups to set new standards using UWB replacing the physical layer standard IEEE 802.15.3 and IEEE 802.15.4 dedicated to wireless personal area networks (WPAN). In the first hand, the IEEE 802.15.3a committee whose terms of reference require data rates exceeding 100 Mbit / s for distances up to 10m. On the other hand, the IEEE 802.15.4a committee designed for the applications based on sensor networks with data rates of the order of hundreds of kbit/s for distances of several hundred meters. The IEEE 802.15.4a committee has already selected using the IR-UWB physical layer.

For 802.15.3a, two consortiums compete, firstly the MBOA alliance (Multi-Band OFDM Alliance) proposing the use of signals using Orthogonal Frequency Division Multiplexing (OFDM). Secondly, a consortium proposing the use of IR-UWB signals that has spread spectrum of type DS-UWB (Direct Sequence - Ultra Wide Band), or TH-UWB (Time-Hopping Ultra Wideband); we will take the latter type into consideration in the current study.

I.2 What is Ultra Wideband?

Ultra Wide Band is a technology that consists of transmitting pulses of very short duration, which results in the use of very wide frequency bands, and it is a high-speed data transfer technology (up to 480 Mbps) at a short distance. This technology looks extremely promising because it could revolutionize communications between devices and electronic components; it consumes little power, and it could increase not only the autonomy of the devices but also improving transfer rates [34, 35].

I.2.1 Principle

Originally, it is called Impulse Radio or communications without a carrier and received the name Ultra-Wideband by the Department of American Defense in 1989. The FCC defines the UWB as any radio technology using a spectrum exceeding 20% of the center frequency or a frequency band of at least 500 MHz [8]. Where the spectrum of Narrow Band systems does not exceed 1% of the center frequency, and between the two there are systems whose spectrum is Wide Band, which is between 1% up to 20% of the center frequency.

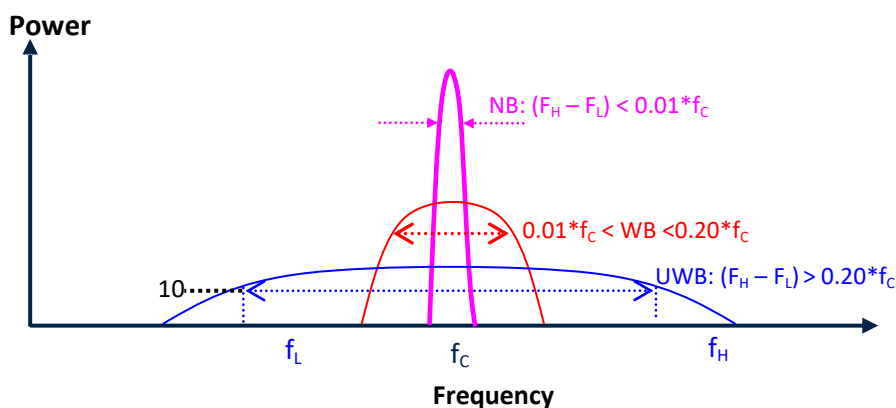


Fig I.1 The spectrum of UWB signals and other signals

I.2.2 UWB and Shannon theorem

We can see clearly the importance of the UWB technology in communications across the Shannon-Hartly equation that represents the maximum capacity of the channel C:

$$C = B \log \left(1 + \frac{S}{N} \right) \quad (I.1)$$

B is the signal bandwidth; S and N are the signal power and noise power respectively. While C varies linearly with B and logarithmically with S/N or SNR. Then we have two possibilities to increase C, by increasing the bandwidth B or by increasing the SNR. The fact that UWB signals assign a very broad band of the order of GHz we can get a huge capacity of the order of hundreds of Mbps.

I.3 UWB Standards

As we have seen the UWB standardization activities currently undertaken by the 802.15 working group of the IEEE standards committee. The general organization of the IEEE 802.15 standard is presented by the following figure. The main specifications are given regarding data rates, ranges and frequencies allocated. In particular, the Bluetooth is used in the IEEE 802.15.1 standard, and the UWB is used in the IEEE 802.15.3a and IEEE 802.15.4a standards.

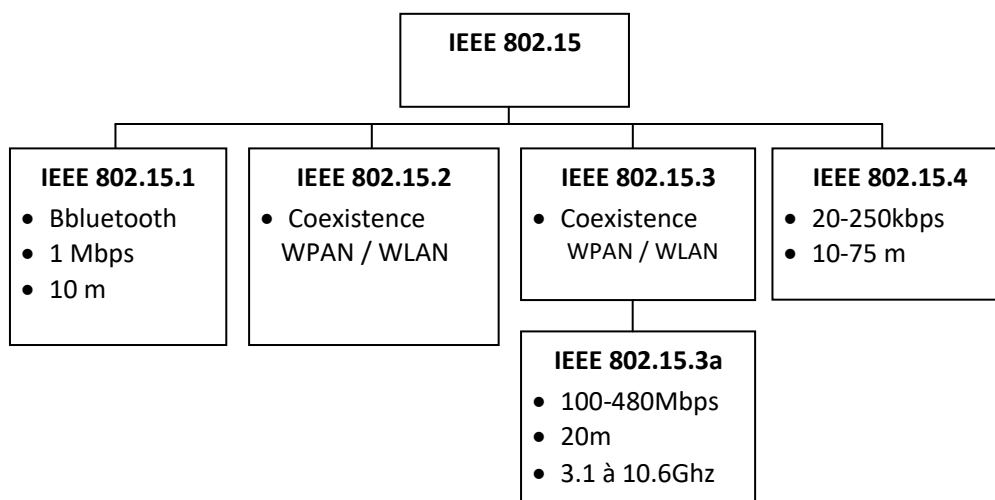


Fig I.2 Organization of IEEE 802.15 [14]

I.4 UWB technology and other technologies

During the last decade, the world witnessed a real enthusiasm from consumers to technologies without wire, because they make the possibility to have a total freedom of movements to communicate. Today, there are wireless systems at several levels: in WPANs (Wireless Personal Area Networks or networks nearby) with Bluetooth; for example, In WLAN (Wireless Local Area Networks or local networks) with WiFi, while in the WAN (Wide Area Networks or large-scale networks) in which we find the most famous system which is GSM.

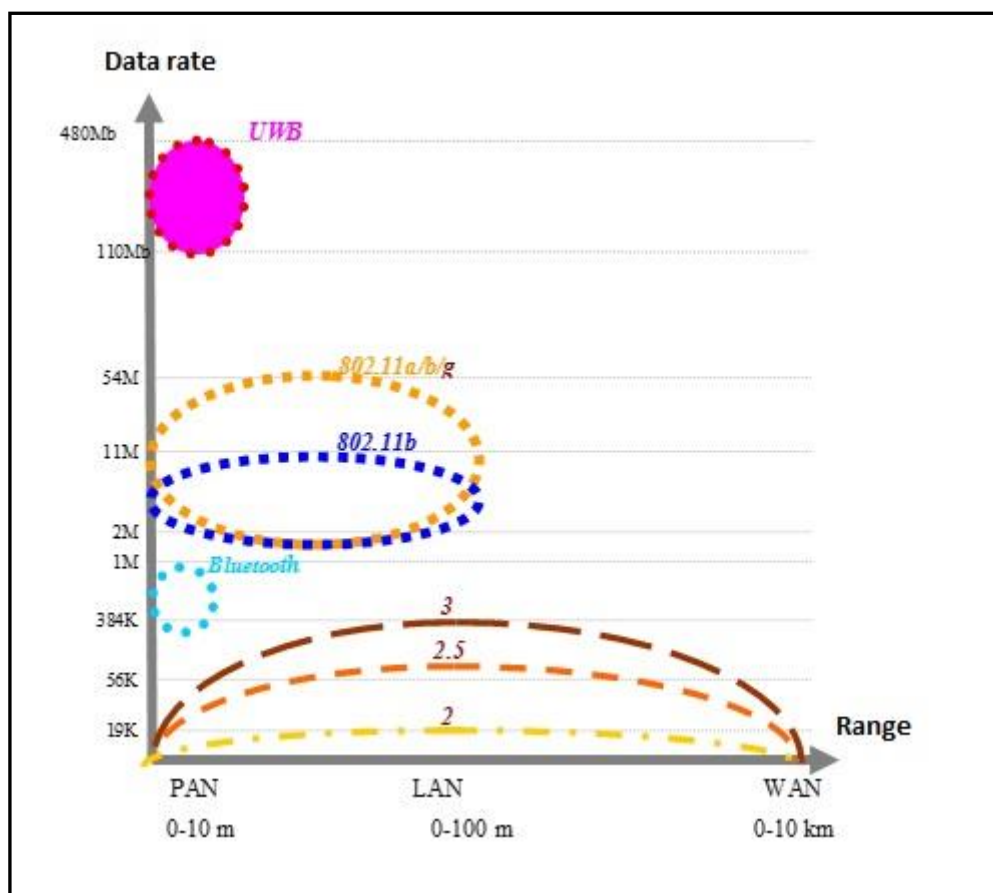


Fig I.3 Summary diagram represents the data rates versus the range

For some years in the WPAN applications, only one technology has been the monopoly, which is Bluetooth. Nevertheless, at the competition with high data rates, Bluetooth could not survive on its rate of 1Mbps. UWB technology is ready for replying this requirement by offering a special rate that can go up to 480 Mbps.

This new technique differs from the preceding ones by the fact that it is not using sine waves. The spectrum obtained by UWB emission is very broad. Since the advent of radio waves, various organizations are responsible for allocating frequency bands for different devices (Frequency bands reserved for cameras, cell phones, television, and so on). These devices have reserved frequency bands to avoid interference from other coexisting equipment.

I.5 Panorama of cohabitation

As has been stated, UWB must coexist with other communications systems without being the source of disturbance or interference to these systems. Some of these systems are illustrated in the following figure:

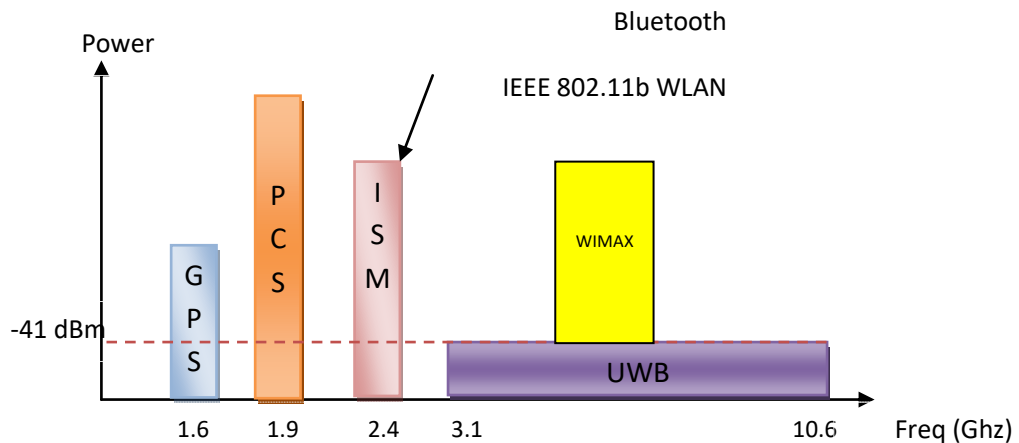


Fig I.4 Different systems coexisting with UWB [14]

I.6 Frequency mask and UWB impulse

Systems based on ultra-wideband occupy a very wide frequency range and overlap of frequency bands already occupied by other systems. For that, it should regulate the emission power regarding the frequency for these UWB systems to avoid disrupting other services. Therefore, when the FCC authorized testing of UWB systems, it imposed drastic transmit power limits within the allowable band [3, 1 GHz - 10 GHz 6]. As shown in Figure (I.5) the Equivalent Isotropically Radiated Power (EIRP) of this band is limited to 41,3 dBm / MHz [15], which corresponds to a maximum total power of 0, 556 mW [13].

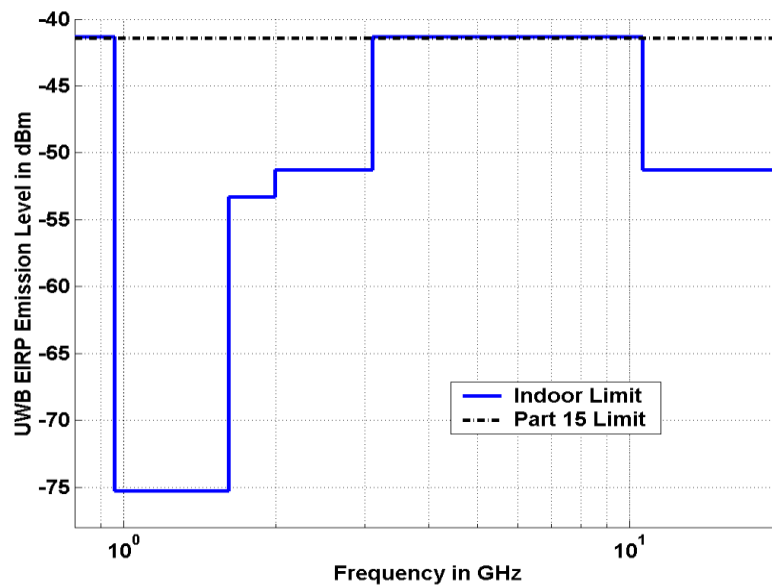


Fig I.5 Transmitted power limits imposed by the FCC for UWB signals [13]

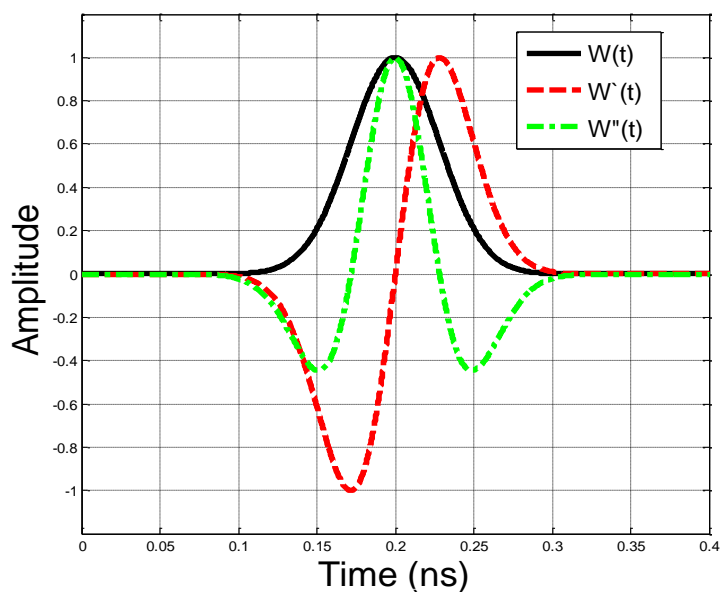
It is now necessary to determine an impulse which can be matched "at best" with the emission mask. In systems dedicated to wireless applications, in particular, in the Time Hopping UWB systems, the signal that respects the mask corresponds to that measured at the transmitting antenna and not to the existing in the modem.

Consequently, to develop and resize properly the impulse that the modem is created, it is necessary to know the transformation that the antenna will make. The transformation that models this adaptation by best manner is the derivative operator [13]. Therefore, the derivative of Gaussian impulse $w'(t)$ must fit the shape of the mask and not $w(t)$, which is the Gaussian impulse generated by the modem. At the reception, the antenna having the same type of behavior, it is the second derivative, which is involved in the processing.

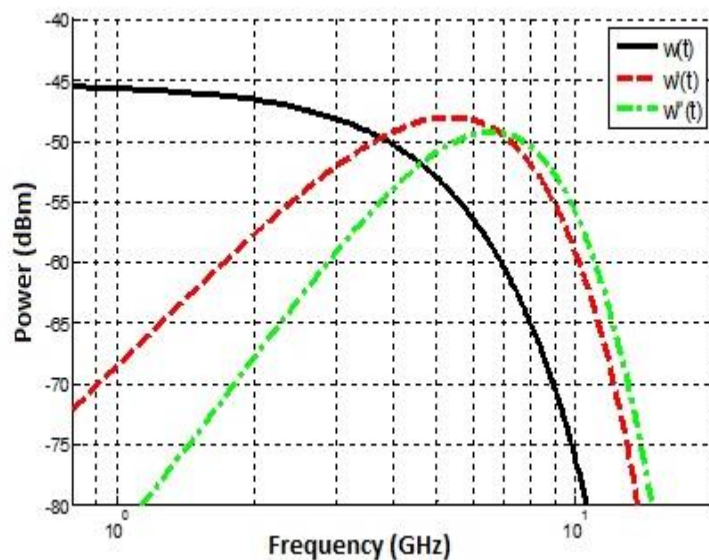
I.7 Impulse waveform

The UWB impulse is based on the transmission and reception of ultrashort impulses (few hundred picoseconds). These short impulses are repeated within a period of a few tens of nanoseconds; thus, they can be modulated in different forms of modulation and combined with Time-Hopping Codes (THC) to avoid interference with other coincident connections.

As against the finesse of impulses require very precise clocks, so expensive. Also, to prevent disruptions on the sub-bands for other uses, it is necessary to complete the filtering; even this may complicate both the transmitter and receiver. Several types of ultrashort pulses are used in UWB impulse transmission systems; the most common are shown in Figure (I.6.a) with their power spectral density in Figure (I.6.b). These impulses are modeled as derived forms of different orders of a Gaussian impulse.



(a)



(b)

Fig I.6 The impulses derived from the Gaussian
(a) time domain; (b) frequency domain

Figure (I.6.a) represents the Gaussian impulses in the time domain: where $w(t)$ represents the Gaussian pulse, $w'(t)$ is Gaussian monocycle, also called the first derivative of the Gaussian, $w''(t)$ is the second derivative of the Gaussian. Figure (I.6.b) represents their spectral densities. These impulses are characterized by very broad spectrum defined over a few MHz to tens of GHz. For the same time width, it is noticed that the center frequency of the spectrum increases when the order of derivation of the impulse increases. These impulses, including the Gaussian monocycle, are most used type in UWB impulse radio. For that reason, we will take the Gaussian monocycle impulse as an impulse form throughout the remainder of this work.

From now on, in the time domain, the Gaussian monocycle will be written as follows:

$$w(t) = \frac{-t}{T_w} \exp\left(-\frac{t^2}{T_w^2}\right) \quad (\text{I.2})$$

T_w is the impulse duration of the monocycle.

In the frequency domain, the spectrum of the monocycle has the following form:

$$w(f) = -j \cdot f \cdot T_w^2 \exp(-f^2 T_w^2) \quad (\text{I.3})$$

Obviously, the more the derivation order increases, the more spectrum is adapted to the frequency mask as noted as well in [12].

I.8 Applications of UWB

Ultra Wideband is a technology of military origin. The resulting applications are therefore not limited to data transfer. There are three types of UWB devices (FCC classification):

- Imaging systems
- Embedded radar equipment
- Communication and measurement devices

I.8.1 Imaging Systems

Imaging systems include the Ground Penetrating Radar (GPR), wall imaging devices, detection devices that can penetrate walls, surveillance systems, and medical devices.

Devices of penetrating ground used to detect buried objects and could help locate underground caches or behind walls. As shown in Figure (I.7.a), this use would be helpful for the police and the army in a conflict. The transmission of signals whose ultra wide spectral band allows achieving results over the entire band from a single measurement, as shown in Figure (I.7.b), where it gives strong power detection since it covers the entire band.



Fig I.7.a GPR can detect multiple targets up to 10m [11]



Fig I.7.b Example of GPR that detects two targets at a distance of 5m [11]

The brevity of impulses with high frequency spectral allows measuring a transient response of target with rich information and separates the received echoes. This peculiarity makes the said technique very robust in the presence of multi-paths.

I.8.2 Embedded radar equipment

This equipment could be used in several areas, notably in the automobile industry, as shown in Figure (I.8), where an example of the embedded radars act as alarms, these devices would be within the frequency bands between (2.2 - 29 GHz) wherein these frequency bands are little used.

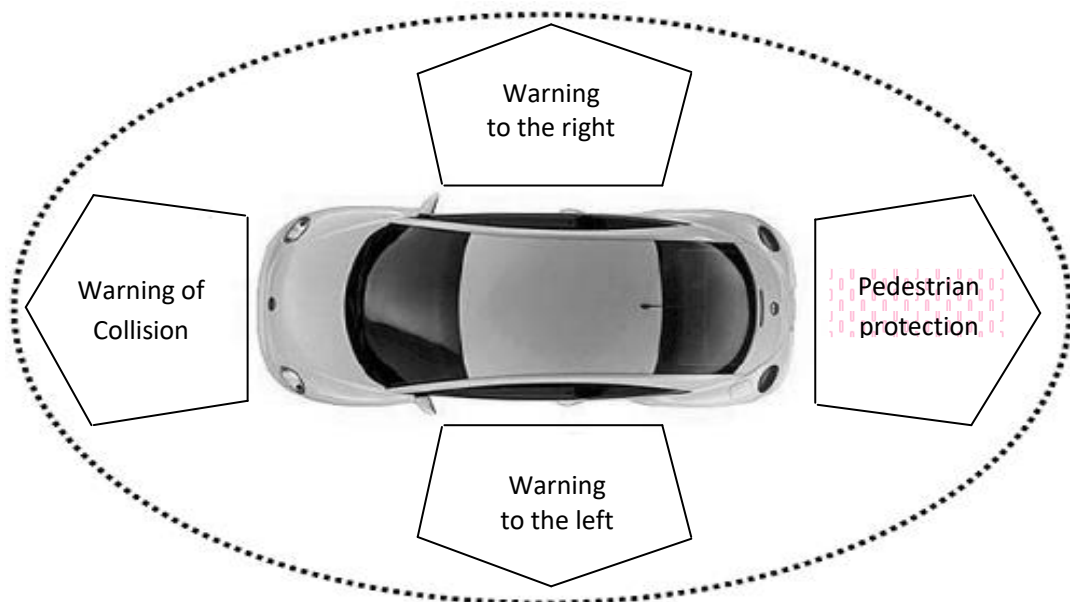


Fig I.8 UWB radar for collision detection

I.8.3 Communication and measurement devices

These applications allow high-speed data transfers and are mainly used in business and homes and between users. However, this technology is very promising in this area; its main objective is to create low-cost devices that can detect and communicate with other devices in their environment. The interconnection capacity and high data rate of wireless are a welcome step forward by the multimedia industry and represents a market of hundreds of millions of devices for users.

The emergence of mobile communication devices, storage and recreation, have showed the need to interconnect these devices easily on a network. The UWB technology is expected to create point-to-point links between electronic devices over short distances, with very high data rates while consuming little energy.



Fig I.9 Typical domestic use of UWB systems

I.9 Advantages and Disadvantages

I.9.1 Advantages

- 1- Efficient use of radio spectrum [10]
- 2- Low cost and small size circuits (can reach a few millimeters) [11]
- 3- Low power consumption (a few milliwatts) [11]
- 4- Simple transmitters [11]
- 5- Low fluctuations of the received power [11]
- 7- The security seems to be an asset of UWB as several protection mechanisms is incorporated at different levels of the protocol, and is transparent to the user

[10]

I.9.2 Disadvantages

- 1- It can be a source of disturbance on other systems. [15]
- 2- The signal/noise ratio decreases with the signal band. It is not interesting to have the widest possible band [11]
- 3- Requires a very precise synchronization [31]

I.10 TH-UWB communication system

As it is indicated in the historical part, in this study we are focusing on Time-Hopping UWB communications systems (TH-UWB) that assure the multiple accesses between users. This technique was made at first time by Scholz [6] and is the source of many academic works.

Time-Hopping Code based on transmitting impulses at instants defined by a pseudo-random sequence; each impulse can be modulated in different modulations such, Pulse Position Modulation (PPM), Orthogonal Pulse Position Modulation (OPPM), Pulse Amplitude Modulation (PAM), On-Off Keying (OOK). During our study, we will describe the TH-UWB system using M-ary PPM modulation.

Multiple accesses are performed by assigning different codes to different users. In the model proposed by Scholtz, a symbol can be repeated several times that adjusts the energy per transmitted bit, while keeping constant the impulse energy (Which ensures a constant power spectral density and therefore compliance with emission mask).

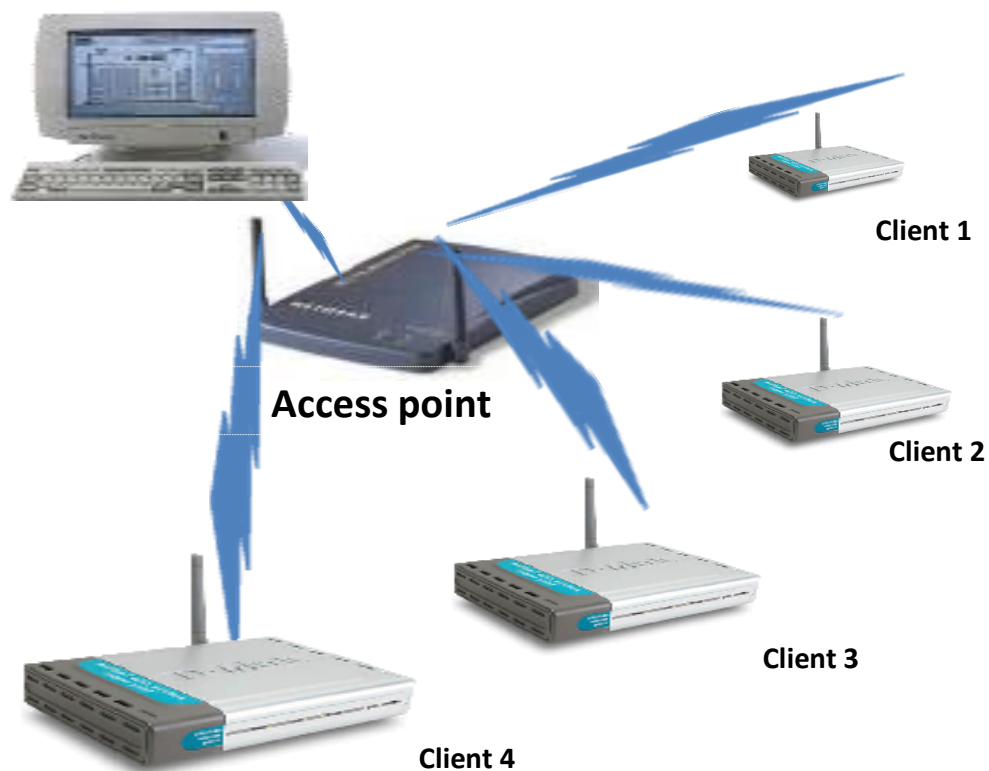


Fig I.10 Example of a UWB system in multi-users case

I.11 Impulse Radio IR-UWB

The Impulse radio principle for the UWB is based on the use of very narrow monocycle train occupying all or a portion of the UWB spectrum. The differentiation between users is performed using the THM technique.

The IR-UWB systems are more economical radio architectures than the MBOA systems; these latter systems require high-quality oscillators, tuned circuits for modulating and demodulating information and intermediate frequency stages. Contrariwise, the IR-UWB transmitters expose baseband signals simplifying architectures (fewer components) and IR-UWB receivers although they have complex architectures a little bit, whereas this matter may be performed through high-speed microprocessors with a good price/performance.

At the IR-UWB receiver, the components related to the different paths of UWB channel could be used constructively to build the reception signal using specific treatments, such as RAKE receivers [14].

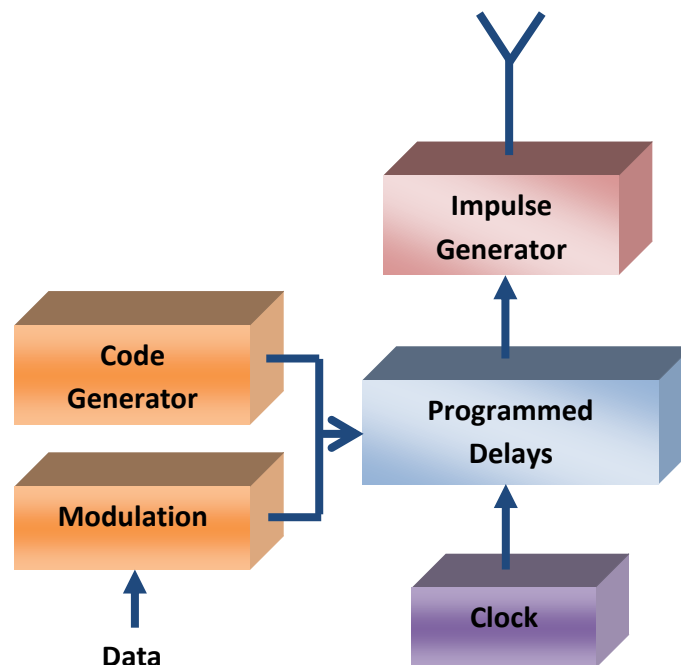


Fig I.11 Block diagram of an IR-UWB transmitter

I.12 TH-UWB signal structure

In multiple access transmission, different users sharing the same physical channel, therefore there's always a risk of interfering with each other. In order to avoid the negative effect of this harmful interference, different multiple access techniques were considered in IR-UWB. Among them, we have the Time Hopping (TH) technique.

The figure (I.12) shows the TH-UWB signal structure consisting of symbols $a^n(k)$ allocated for the user n . As it is depicted, the state of a symbol is (0 or 1) for the 2-PPM modulation according to the shifted delay δ .

Indeed the impulse is much shorter than the symbol duration T_s , for that reason the spectrum is spread, so it is possible during the time T_s seconds time interval to repeat several times that impulse. This matter creates a separation between users based on the technique of time hopping. The latter technique combines a specific code to each user to

set up the impulses' locations within the symbol T_s . Therefore, the TH-UWB signal associated with the same information symbol is composed of N_f duration of T_f frames. Each frame comprises several impulses destined to different users, but only one impulse of them in the frame duration is taken into account for a specified user [6, 26].

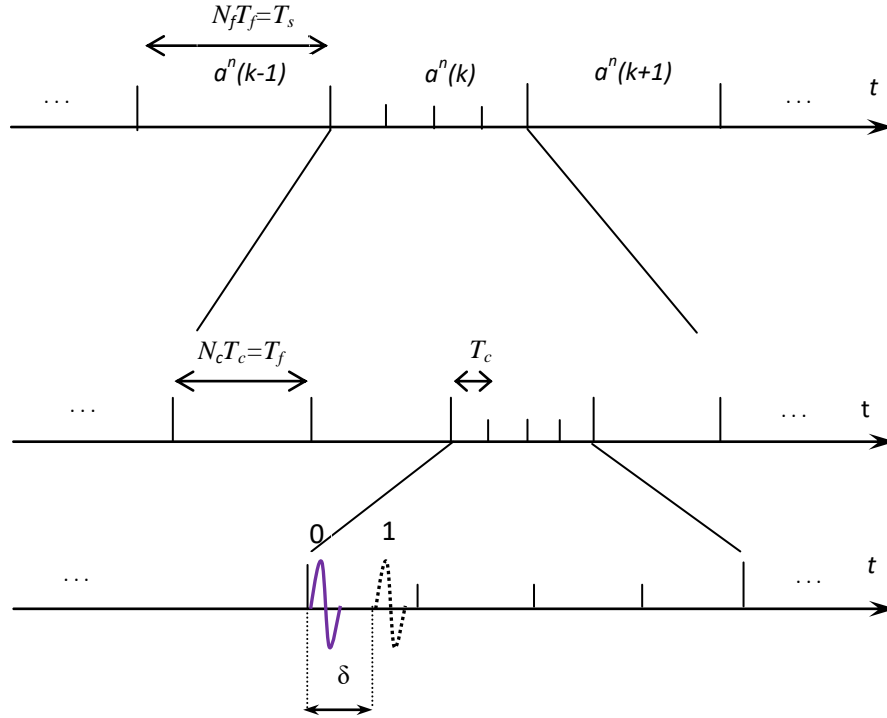


Fig I.12 TH-UWB signal structure for PPM modulation

To determine the position of the impulse within the frame, this latter is divided into N_c chips of duration T_c to facilitate extracting codes of the impulse positions of each user. A specific code determines the position of the impulse within the frame (chip number) to each user. These codes are chosen to avoid interference between different users, and they are periodic codes over the number of frames in each symbol

I.12.1 PPM Modulation (Pulse Position Modulation)

Previously, the PPM has been used for optical communications as a classical modulation, whereas it remains untraditional for wireless communications. The interest in PPM increased with IR-UWB that has a very fine time resolution [32]. This modulation distinguishes between “0” and “1” through a small delay δ .

Basing on what it is mentioned before, the equation that represents the PPM modulation assigned to the signal transmitted for the desired user n is [13]

$$S^n(t) = \sqrt{E^n} \sum_{k=-\infty}^{+\infty} \sum_{j=-\infty}^{N_f-1} w(t - kN_f T_f - jT_f - \tilde{c}_n(j)T_c - \delta a^n(k)) \quad (I.4)$$

- E^n : Signal energy associated with the user n
- T_f : Frame duration
- T_c : Chip duration
- N_f : Number of frames
- N_c : Number of chips
- $w(t)$: Impulse shape, where $T_w < T_c$
- $a^n(k)$: Transmitted symbols $a^n(k) \in \{0, 1\}$
- $\tilde{c}_n(j)$: Time hopping code THC associated with the user n , with integer values in $\{0, N_c-1\}$ and periodic with period equals to N_f
- δ : Modulation factor

The Figure (I.13) below shows the architecture of one information symbol (0 or 1), where just a multiple access of two users with allocated THCs are considered here using the PPM modulation. In this example the information symbol contains $N_f=2$ frames, each frame contains $N_c=5$ chips whose duration T_c , the THC for each user is attributed depending on the location of the impulse in each frame as following:

$\tilde{c}_1 = \{0, 1\}$ for the user designed by the continuous impulses.

$\tilde{c}_2 = \{2, 4\}$ for the user designed by the discontinuous impulses.

It is clear to show that the user whose continuous impulses has transmitted "0" and the other one has transmitted "1".

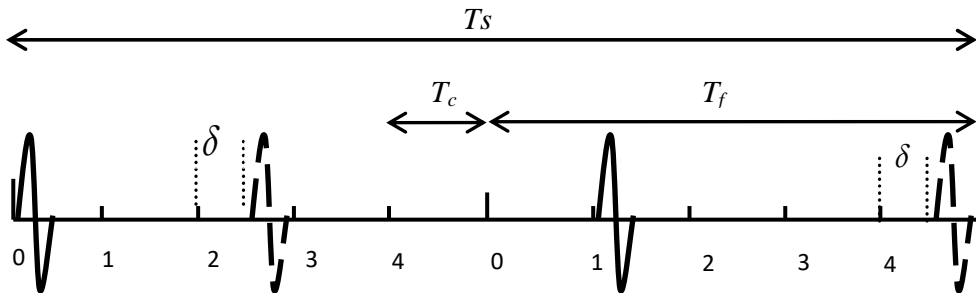


Fig I.13 Two states "0" and "1" modulated in PPM for two users

I.12.2 M-Ary PPM Modulation

This modulation is based on the previous one, where we can modulate the information symbol in several states across several delays x . Where the number of possible states is $M = 2^b$, knowing that b is the number of the associated bits, where M can take the following values (2, 4, 8, 16 ... etc.).

The following figure shows the structure of this modulation.

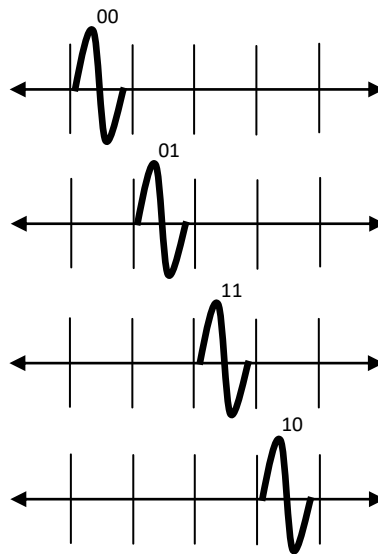


Fig I.14 M-Ary PPM Modulation (M=4)

I.12.3 TH-UWB signal form

In this case, Time Hopping Code signal using a PPM modulation is taken in detail. The following figure shows an example of a multiple access scenario for three users only and represents two information symbols (0 or 1) with the following parameters.

- Data Rate: $R_d=200\text{Mbps} \Rightarrow T_s = 5 \text{ ns}$
- $N_f = 2 \Rightarrow T_f = T_s/N_f = 2.5 \text{ ns}$
- $N_c = 5 \Rightarrow T_c = T_f/N_c = 0.5 \text{ ns}$
- $T_w = 0.2 \text{ ns}$ (the impulse duration with a normalized amplitude to 1).
- THC time hopping codes
 - $\tilde{C}_1 = \{0, 3\}$ for the user of the red color
 - $\tilde{C}_2 = \{2, 4\}$ for the user of the purple color
 - $\tilde{C}_3 = \{3, 1\}$ for the user of the green color

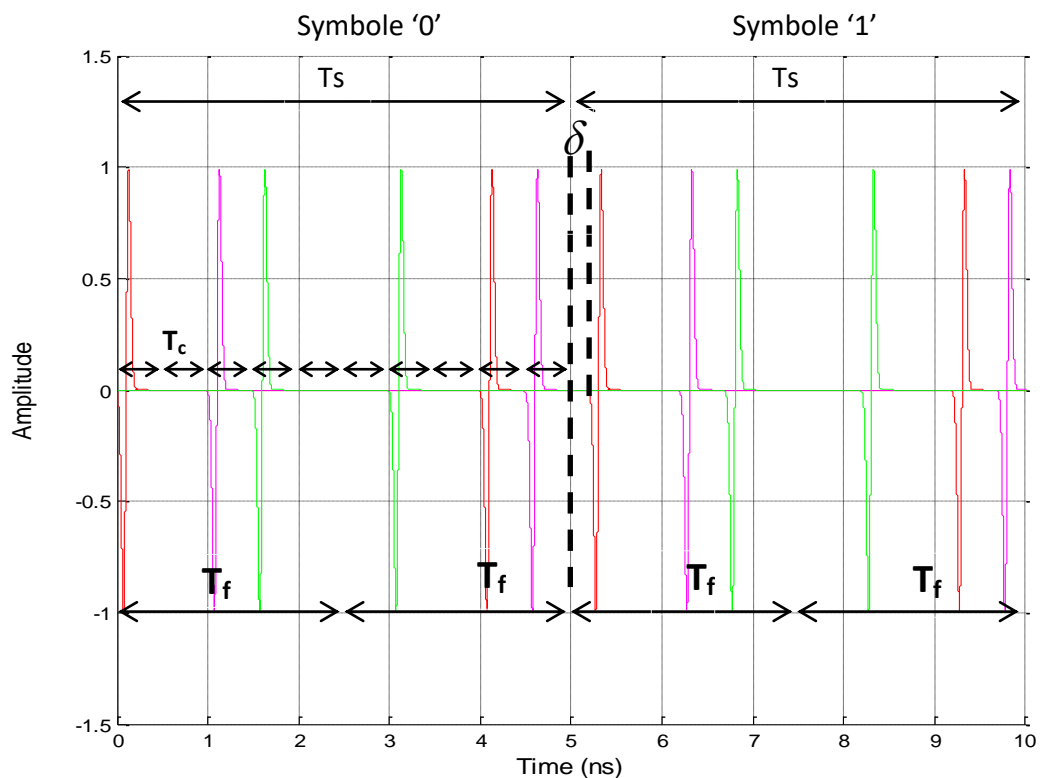
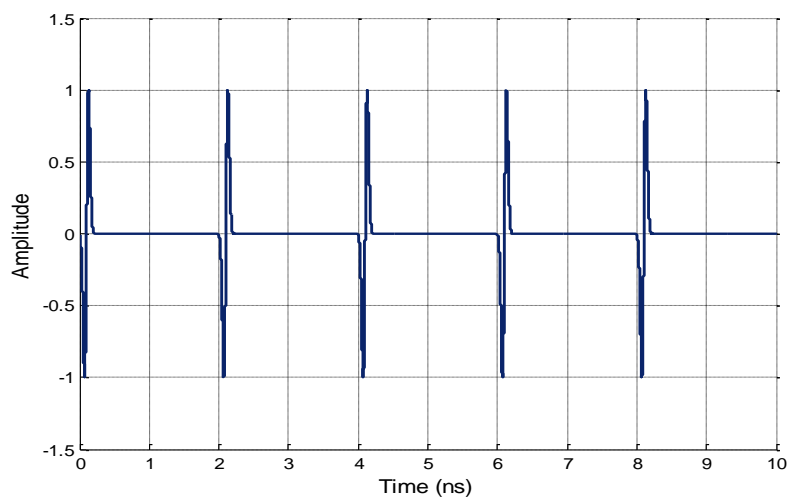


Fig I.15 TH-UWB signal for three users

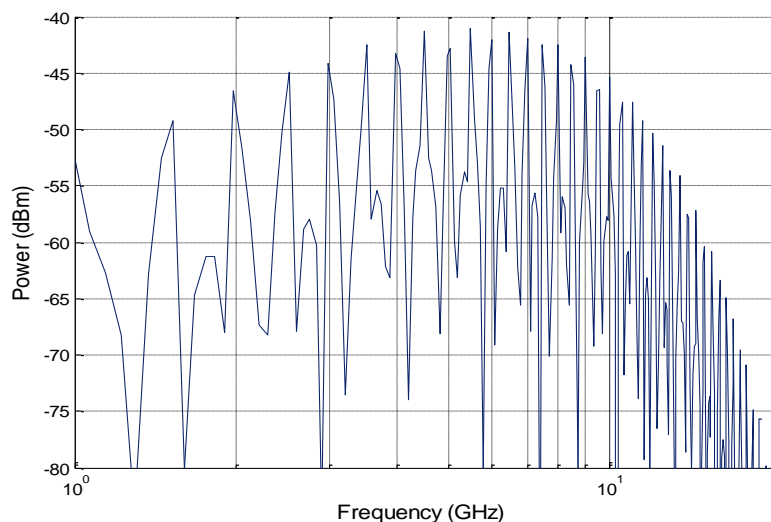
I.13 THC effect on the transmitted signal spectrum

The way of transmitting the impulses by the user according to the Time Hopping Code (THC) has a great influence on the signal spectrum, where transmitting the impulses at regular intervals might cause spurious peaks in the frequency domain, these parasitic peaks are associated with temporal periodicities of the signal [33].

Figure (I.16) shows a sequence of Gaussian monocycles in time and frequency domain where the impulses are regularly transmitted:



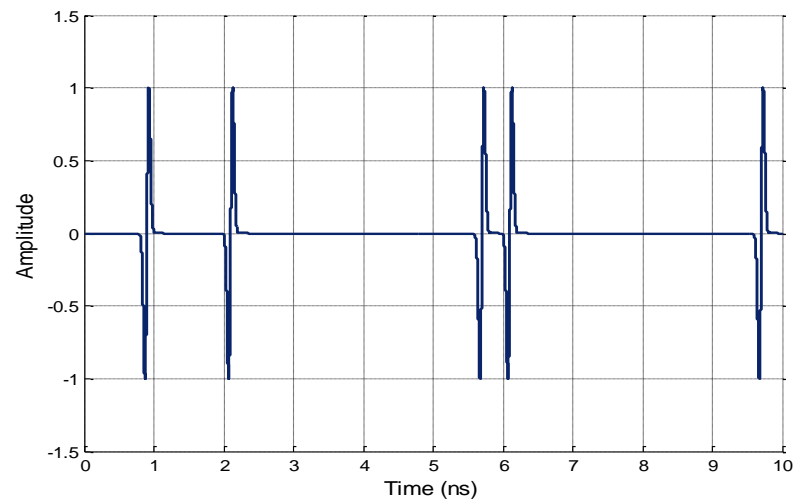
(a)



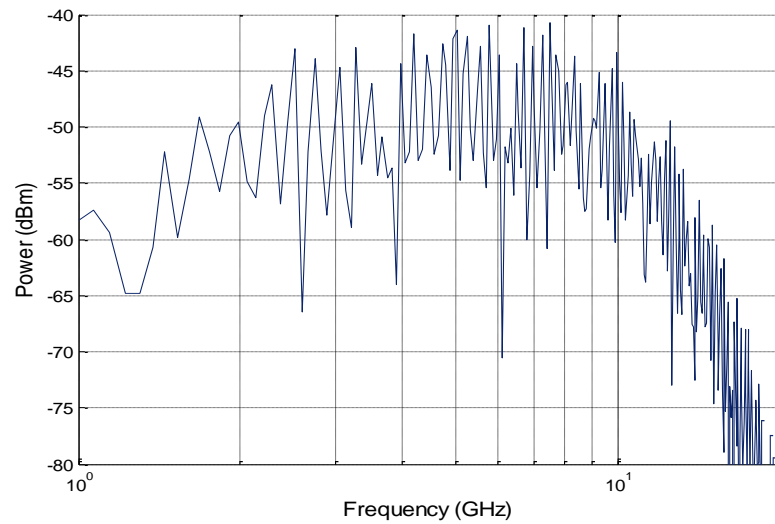
(b)

Fig I.16 Sequence of regular monocycles impulses
(a) in time domain; (b) in frequency domain

In the frequency domain, the Gaussian monocycles' sequence generates rays spectrum. Thus, the impulses train may interfere with conventional short-range radio systems. These rays can be eliminated by varying the time interval from one impulse to another figure (I.9). That means making time hopping codes for each user appropriately.



(a)



(b)

Fig. I.17 Sequence of irregular monocycles impulses
(a) in the time domain; (b) in the frequency domain

I.14 Summary

The UWB technology from day to day proves that it would conquer the field of personal communications to replace the current personnel systems such as Wi-fi, Bluetooth. Despite the fact that the abovementioned systems have their advantages, but they present a significant weakness in the level of transmission data rate which has become a recommended need of the consumers and the world market. Under these conditions, the UWB technology has made the object of these recommendations. Moreover, since it offers an unlicensed wide frequency band allowing a large number of users to communicate each other with a very high transmission rate. Also, the fact that the temporal resolution is inversely proportional to the bandwidth of the signal, therefore this technology is enriched by another fantastic feature particularly in the field of imaging.

In this chapter, we have addressed the necessary key concepts for understanding UWB communications system, where we have shown the THC signal structure that is based on transmitting impulses' sequences according to each user, these sequences are arranged by time hopping codes to establish a smooth multiple access communication without perturbing each other. Furthermore, we have selected and presented a known modulation in UWB domain which will be used in future numerical results, i.e., M-ary PPM Modulation.

Moreover, the manner of transmitting the impulses has a major impact on the nearby systems, where it is clearly proved that the impulses sequences should be regularly transmitted to keep the signal's spectrum as slick as possible without rays through neatly choosing the THC.

The next chapter will be devoted to the channel modeling in which a deep studied should be done for characterizing the UWB channel nature to be able to deal with it.

Chapter II

Modeling of UWB multipath channel

Chapter II

Modeling of UWB multipath channel

II.1 Overview

The channel modeling is a well-known problematic in the development of communications systems, but when it comes to multipath phenomena, indeed the problem would be a great challenge in dealing. In fact, to conceive a communication system or analyze its performance, it is necessary to take into account the characteristics of the channel associated with the system. Wireless propagation channels have been studied for over 50 years, and many models have been proposed. However, UWB systems require developing new models because the propagation phenomena involved have different aspects than those of conventional channels due to the frequencies band used.

In 1990, the first measurement campaigns of UWB propagation channels were made, and in 2001 the first UWB channel models emerged. These studies (measurements and modeling) were then widely stimulated conjointly with the development of standardization works IEEE 802.15.3a and IEEE 802.15.4a. Many experiments and research topics were then performed in a variety of environments corresponding to various applications envisaged for UWB channels, and several models have been proposed.

Among these researches, in 2002 the IEEE has proposed a first channel model dedicated to standard IEEE 802.15.3a (high data rate communication applications for WPAN), which is called "IEEE 802.15.3a Channel Model" or "Model 3a". Where the main objective is to allow a comparison of various UWB devices proposed for the physical layer [18].

Although this model does not measure the absolute performance of the systems due to various simplifications made, however, it is sufficiently realistic to study the behavior on the different proposals. Furthermore, this model is a statistical model derived from measurements; it is the most used for UWB channels and is available as Matlab files [14].

In this chapter, we will focus on the IEEE 802.15.3a channel model highlighting the characteristics of UWB multipath channel to understand the specifics of the UWB propagation.

II.2 IEEE 802.15.3a Channel model (Model 3a)

II.2.1 Presentation

The IEEE 802.15.3a standard was developed with major constraints to take into account the attenuation losses and aspects related to multipath phenomena, this for many types of indoor environments (offices and residential) including several distances (between 0 and 10 meters) and scenario of Line-of-Sight (LOS) and No Line-of-Sight (NLOS).

Four scenarios or Channel Models (CM) were taken into account:

- LOS with a distance of 0-4 m between transmitter/receiver (CM1).
- NLOS for a distance of 0-4 m (CM2)
- NLOS for a distance of 4 to 10 m (CM3)
- NLOS very dense multipath (CM4)

The model had to be relatively simple to be used easily and quickly, and also transparent to the different measures. Its development is based on many contributions resulting from various measurement campaigns and proposed models that are listed in [17].

In the experimental part, the various works are distinguished by the experimental premises (architectures and materials); and channel sampling techniques: measurements in the time domain (requiring an impulse generator and a fast digital oscilloscope); measurements in the frequency domain (vector network analyzer), distances of planned transmissions, signals types and used antennas, ranges of frequencies surveyed.

For the modeling part, both conventional approaches could be considered: deterministic theoretical approach and experimental approach. The deterministic theoretical approach is intended for a given environment but has the disadvantage of being difficult to generalize it over different contexts. For that, the experimental approach was preferred. Thus, most of the proposed models were determined empirically and based on a probabilistic model derived from a physical reasoning.

II.2.2 Modeling of multipath channel

Generally, in the presence of obstacles between the transmitter and the receiver (the common case in indoor propagation), the UWB signal transmitted under wave form is received as a plurality of delayed and attenuated signals from different paths. Thus the attenuations and delays vary according to paths which are due to various obstacles. The superposition of different propagation paths then leads to a so-called multipath propagation figure (II.1).

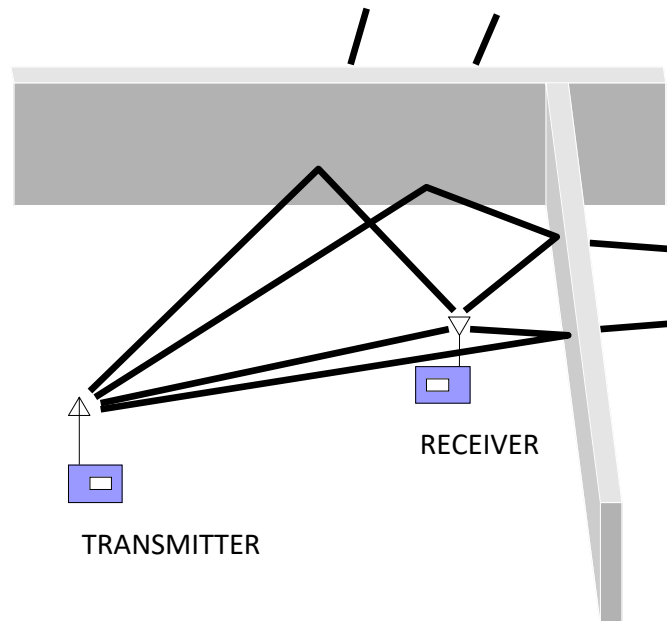


Fig II.1 Illustration of the propagation mechanisms

In a real environment, the paths are variable in number and undergo different effects depending on the nature of the interaction between the wave and the components of the environment (Reflection, diffraction, diffusion, guiding-wave). The signal obtained at the receiving antenna corresponds to a recombination of these waves, which have undergone an attenuation and a different rotational phase. Therefore, the presence of multipath propagation may lead to significant distortions of the received signal, especially inside buildings, where paths of Line-of-Sight (LOS) are not always available where the paths of No Line-of-Sight (NLOS) are more dominant. Figure (II.2) illustrates the multipath mechanisms.

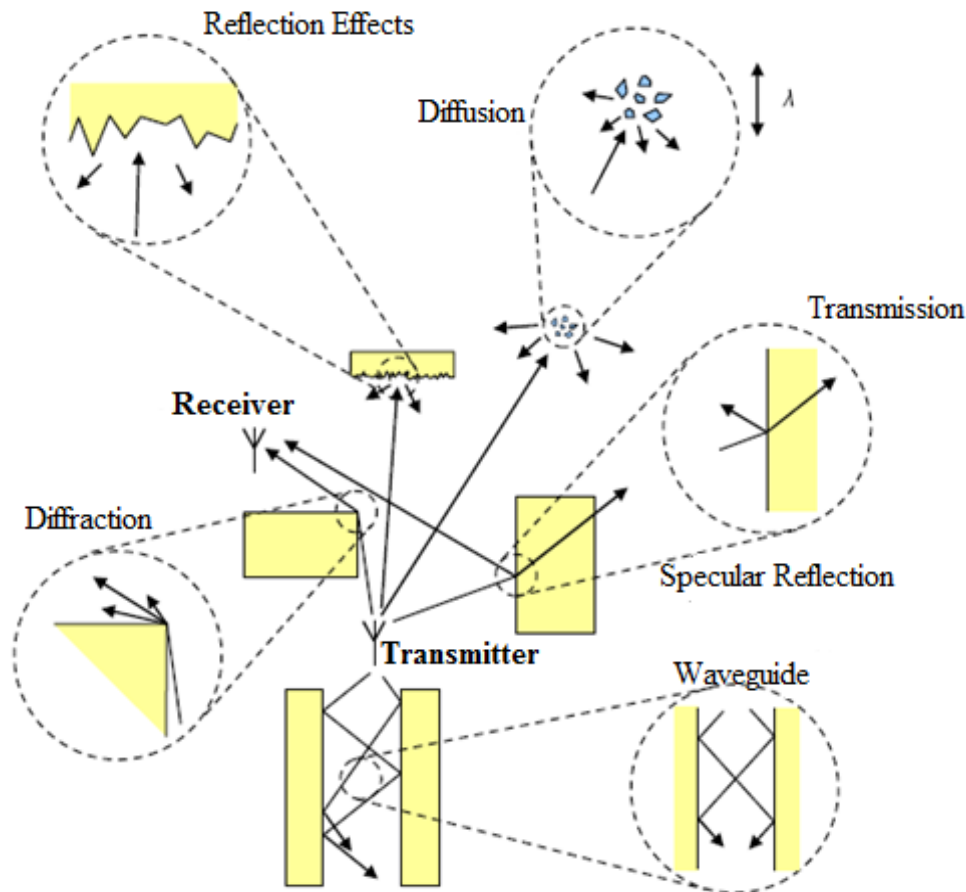


Fig II.2 Main multipath mechanisms [13]

The different campaigns of channel measurements highlighted some specific features for the UWB case. On the one hand, the different paths arrive in successive packets (clusters) such is depicted in the figure (II.3). This property has guided the choice of the model to the one proposed by Saleh-Valenzuela (SV) [21], which has been then adapted to the UWB case. The Rayleigh distribution translating paths' amplitudes has been replaced by a log-normal distribution that is best suited to the obtained measurements. On the other hand, the fading phenomenon associated with each packet and each path has been assumed to be independent of each other. Furthermore, the arrivals of packets are modeled by a Poisson process, the same thing for paths' arrivals that are also modeled by another Poisson process. The arrival of all paths obeys a double Poisson process of various parameters adapted to the time scale (packet or path).

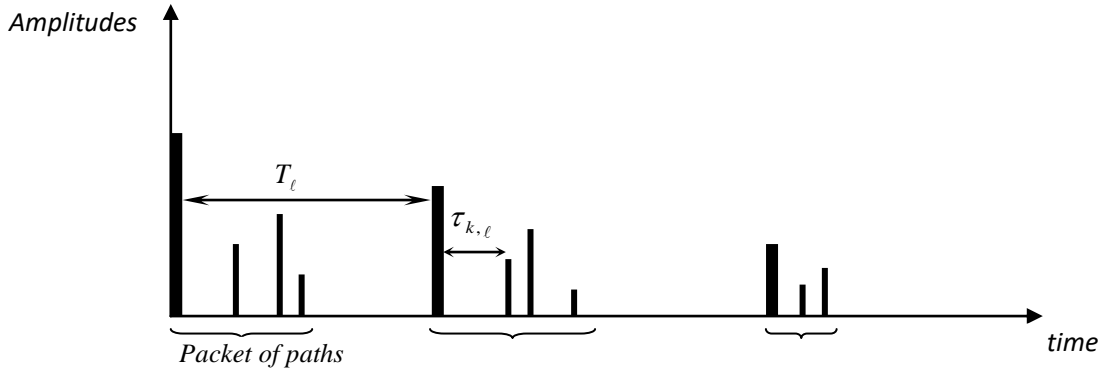


Fig II.3 Synoptic illustration of the impulse response of a UWB multipath channel [14]

The impulse response of multipath model is then given by the following relation

$$h(t) = X \sum_{l=0}^L \sum_{k=0}^K \alpha_{k,l} \delta(t - T_l - \tau_{k,l}) \quad (\text{II.1})$$

Where the parameters are defined below

- L : number of packets
- K : number of paths per packet
- X : global "shadowing" effect
- $\{\alpha_{k,l}\}$: attenuation coefficient of paths
- $\{T_l\}$: arrival time of the 1st path of the l^{th} packet
- $\{\tau_{k,l}\}$: delay of the k^{th} component of paths of the l^{th} packet, according to the arrival time of the 1st path ($\tau_{1,l}=0$)

The probability densities of the difference between arrival times of two packets and two consecutive paths are given by these equations respectively [14]

$$p(T_l | T_{l-1}) = \Lambda \exp[-\Lambda(T_l - T_{l-1})], \quad l > 0 \quad (\text{II.2})$$

$$p(\tau_{k,l} | \tau_{(k-1),l}) = \lambda \exp[-\lambda(\tau_{k,l} - \tau_{(k-1),l})], \quad k > 0 \quad (\text{II.3})$$

Where Λ describes the arrival rate of a packet and λ describes the arrival rate of a path within a given packet.

These equations involve exponential functions because if the arrival times follow a Poisson process, the difference between two times follows an exponential distribution.

The channel coefficients are defined as follows

$$\alpha_{k,l} = p_{k,l} \xi_\ell \beta_{k,l} \quad (\text{II.4})$$

ξ_ℓ represents the fading associated with ℓ^{th} packet, $\beta_{k,l}$ represents the fading associated with k^{th} path of the ℓ^{th} packet, $p_{k,l}$ represents the random inversions of impulses due to reflections.

Regarding the modeling, $p_{k,l}$ takes the values ± 1 with equal probability, while ξ_ℓ and $\beta_{k,l}$ obey to log-normal distributions whose values are calculated from the following relations.

$$20 \log_{10}(\xi_\ell \beta_{k,l}) \propto \text{Normal}(\mu_{k,l}, \sigma_1^2 + \sigma_2^2) \quad (\text{II.5})$$

and

$$\left| \xi_\ell \beta_{k,l} \right| = 10^{(\mu_{k,l} + n_1 + n_2)/20} \quad (\text{II.6})$$

with $n_1 \propto \text{Normal}(0, \sigma_1^2)$ and $n_2 \propto \text{Normal}(0, \sigma_2^2)$ which are independent and which respectively correspond to the fading of each packet (large scale fading) and each path (small scale fading). The modeling of two fadings was chosen particularly because the sum of two log-normal distributions also provides a log-normal distribution, which explains their consideration at the same time.

The energy attenuation is given by [18]

$$E \left[\left| \xi_\ell \beta_{k,l} \right|^2 \right] = \Omega_0 e^{-T_l/\Gamma} e^{-\tau_{k,l}/\gamma} \quad (\text{II.7})$$

Ω_0 average energy of the first path of the first packet, γ is the decay factor of a path and Γ is the decay factor of a packet.

Figure (II.4) shows the energy attenuation versus the delays

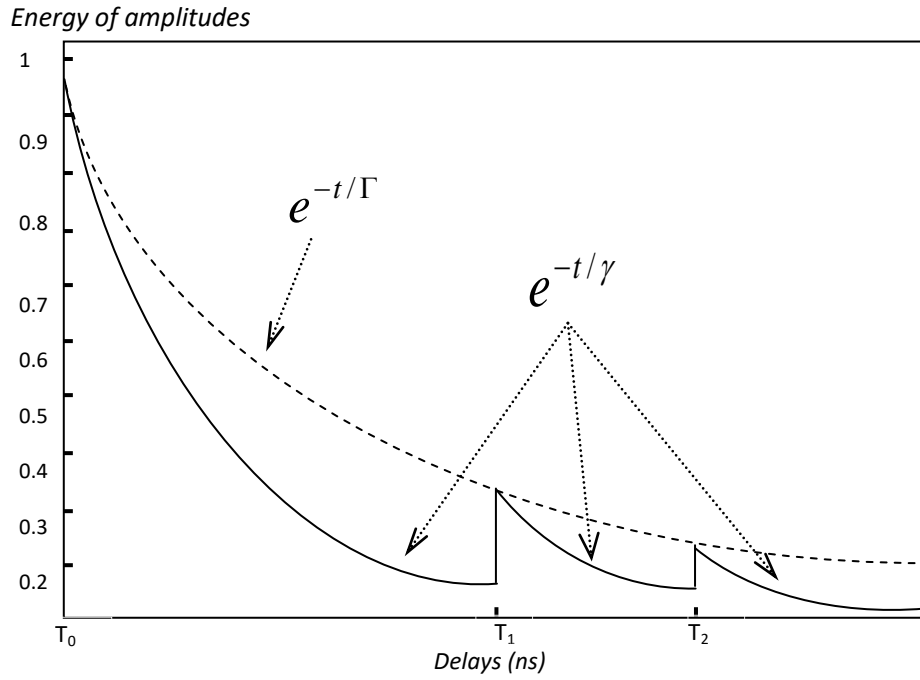


Fig. II.4 The energy attenuation versus the delays

The expectation is expressed as

$$\mu_{k,\ell} = \frac{10\ln(\Omega_0) - 10T_l/\Gamma - 10\tau_{k,l}/\gamma}{\ln(10)} - \frac{(\sigma_1^2 + \sigma_2^2)\ln(10)}{20} \quad (\text{II.8})$$

The total energy contained in the terms $\{\alpha_{k,l}\}$ is normalized, which means

$$\sum_{\ell=1}^L \sum_{K=1}^K |\alpha_{K,\ell}|^2 = 1 \quad (\text{II.9})$$

An additional term X of "shadowing" is then added. It is characterized by a log-normal distribution defined by the following relation

$$20\log_{10}(X) \propto \text{Normal}(0, \sigma_x^2) \quad (\text{II.10})$$

The channel is characterized by the impulse response described by the relation (II.1) and the following seven parameters define the multipath channel model

- Λ : arrival rate of a packet

- λ : arrival rate of a path within a given packet
- Γ : decay factor of a packet
- γ : decay factor of a path
- σ_1 : standard deviation of lognormal fading characterizing a packet
- σ_2 : standard deviation of lognormal fading characterizing a path
- σ_x : standard deviation of lognormal characterizing the global "shadowing"

Conventionally simpler parameters are extracted to characterize the channel quickly. For this reason, three major characteristics of UWB channel have been identified and are used to adjust the variables of the model by comparing the values of these characteristics obtained from measurements and model. These characteristics are the following

- $\bar{\tau} = \tau_m$: mean delay of propagation corresponding to the gravity center of the profile
- τ_{rms} : root mean square delay spread (rms delay spread)
- NP : number of multipath components.

The delay spread τ_{rms} is the square root of the moment of 2nd order of $|h(\tau)|^2$ and is defined by [14]

$$\tau_{rms} = \sqrt{\overline{\tau^2} - (\bar{\tau})^2} \quad (\text{II.11})$$

with

$$\bar{\tau} = \frac{\sum_k \tau_k |h(\tau_k)|^2}{G}, k = 1, 2 \quad (\text{II.12})$$

Where $h(\tau)$ is the measured response in time scale, τ_k are the delays of different responses, and the gain of multipath G is

$$G = \sum_k |h(\tau_k)|^2 \quad (\text{II.13})$$

The delay spread is a dispersion parameter. It increases if the channel impulse response contains paths delayed with large amplitudes. Its physical interpretation in the time domain is simple and allows understanding its importance. Indeed, imagining the propagation of an impulse train periodically transmitted in the period T_s . If $T_s > \tau_{rms}$, then the time between two successive impulses is large enough so that the echoes due to the multipath do not interfere with a symbol to another. By against if $T_s < \tau_{rms}$, an inter-symbol interference appears. Note that if this example seems to show that the multipath reduces the possibility of transmitting a signal with high data rate (i.e., small T_s), in IR-UWB this limitation is still far less restrictive than narrowband signals because the duty cycle of UWB impulse trains is extremely low.

Figure (II.5) shows an illustration of the physical meaning of these parameters, where it should also be noted that the amplitude of the first path is not necessarily the greatest due to the influence of shadowing.

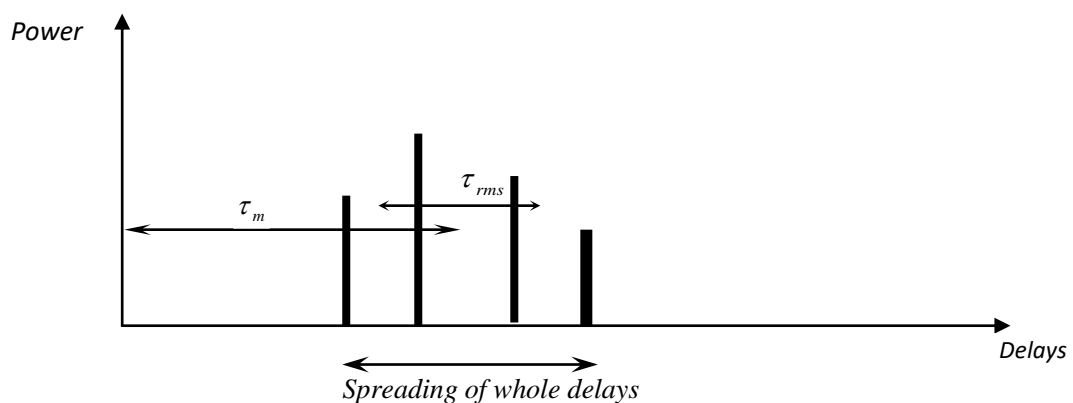


Fig. II.5 Illustration of the channel parameters [14]

II.2.3 Evaluation of modeling

A meaningful evaluation of the model can be given by comparing the values of the following four characteristics obtained from measurements and models

- The *mean delay*
- The standard deviation of the delays
- The number of amplitudes' paths having attenuation more than 10 dB from the strongest path

- The number of paths representing 85% of the channel energy.

These characteristics were selected to represent quickly and accurately the four scenarios of indoor channels (CM1 to 4) taken into account by the model of 3a. The table in (Appendix B.1) gives the values of these characteristics (averaged from many measures), where the parameters of the different models are also shown. They were obtained experimentally from measurements and extraction algorithms. Among these algorithms two are commonly used in UWB: SAGE algorithm [22, 23] and the CLEAN algorithm [24].

II.3 Critique of modeling

The model 3a was proposed with the aim of providing a fast and efficient way to compare the various proposals for UWB systems developed for the standard IEEE.802.15.3a. It is important to quickly get a UWB channel model that models the typical environments (four scenarios) for this standard. Some simplifying assumptions have therefore been made voluntarily because of lack of available measures. This modeling is still incomplete and but meets the objective that was set.

The additional study presented in [25] is interesting because it shows that some model parameters have more influence than others. The article compares the results obtained during transmission where the three following channels are considered: model IEEE, a model where the log-normal distribution is replaced by a Rayleigh distribution and a model in which the notion of the arrival of paths per packet is removed. Anyway, the obtained results are very similar in all three cases. The study concludes that the main modeling parameters are the number of significant paths and the arrival time of the paths.

II.4 Simulation of IEEE 802.15.3a Channel

This channel has the advantage of being widely used in various studies of UWB systems because it reflects a seamless interaction between UWB signals and the real environment. As an example, the Figure (II.6) illustrates the impulse response of 100 realizations for the model CM3.

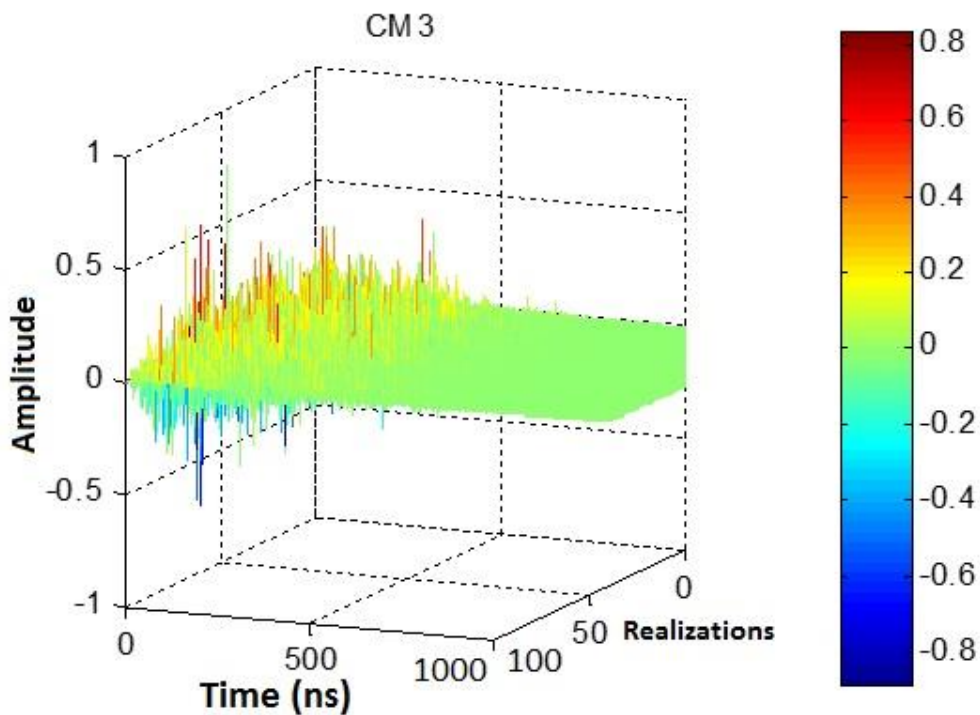
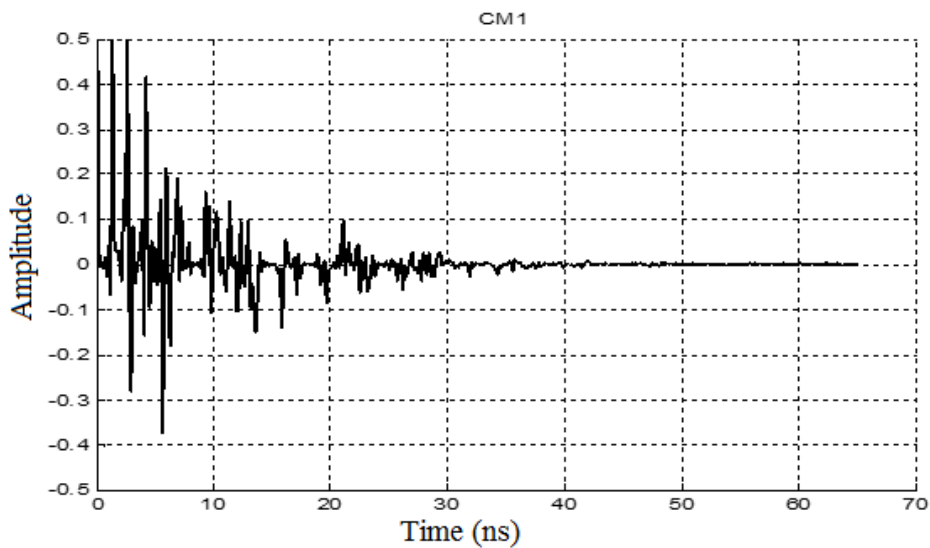


Fig II.6 100 realizations generated by the Model CM3

The figures presented below, illustrate a typical realization of the channel impulse response for the four models of IEEE 802.15.3a channel



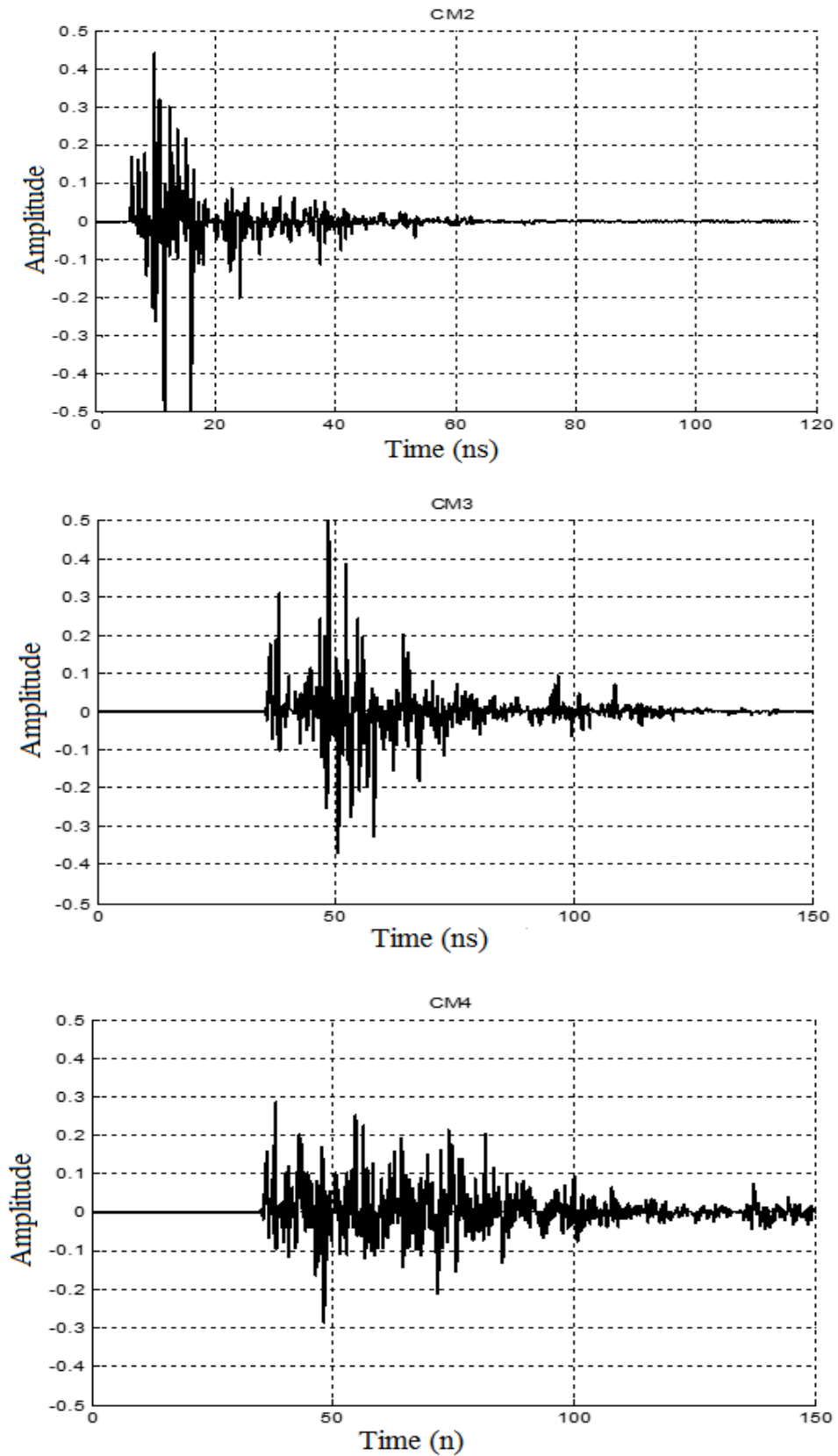


Fig. II.7 Some typical impulse responses for Models CM1, CM2, CM3, CM4

II.5 Summary

In a real environment, the transmission of a signal is usually done with a possible direct path and other propagation paths. These paths vary in number and undergo different effects depending on the nature of the interaction between the wave and an element of the environment as we have seen.

In this chapter, we have described all the different phenomena of UWB signals propagation. We have found that the models proposed by the IEEE have the advantage to model various environments fairly accurately. They are a very interesting tool to develop and study UWB signals from almost a practical viewpoint considering the different propagation phenomena. These models have the merit to be as references for UWB systems studies. They are applied inside short range indoor environments for high data rate communications.

However, there are some improvements to be added such as the Doppler Effect to make them more realistic, and enabling to combat more efficiently against the negative effects of the environment due to other communication devices. Moreover, an important characteristic is not taken into account by the IEEE models which is the angular dispersion. Nevertheless, to make the IEEE models more realistic, the modeling of the channel is characterized by different parameters. We note some parameters like the packet and path arrival rates, the exponential decay coefficients of the packets and paths, the amplitude fluctuations of the paths are modeled by a lognormal distribution; a random inversion coefficient is introduced for simulating the phase inversions of the paths due to reflections. For that reason, this fairly complete model has the merit of being a reference for the studies of UWB systems.

Finally, in the next chapter, many interesting aspects of the channel estimation and the acquisition of UWB signals are discussed, where different parameters will be assessed to study their impacts on the UWB system performance.

Chapter III

UWB channel estimation and acquisition of signals

Chapter III

UWB channel estimation and acquisition of signals

III.1 Overview

After detailing the TH-UWB communication system and the transmission channel modeling, we get to the stage of UWB channel estimation and acquisition of signals. In fact, by the reason of the different fluctuations of the channel parameters caused by the presence of the multipath phenomenon and noise, the acquisition requires a prior channel estimation procedure, where the channel parameters (amplitudes and delays associated with each path) must be approximately known at the receiver. For that, we address in this sense, two contexts of estimation using Maximum Likelihood estimator (ML); the first is a supervised estimation through known sequence estimation (Data Aided (DA)), and the other by a self-estimation through unknown sequence estimation (Non-Data Aided (NDA)).

Many works have been done on the design of UWB receivers, where the assumption of a perfect knowledge of channel parameters was considered at the receiver [26, 29]. In [28], the authors proposed an ML estimator in a realistic arrangement of multiple-access using Time Hopping Code (TH-UWB) and in both contexts (DA) and (NDA). In [30], an estimator of ML in the DA context is performed while one impulse is transmitted in a symbol, where the influence of estimation errors on the rake receiver is made numerically. In [28, 30], the collisions occurring between the incoming impulses from different multipath are neglected, and assuming that the multipath signals are orthogonal. In [31], the author presents the ad hoc estimator to estimate the channel in the frequency domain, where the received signal is firstly passed per a low-pass filter for a practical reason. This filter is characterized by a bandwidth less than the bandwidth of UWB signal and then sampled at the Nyquist frequency. However, since the time resolution is inversely proportional to the bandwidth of the signal, the low-pass filtering reduces the resolution of multipath.

III.2 TH-PPM UWB Signal Format

Typically, the signal reconstitution is to find the information transmitted by exploiting the received signal accurately. Indeed, this is difficult especially in the UWB domain, because the transmitted signal undergoes many distortions related mainly to the propagation channel as well as antennas and electronic circuits. It is well known that the IR-UWB signals are composed of a suite of impulses whose short durations, which are confined within a specific time interval.

The received signal is a combination of different replicas of the transmitted signal that have undergone numerous deformations resulting mainly from the Inter-Symbol Interference (ISI), and from the Multi-User Interference (MUI) as well as the different noises due from coexisting systems signals (UWB and / or "narrowband").

The TH-PPM UWB signal for one user $s(t)$ is defined by the following expression according to the notation (I.4)

$$s(t) = \sqrt{E} \sum_{k=-\infty}^{+\infty} \sum_{j=-\infty}^{N_f-1} w(t - kN_f T_f - jT_f - \tilde{c}(j)T_c - \delta a(k)) \quad (\text{III.1})$$

Thus, the UWB channel has the following expression from the notation of (II.1)

$$h(t) = X \sum_{l=0}^L \sum_{k=0}^K \alpha_{k,l} \delta(t - T_l - \tau_{k,l}) \quad (\text{III.2})$$

Then the expression of the received signal is given as follows

$$r(t) = X \sqrt{E} \sum_{k=-\infty}^{+\infty} \sum_{j=-\infty}^{N_f-1} \sum_{l=0}^{L_c} \sum_{k=0}^K \alpha_{k,l} \tilde{w}(t - kN_f T_f - jT_f - \tilde{c}(j)T_c - \delta a(k) - T_l - \tau_{k,l}) + n(t) \quad (\text{III.3})$$

Where $\tilde{w}(t)$ is the received impulse (distorted from that transmitted $w(t)$)

The diagram of various blocks of the TH-UWB transmission link is illustrated in the following figure

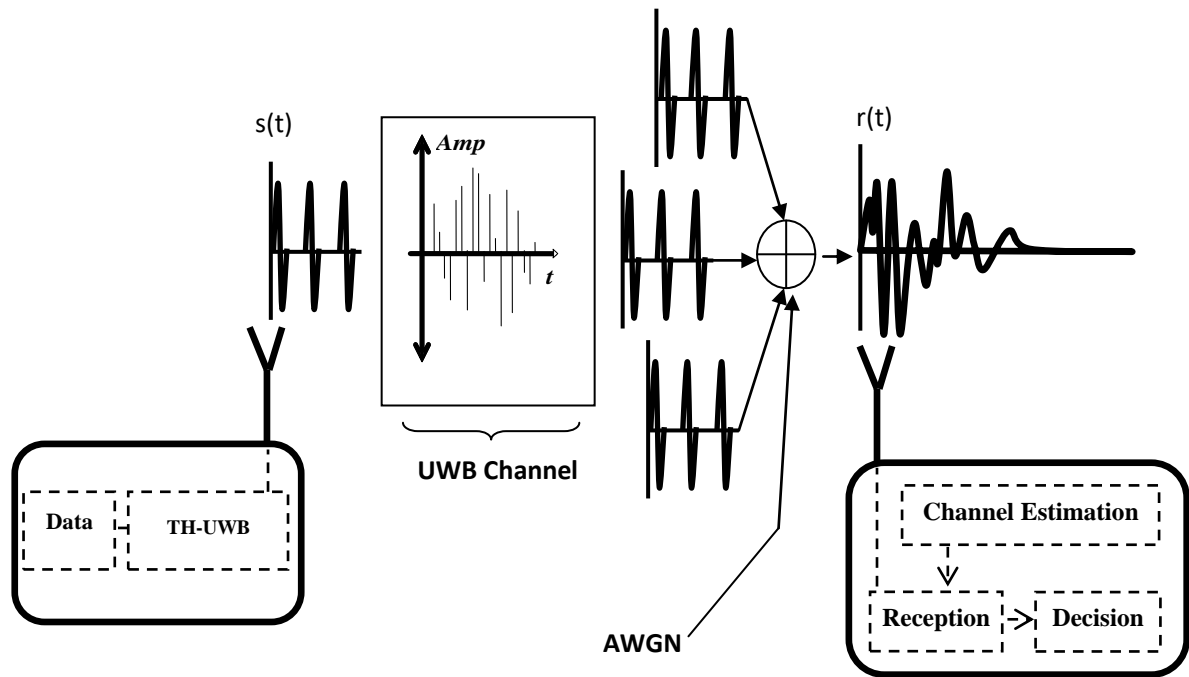
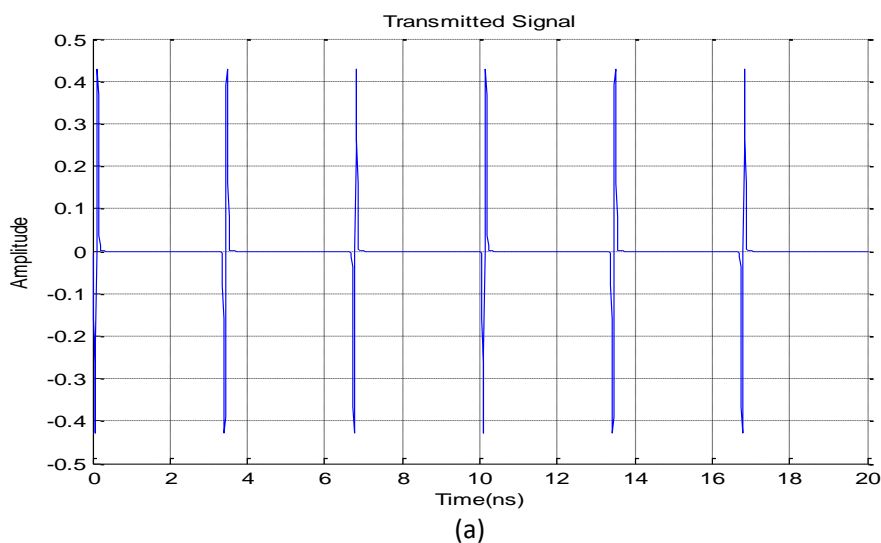
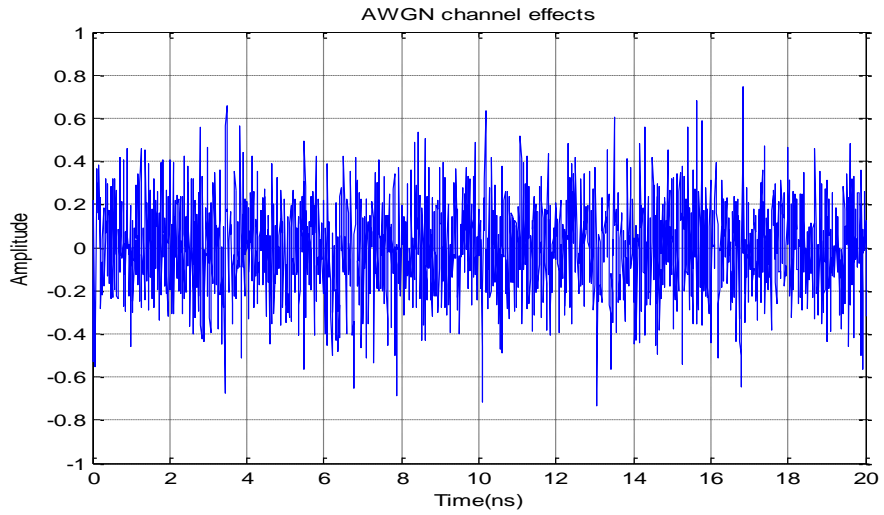


Fig III.1 Block diagram of the TH-UWB transmission link

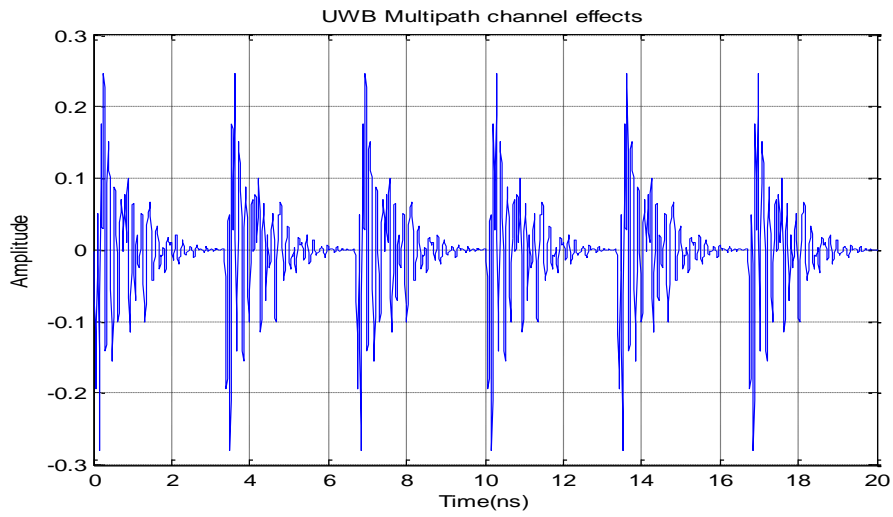
At the receiver, the signals affected by the UWB channel might be arrived by constructive or destructive manner causing different attenuations and changes due to various delays of multipath.

Figure (III.2) illustrates the transmitted UWB signal, noise effects, the effects of the UWB multipath channel (CM1) and the received signal form. The fact that the MUI interference is difficult to be removed in the time domain, we approximate that MUI is represented as a white Gaussian noise added to $n(t)$, this approximation is justified by ensuring an equal power distribution as considered in [26].

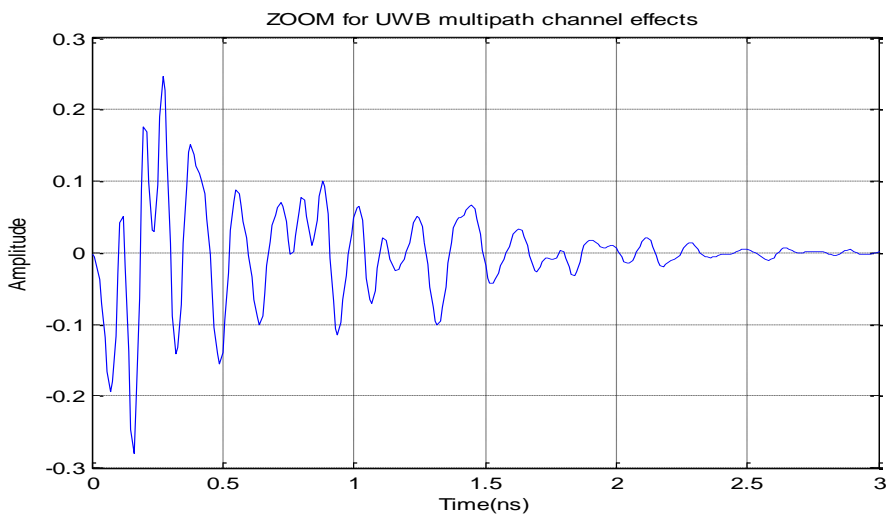




(b)



(c)



(d)

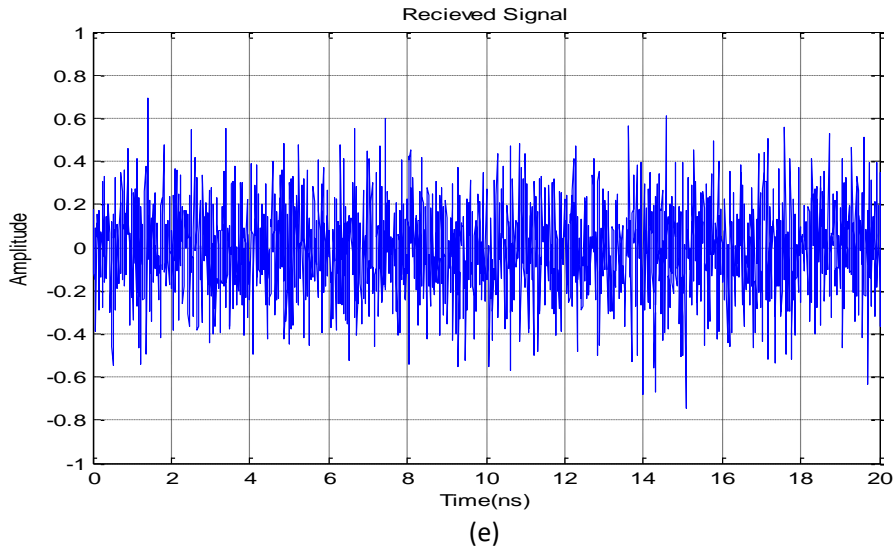


Fig III. 2 Illustration for a TH-UWB signal with PPM modulation

- a) transmitted signal, b) transmitted signal with noise 20dB, c) UWB channel effects
d) Zoom of a spread impulse e) UWB signal at the receiver

The Figure (III.2 (e)) gives in evidence how the impulses are distorted and affected by UWB channel. At the receiver, to reconstitute the transmitted signal we should compensate the multipath effects through a channel estimation to increase the power of the received signal.

III.3 Working principle of rake receiver

The rake receiver belongs to the correlation receivers. Its general idea is to use the various components of the multipath to improve the final decision. This decision is practically limited because the receiver can analyze only a finite subset of L_c contributions which are called fingers (branches) of the rake receiver.

The rake receiver consists of several fingers of which the number corresponds to the number of multipath components taken into account. For each finger the phase correlation is performed as the following description. The received signal is multiplied by a signal "template" $m_l(t - kN_f T_f - \tilde{\tau}_l)$ which is adapted to the l^{th} finger of the rake, then it is integrated over the information symbol's duration to give the decision signal. At this stage, a threshold detector based on the result of the correlator is sufficient to demodulate and determine the received symbol.

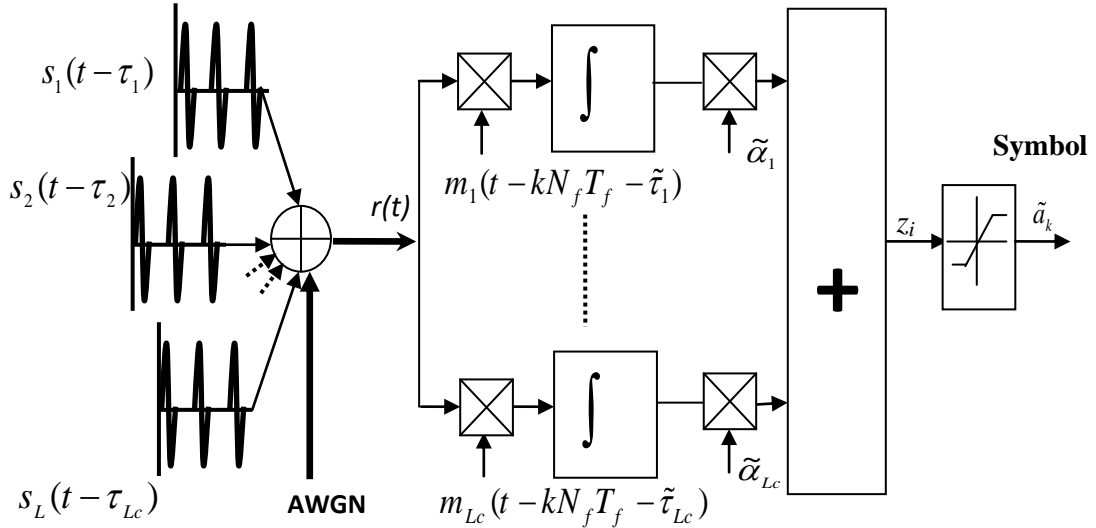


Fig III.3 General structure of the rake receiver

In the case of PPM modulation, a single template signal is used to give the decision signal, where the detector performs a comparison against the zero by seeing the sign of the result given by the correlator. The formula of the template signal for PPM modulation is given by

$$m(t) = b(t) - b(t - \delta) \quad (\text{III.4})$$

where $b(t)$ represents a block of an information symbol.

The resulting signal is integrated over a duration corresponding to the duration T_s of an information symbol. The weighted sum of the correlation results is then applied to a detector which determines the received symbol \tilde{a}_k . The decision variable z_i is given by the following expression

$$z_i = \sum_{l=1}^{L_c} \alpha_l \int_{kN_f T_f}^{(k+1)N_f T_f} r(t) m(t - kN_f T_f - \tau_l) dt \quad (\text{III.5})$$

The following figure shows an example of a modulated signal with PPM and represented for one finger of the rake receiver.

In practice, the parameters $\{\alpha_l\}$ and $\{\tau_l\}$ are unknown a priori and should be estimated through a channel estimation process.

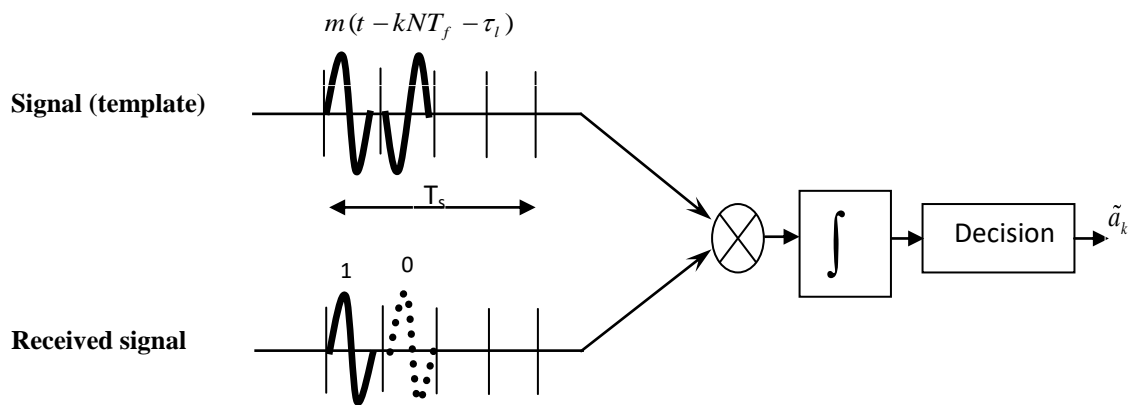


Fig. III.4 Demodulating a symbol with the PPM modulation

Figure (III.5) represents the rake receiver and its detailed blocks for a single user, including channel estimation block as well as the blocks of synchronization and time control. It is very interesting to indicate that the synchronization process has a pivotal role to ensure a good coincidence of the received signal with the template signal. The synchronization allows to determine the exact time of the first path at the receiver; indeed this operation affects the estimate process, for that this operation is very complex, especially in the presence of the multipath, noises, and Multi-Users Interference (MUI) due from other users.

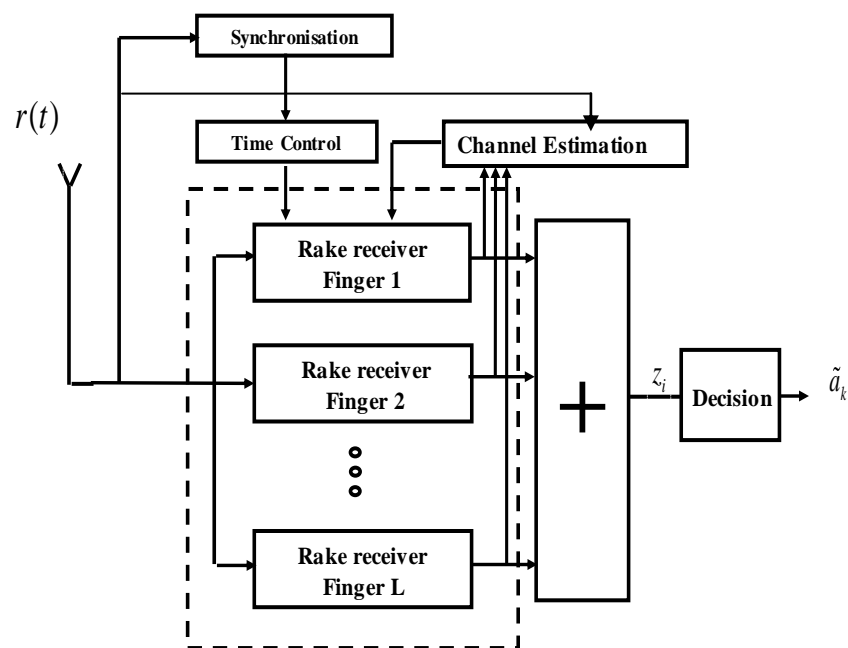


Fig. III.5 Generic diagram of the rake receiver for a single user

Several options are also possible for the number of branches or fingers constituting the rake receiver; i.e. the number of components included that define the type of rake receiver. By this reason, there are three Rake receiver types that are described as follows:

III.3.1 A-Rake Receiver (All Rake)

It takes into account all the received paths, for that it may become very complex. In practice, it is so difficult to carry out this type of receivers because the numerous number of paths.

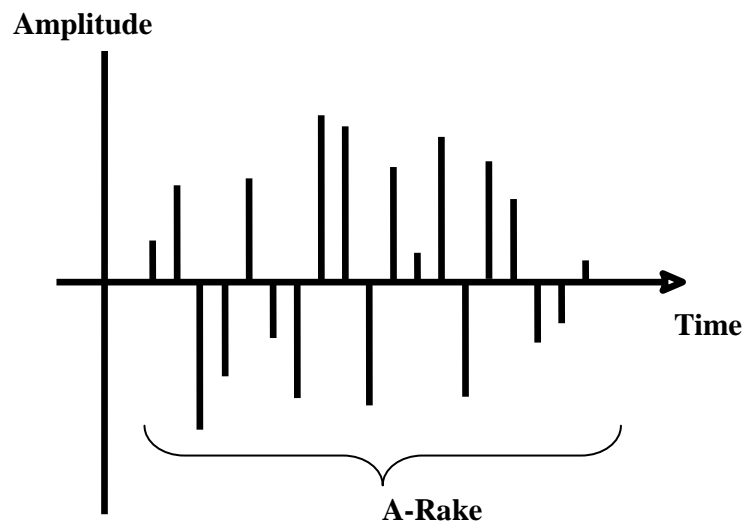


Fig. III.6 The paths that are taken into account by A-Rake

III.3.2 P-Rake receiver (Partial Rake)

In this type, only the first paths are considered at the receiver without any distinction between them.

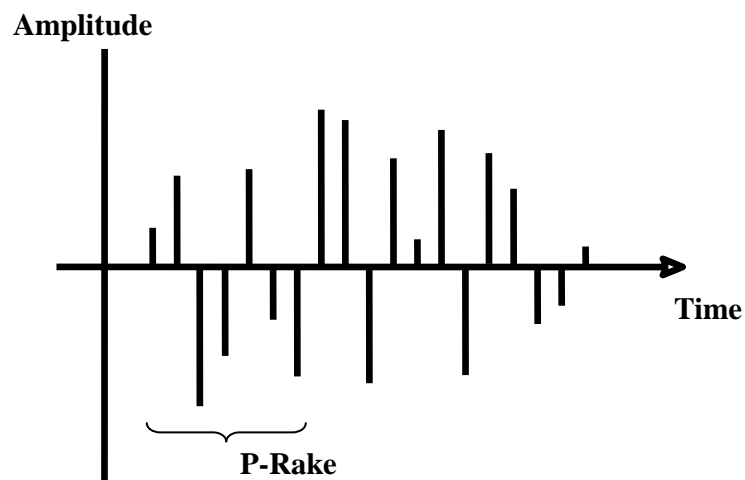


Fig. III.7 The paths that are taken into account by P-Rake

III.3.3 S-Rake receiver (Selection Rake)

This type of receivers picks up only the most important paths are taken into consideration. According to the IEEE channel, the concerned paths are those having undergone an attenuation of more than 10 dB compared to the strongest path, not necessarily the first arrived path, (the remains α_l will be null, except one that corresponds the best path which is equal to the fading coefficient of the corresponding path).

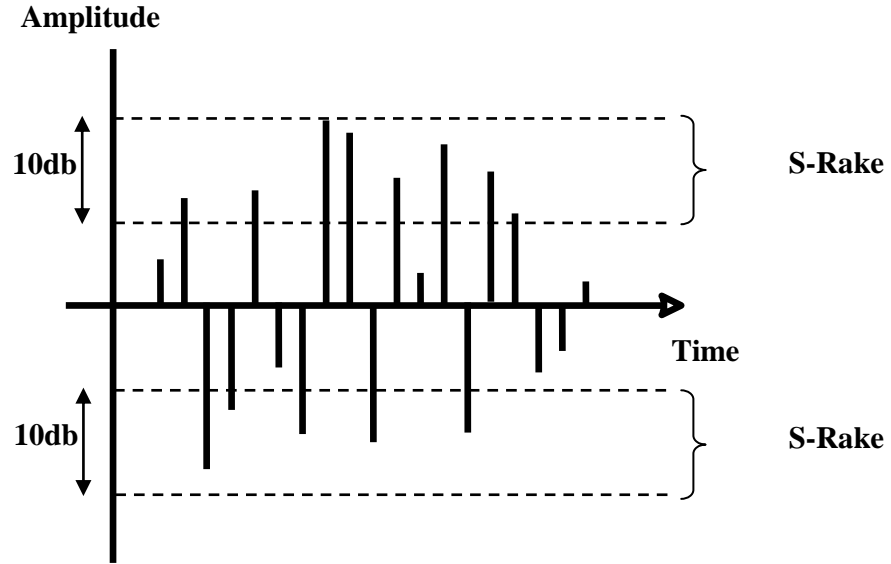


Fig. III.8 The paths that are taken into account by S-Rake

III.4 UWB channel estimation

After having seen the relationship between the rake receiver and the channel estimation; now we will give a bit of detail about the channel estimation process through a maximum likelihood method basing on the work done in [28]. This method consists of two contexts; the first is a supervised estimation through a known data sequence DA, and the other by a self-estimation through an unknown data sequence NDA.

First of all, we recall that the TH-UWB signal $s(t)$ is given by

$$s(t) = \sqrt{E} \sum_{i=-\infty}^{+\infty} \sum_{j=-\infty}^{N_f-1} w(t - iN_fT_f - jT_f - \tilde{c}(j)T_c - \delta a(i)) \quad (\text{III.6})$$

Then the signal transmitted by the desired user is modulated by [26], [27]

$$s(t) = \sum_i b(t - iN_fT_f - \delta a_i) \quad (\text{III.7})$$

with

$$b(t) = \sum_{j=0}^{N_f-1} w(t - jT_f - \tilde{c}_j T_c) \quad (\text{III.8})$$

Noting that $b(t)$ is a block which represents the duration of an information symbol.

We recall as in [28], it is easy that the symbols might be overlapped to each other partially due to the distance of the adjacent blocks. Everything depends on the values of T_f , δ , T_c and \tilde{c}_j , the overlap should be avoided because that may cause the ISI. Furthermore, the minimum distance between the monocycle impulse that crosses a block and the next impulse in the other block is found equal

$$d_{\min} = T_f - \delta - T_c (\tilde{c}_{N_f-1} - \tilde{c}_0) \quad (\text{III.9})$$

III.4.1 Data-Aided Channel estimation

In this part, we focus on the channel estimation through a known sequence data (Data Aided (DA)), so from the relation (III.3) we have

$$r(t) = \sum_{l=0}^{L_c} \alpha_l s(t - \tau_l) + n(t) \quad (\text{III.10})$$

The global noise $n(t)$ has a spectral density of $N_0/2$, and assuming that $\tau = (\tau_1, \dots, \tau_{L_c})$ and $\alpha = (\alpha_1, \dots, \alpha_{L_c})$ as unknown deterministic quantities.

The signal affected by the multipath $\tilde{s}(t)$ is given by

$$\tilde{s}(t) = \sum_{l=1}^{L_c} \tilde{\alpha}_l s(t - \tilde{\tau}_l) \quad (\text{III.11})$$

The log-likelihood function is given by the following expression [3]:

$$\log[\Lambda(\tilde{\alpha}, \tilde{\tau})] = 2 \int_0^{T_0} r(t) \tilde{s}(t) dt - \int_0^{T_0} \tilde{s}^2(t) dt \quad (\text{III.12})$$

By replacing the relation (III.11) into (III.12), and neglecting the correlation between signal echoes, we get

$$\frac{\int_0^{T_s} s(t - \tilde{\tau}_{l_1})s(t - \tilde{\tau}_{l_2})}{\int_0^{T_s} s(t)dt} \approx 0 \quad l_1 \neq l_2 \quad (\text{III.13})$$

This approximation reflects the fact that, the impulses occurring in $s(t)$ are widely separated from each other.

After some manipulation the log-likelihood function becomes

$$\log[\Lambda(\tilde{\alpha}, \tilde{\tau})] = 2 \sum_{l=1}^{L_c} \tilde{\alpha}_l \sum_{i=0}^{M-1} z_i(\tilde{\tau}_l, a_k) - ME_b \sum_{l=1}^{L_c} \tilde{\alpha}_l^2 \quad (\text{III.14})$$

where E_b represents the energy of $b(t)$:

$$E_b = \int_0^{NfT_f} b^2(t) \quad (\text{III.15})$$

$z_i(\tilde{\tau}_l, a_k)$ represents the response of the matched filter $b(-t)$ in $t = kN_fT_f + \delta a_k + \tilde{\tau}_l$

$$z_i(\tilde{\tau}_l, a_k) = [r(t) \otimes b(-t)]_{t=kN_fT_f + \delta a_k + \tilde{\tau}_l} \quad (\text{III.16})$$

where \otimes is the convolution operation

From the relation (III.16), it is clear that $\{z_i(\tilde{\tau}_l, a_k)\}$ are sufficient statistics to calculate the Maximum Likelihood (ML) and to estimate (α, τ) .

These statistics can be calculated by replacing the relation (III.10) into (III.16) as follows

$$z_i(\tilde{\tau}_l, a_k) = \left[\sum_{j=0}^{N_f-1} (r(t)w(t)) \right]_{t=(kN_f+j)T_f + \delta a_k + \tilde{\tau}_l + c_jT_c} \quad (\text{III.17})$$

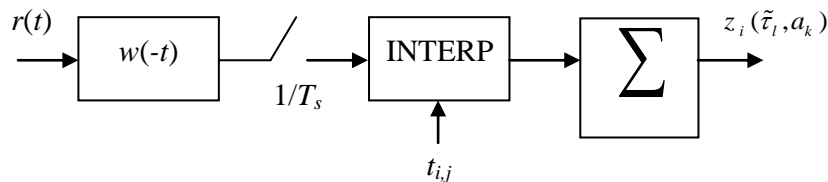


Fig. III.9 Sufficient statistics [28]

$z_i(\tilde{\tau}_l, a_k)$ is obtained by the correlation between $r(t)$ and the matched filter in accordance with the Gaussian monocycle impulse shape and sampling at intervals:

$$t_{i,j} = (kN_f + j)T_f - \delta a_k - \tilde{\tau}_l - c_j T_c, \text{ with } 0 \leq j \leq N_f - 1$$

In practice, the output of the filter is sampled with an appropriate sampling time $1/T_s$ and then interpolated as shown in the previous figure.

Returning to relation (III.14), $\log[\Lambda(\tilde{\alpha}, \tilde{\tau})]$ which is based on $\tilde{\alpha}$ and $\tilde{\tau}$ should be maximized; this can be done in two steps. Firstly, by varying $\tilde{\alpha}$ while maintaining $\tilde{\tau}$ fixed until finding out the maximum of $\tilde{\alpha}(\tilde{\tau})$. Secondly by replacing $\tilde{\alpha}(\tilde{\tau})$ instead of $\tilde{\alpha}$ in $\log[\Lambda(\tilde{\alpha}, \tilde{\tau})]$ and seeking for the maximum of $\log[\Lambda(\tilde{\alpha}(\tilde{\tau}), \tilde{\tau})]$.

Then the first step gives

$$\tilde{\alpha}_l = \frac{1}{ME_b} J(\tilde{\tau}_l) \quad 1 \leq l \leq L_c \quad (\text{III.18})$$

$$J(\tilde{\tau}) = \sum_{k=0}^{M-1} z_i(\tilde{\tau}, a_k) \quad (\text{III.19})$$

By substituting (III.18) in (III.14), the problem reduces to maximize

$$\sum_{l=1}^{L_c} J^2(\tilde{\tau}_l) \quad (\text{III.20})$$

When the maximum of (III.20) is found out by maximizing each term in the sum, the problem reduces to seek delays where there is a maximum in $J(\tilde{\tau})$, Once they are found, multipath amplitudes follow the relation (III.18).

Having estimated the parameters of the UWB channel, the estimation error is represented as the Mean Square Error (MSE) given by the following two relations

$$MSE_\tau = \frac{\sum_{l=1}^{L_c} (\tau_l - \tilde{\tau}_l)^2}{L_c} \quad (\text{III.21})$$

$$MSE_{\alpha} = \frac{\sum_{l=1}^{L_c} (\alpha_l - \tilde{\alpha}_l)^2}{L_c} \quad (\text{III.22})$$

III.4.2 Non-Data Aided channel estimation

In this part, we study the channel estimation based on the previous estimation where the received symbols are unknown (Non-Data Aided (NDA)). To deal with this problem, the ML method is always adopted but, as it is shown in [28], a low SNR should be assumed to simplify the algorithm. The procedure is as detailed above, except that the symbols are now seen as unknown parameters.

The symbols $a_k = (a_1, a_2, \dots, a_{M-1})$ are unknown, the likelihood function is given by [3]

$$\Lambda(\tilde{\alpha}, \tilde{\tau}) = \int \Lambda(\tilde{\alpha}, \tilde{\alpha}, \tilde{\tau}) p(\tilde{\alpha}) d\tilde{\alpha} \quad (\text{III.23})$$

The values a_k are independent and taking the value zero and one with the same probability, so the probability of the estimated data can be written by

$$p(\tilde{\alpha}) = \prod_{k=0}^{M-1} \frac{[\delta(\tilde{\alpha}_k) - \delta(\tilde{\alpha}_k - 1)]}{2} \quad (\text{III.24})$$

where $\delta(\tilde{\alpha})$ is the Dirac impulse

Basing on the previous estimation by DA we get

$$\Lambda(\tilde{\alpha}, \tilde{\alpha}, \tilde{\tau}) = \exp \left\{ \frac{1}{N_0} \left[2 \sum_{l=1}^{L_c} \tilde{\alpha}_l \sum_{k=0}^{M-1} z_i(\tilde{\tau}_l, \tilde{\alpha}_k) - ME_b \sum_{l=1}^{L_c} \tilde{\alpha}_l^2 \right] \right\} \quad (\text{III.25})$$

After some mathematical manipulations, the relation can be written by

$$\Lambda(\tilde{\alpha}, \tilde{\alpha}, \tilde{\tau}) = \exp \left\{ \frac{-ME_b}{N_0} \sum_{l=1}^{L_c} \alpha_l^2 \right\} \times \prod_{k=0}^{M-1} \exp \left\{ \frac{2}{N_0} \sum_{l=1}^{L_c} \tilde{\alpha}_l z_i(\tilde{\tau}_l, \tilde{\alpha}_k) \right\} \quad (\text{III.26})$$

From the relation (III.23), the likelihood function can be given by

$$\Lambda(\tilde{\alpha}, \tilde{\tau}) = \exp \left\{ \frac{ME_b}{N_0} \sum_{l=1}^{L_c} \tilde{\alpha}_l^2 \right\} \prod_{k=0}^{M-1} \left[\frac{1}{2} \exp \left\{ \frac{2}{N_0} \sum_{l=1}^{L_c} \tilde{\alpha}_l z_k(\tilde{\tau}_l, 0) \right\} + \frac{1}{2} \exp \left\{ \frac{2}{N_0} \sum_{l=1}^{L_c} \tilde{\alpha}_l z_k(\tilde{\tau}_l, 1) \right\} \right] \quad (\text{III.27})$$

The problem with this term is that the maximization includes very intense calculations since it requires a digital search through a multi-dimensional space generated by $(\tilde{\alpha}, \tilde{\tau})$.

Moreover, as the surface $\Lambda(\tilde{\alpha}, \tilde{\tau})$ could get several incorrect maximums, the estimation will be difficult to achieve due to dramatic degradations of the signal at the receiver, where this can cause a heavy estimation. For this reason, some dispositions are needed to avoid such obstacles.

Firstly, we choose to maximize $\log[\Lambda(\tilde{\alpha}, \tilde{\tau})]$ rather than $\Lambda(\tilde{\alpha}, \tilde{\tau})$, then the relation (III.27) becomes

$$\log[\Lambda(\tilde{\alpha}, \tilde{\tau})] = \frac{-ME_b}{N_0} \sum_{l=1}^{L_c} \tilde{\alpha}_l^2 + \sum_{i=0}^M \log \left[\frac{1}{2} \exp \left\{ \frac{2}{N_0} \sum_{l=1}^{L_c} \tilde{\alpha}_l z_i(\tilde{\tau}_l, 0) \right\} + \frac{1}{2} \exp \left\{ \frac{2}{N_0} \sum_{l=1}^{L_c} \tilde{\alpha}_l z_i(\tilde{\tau}_l, 1) \right\} \right] \quad (\text{III.28})$$

The SNR is assumed to be low, and then this approximation may be made in (III.28)

$$\log \left[\frac{1}{2} \exp \{2x\} + \frac{1}{2} \exp \{2y\} \right] \approx x + y \quad |x|, |y| \ll 1 \quad (\text{III.29})$$

For that, the relation (III.29) can be written as

$$\log[\Lambda(\tilde{\alpha}, \tilde{\tau})] \approx 2 \sum_{l=1}^{L_c} \tilde{\alpha}_l \sum_{i=0}^{M-1} \frac{z_i(\tilde{\tau}_l, 0) + z_i(\tilde{\tau}_l, 1)}{2} - ME_b \sum_{l=1}^{L_c} \tilde{\alpha}_l^2 \quad (\text{III.30})$$

The latter relation is important and similar to the relation (III.14) of the DA estimation. In fact, the two relations are identical, provided that $z_i(\tilde{\tau}_l, a_i)$ in (III.14) is replaced by

$$\left[\frac{z_i(\tilde{\tau}_l, 0) + z_i(\tilde{\tau}_l, 1)}{2} \right].$$

It is necessary to note that the maximization method developed earlier in the sense of AD is still valid with the indicated minor modification. The purpose of the approximation is to allow moving from (III.28) to (III.30) in order to simplify the estimation algorithm [27].

III.5 TH-UWB system description

The study consists of analyzing each block constituting the UWB transmission link. The following figure briefly explains the various blocks of the transmission link.

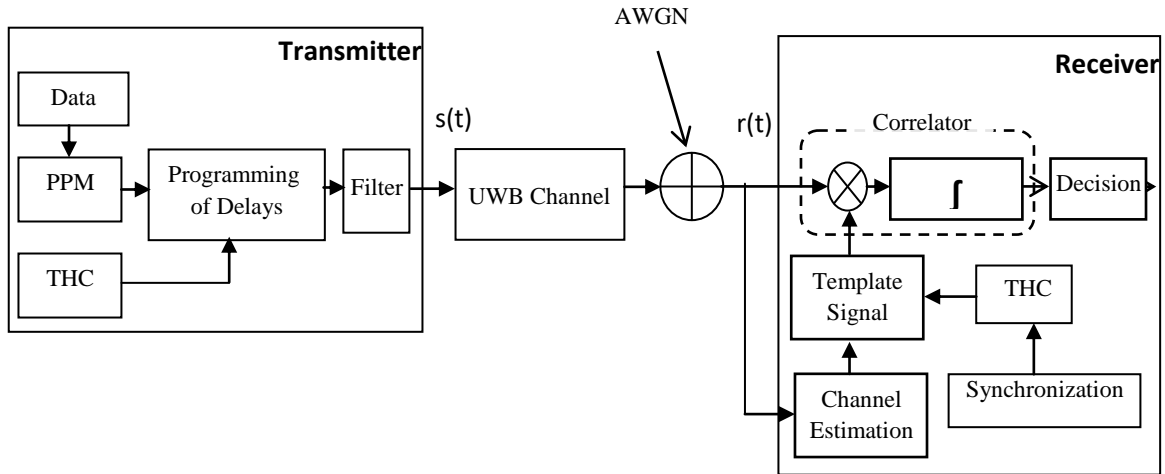


Fig. III.10 Block diagram of TH-UWB transmission link

For reasons of simplification, the side of the receiver shown above is given for a single finger. After generating the UWB signal according to the TH-UWB transmission system, a shaping filter is chained to designate the impulse shape; then the signal is passed through the UWB channel characterized by the multipath phenomenon; we get to the stage of correcting of signals by the rake receiver. As noted previously, the rake receiver uses a matched filter to estimate the UWB channel. The estimation is used for correlating the received signal with a predefined template signal; this according to the used modulation or the desired user. The template signal uses the same time hopping codes employed by the transmitter for detecting the temporal position of the impulses, and then integration is made over the duration of a symbol T_s . All previous steps should be applied on all fingers of the rake receiver. Also, the matter could be becoming more complex at the receiver in the case of a multiple access of multiple users. Finally, a threshold detector is set up to distinguish the received information.

III.6 Organization of the transmitted data

Some words are useful for the practical implementation of the system in the time domain. The known approach is to organize the data model as groups, Firstly a group comprising a preamble of M symbols for the UWB channel estimation is sent, followed by a guard interval, then $Q \times M$ information symbols as illustrated in the figure (III.11).

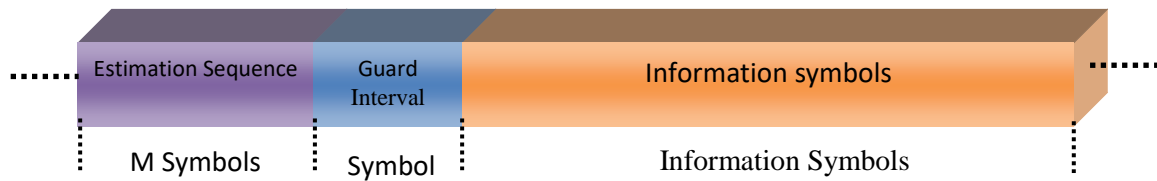


Fig. III.11 Organization of the transmitted data

The channel estimation through a pre-established sequence is used to detect useful information that follows it. The integer M must be large enough to ensure an accurate estimate. According to [28] showed that M must be in the order of a hundred or more.

III.7 Simulation results

In this part, all results have been done using Matlab simulations; in view of most famous works such as [28, 30, 31], it is necessary to note that two assumptions are taken into consideration during all simulations of this chapter:

- The arrival time of the first path is known
- Perfect synchronization between the transmitter and receiver

III.7.1 Simulation parameters

The TH-UWB signal is modulated with PPM modulation and built according to the following parameters:

- Data rate: $R_b=50\text{Mbps}$
- Number of frames in a symbol $N_f=2$
- Number of chips in a frame $N_c=10$, where $\tilde{c}_n(j)$ is the Time Hopping Code (THC) associated with the desired user in j^{th} frame and it is between $\{0, N_c-1\}$
- Signal energy E^n is normalized to "1"
- Impulse duration is $T_w=0.2\text{ns}$
- Modulation factor $\delta = 0.2\text{ns}$.
- Sampling rate 25 GHzs.
- The length of the estimation sequence $M=100$ bit and $Q=30$.

In the beginning, let us cast a glance at one realization generated by the model CM2 and its corresponding estimated one respectively as shown in the figures (III.13 .a) et (III.13 .b), where it is clear that most of the received paths are resolved for the estimation.

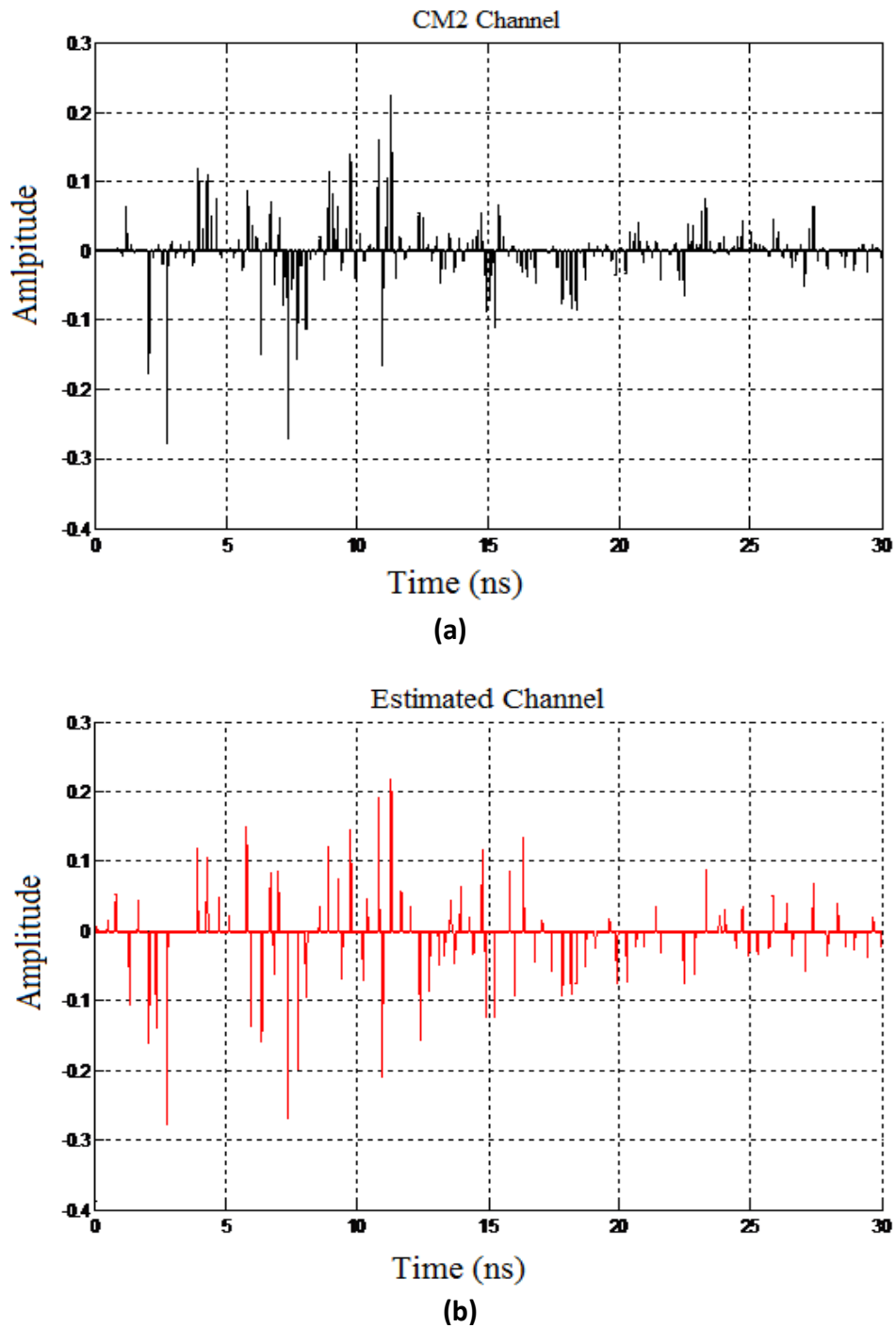


Fig III.12 Example for the model CM2

a) Generated realization, b) Its corresponding estimated one with SNR=20dB

III.7.2 Channel estimation error

After estimating the channel according to DA and NDA contexts, we represent the Mean Square Error (MSE) of the channel estimation versus the Signal to Noise Ratio (SNR). The results are carried out in terms of amplitudes and delays respectively as indicated by the two figures (III.12.a) and (III.12.b), where the SNR is shown here as E_b/N_o .

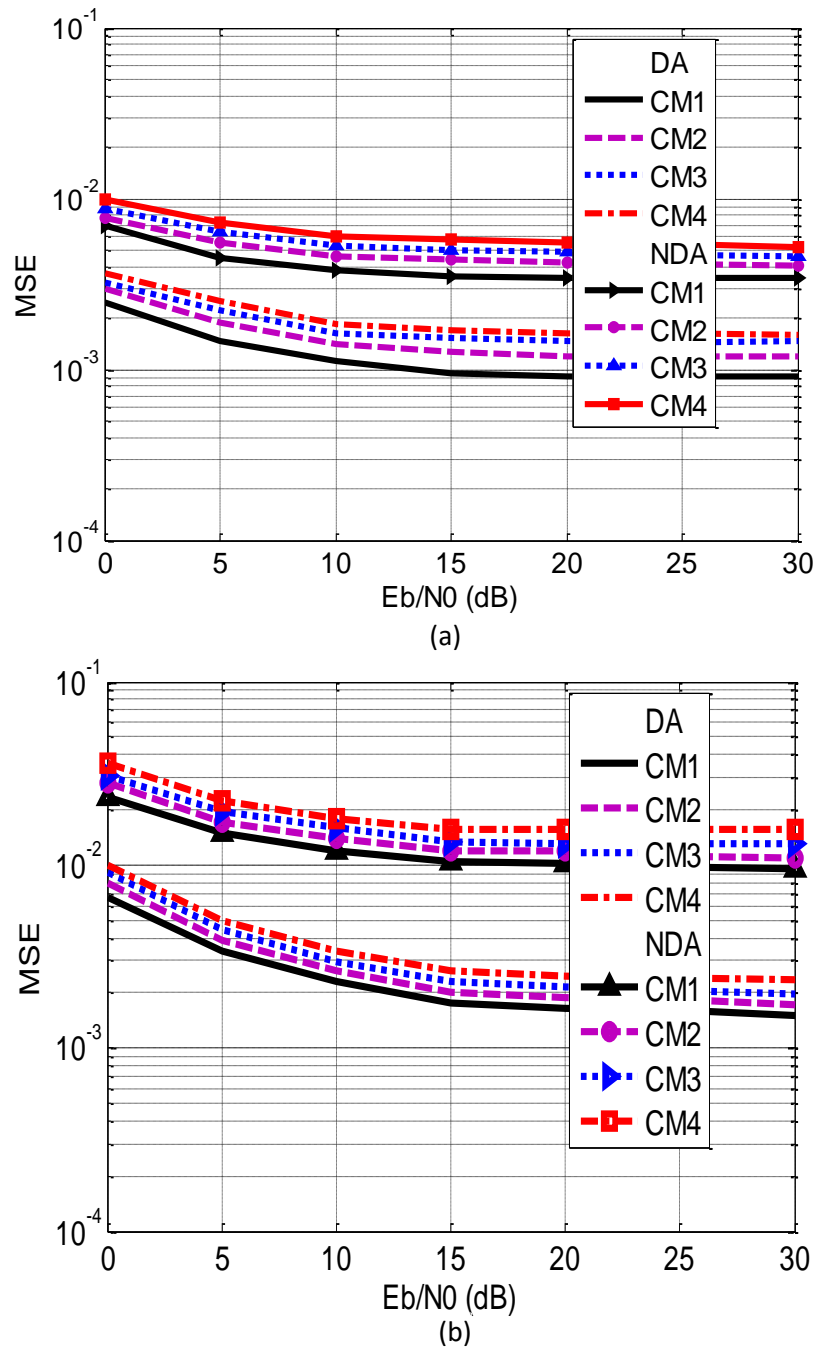


Fig. III.13 MSE versus SNR,
a) for amplitudes b) for delays

It is observed that the MSE of the channel estimation for the amplitudes is well estimated compared to delays due to the multipath effects, and a significant difference between the two estimation contexts is clearly observed. Thus, the DA estimation keeps always a better estimation compared to the NDA for the both estimations of amplitudes or delays. For the amplitudes, the difference between the two contexts regarding the MSE is around $2,5 \cdot 10^{-3}$ and for the delays is around $8 \cdot 10^{-3}$. It can be remarked also that from SNR = 15 dB the estimation almost remains constant.

To show the performances of the transmission link, some evaluations regarding the MSE and the bit error rate BER were plotted, where different evaluation parameters that might affect the channel estimation and the communication system are handled, these parameters are as follows

- The estimation context
- The transmission data rate
- The Influence of the multiple-access
- The estimation sequence length
- The modulation factor
- The paths number
- The receiver type

III.7.3 Influence of the estimation context

UWB communication based on PPM modulation is performed using two estimation contexts mentioned previously. The four models of the UWB channel are evaluated here in terms of BER versus SNR. The Fig III.14 shows the BER versus E_b/N_0 for different channel models based on DA and NDA estimation. The AWGN channel is embedded in parallel with UWB channel models to show the marginal differences between them. It is clear that by increasing the model order, the BER is affected brusquely.

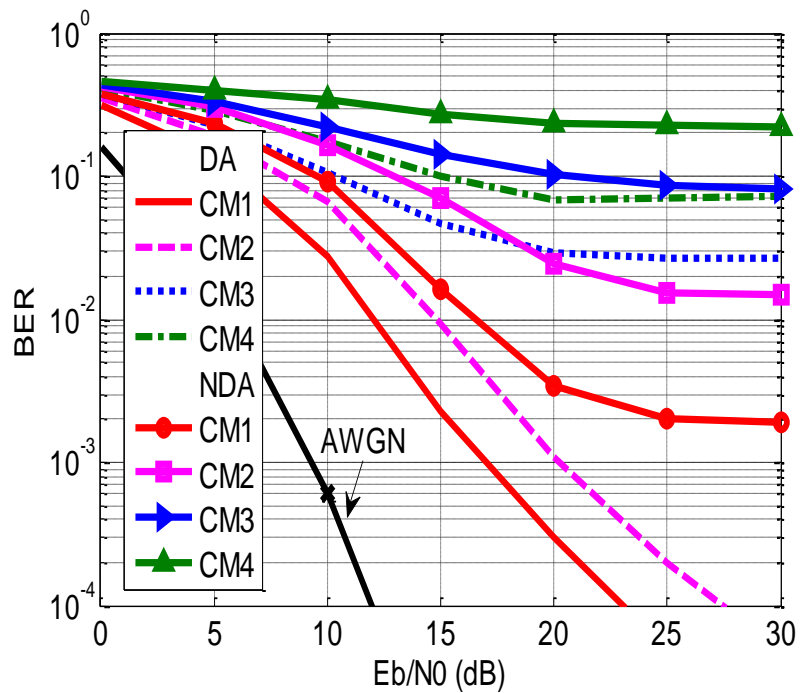
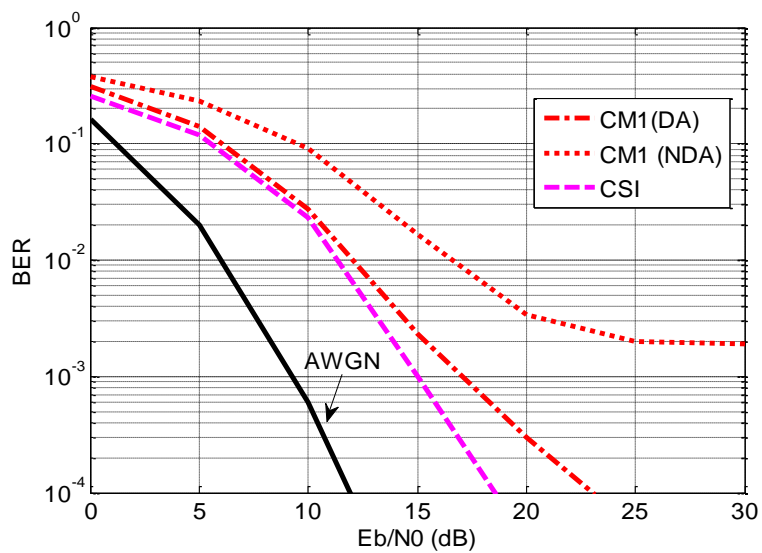
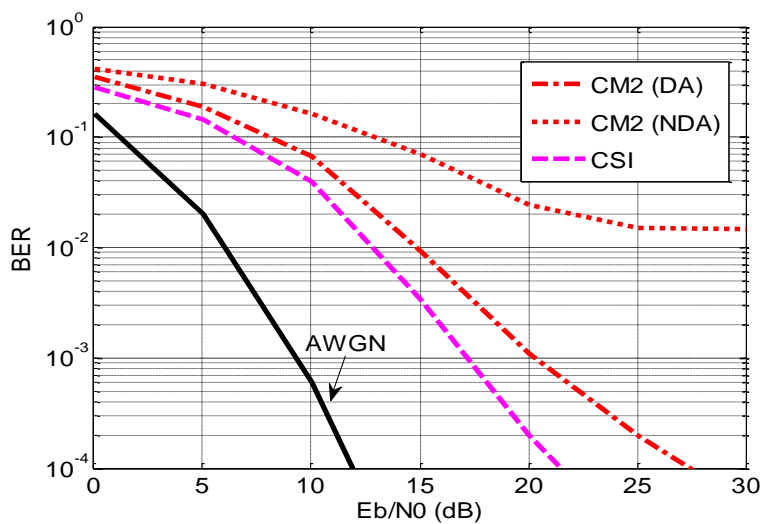


Fig III.14 BER performance for DA and NDA estimation

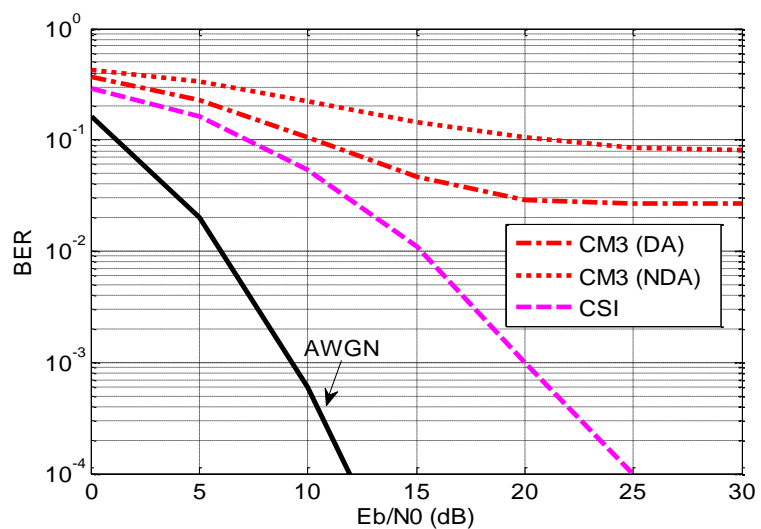
In the following figures, we evaluated the four channel models in terms of BER versus E_b/N_0 . However, in order to clarify the performance of each channel model separately, we plotted both the AWGN channel and the case of a perfect knowledge of the Channel State Information (CSI); this latter is assumed as available at the receiver as shown in Fig (III.15. a, b, c, d). An evaluation was also made by assuming an Additive White Gaussian Noise (AWGN) channel, where after the estimation and correction operation, a notable difference between the AWGN channel and the different models of IEEE 802.15.3a is observed. Obviously, the DA estimation is better than the NDA estimation; the models CM3 and CM4 didn't give a good result in comparison with the models CM1 and CM2, knowing that the number of paths taken into account is 40 paths.



(a)



(b)



(c)

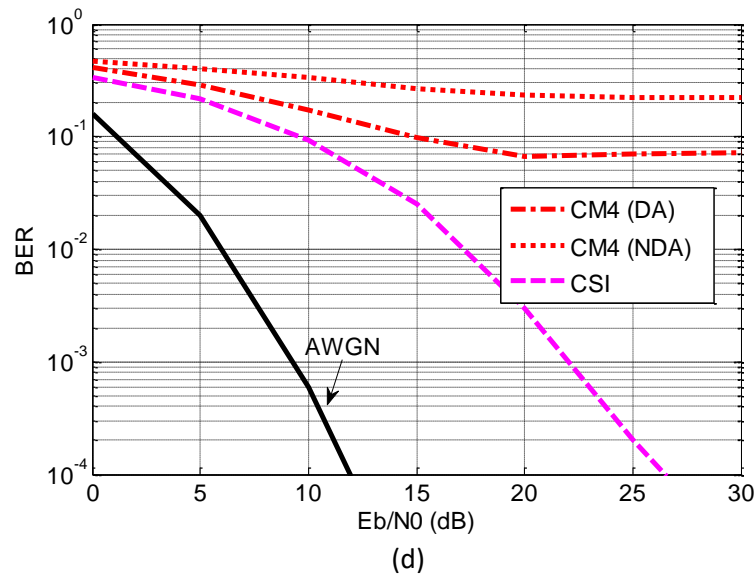
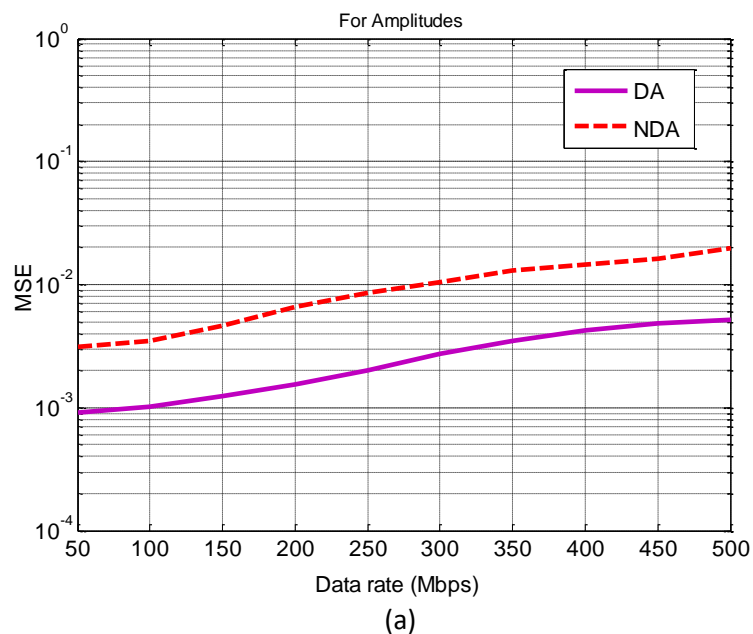
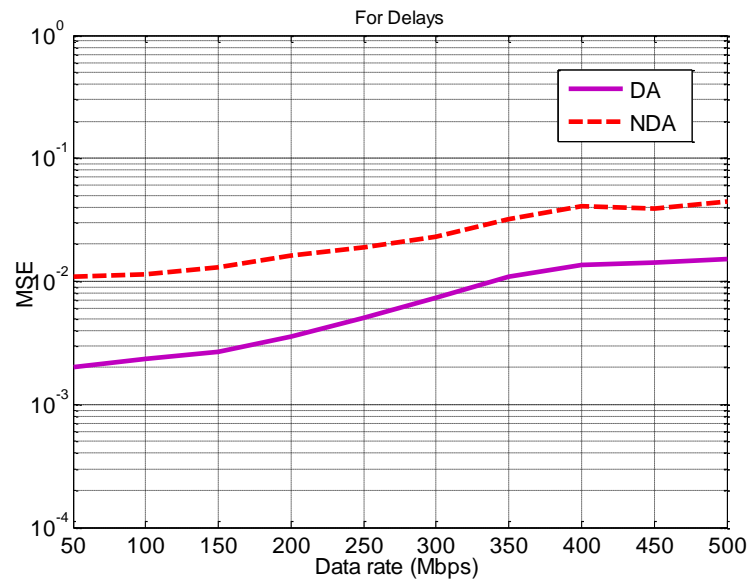


Fig. III.15 BER versus SNR for PPM modulation using DA and NDA estimation
 a) CM1, b) CM2, c) CM3, d) CM4

III.7.4 Influence of the data rate

The figures (III.16.a) and (III.16.b) show the mean squared error for the model CM1 versus data rate in terms of amplitudes and delays respectively. It is noted that the MSE increases with an almost constant change in both contexts.

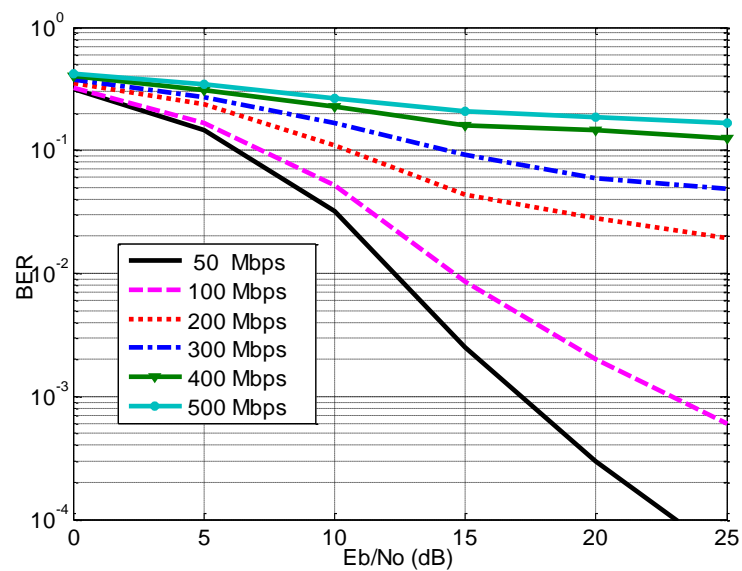




(b)

Fig. III.16 MSE of the channel estimation (for CM1 in this case) versus data rate; with SNR=20dB. a) for amplitudes b) for delays

After having estimated the CM1 model, we represent in the figure (III.17.a) the BER versus SNR for different data rates using context DA, with ranging from 50Mbps up to 500Mbps. We also represent in the figure (III.17.b) the BER versus data rate using the two estimation contexts; it is observed that the data rate has highly affected the BER.



(a)

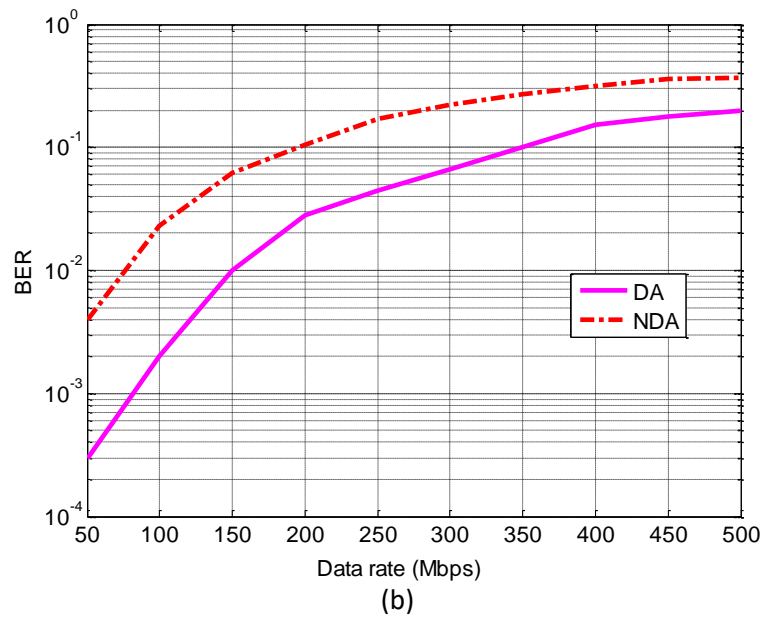
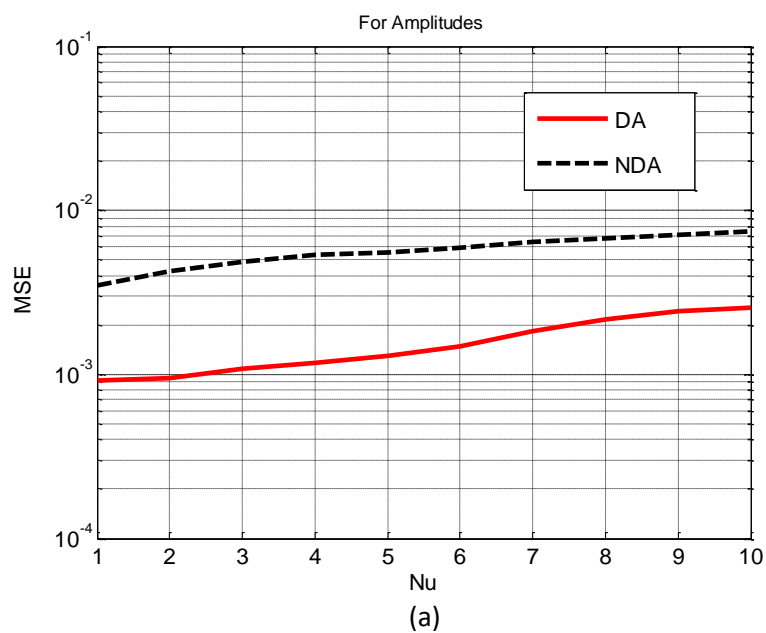


Fig. III. 17 BER evaluations for the model CM1
 a) versus SNR for different data rates,
 b) versus data rate, SNR = 20dB

III.7.5 Influence of the multiple-access

In this case, multiple users in the radio channel model CM1 are assumed, knowing that the number of users N_u is from 1 up to 10 users. Figures (III.18a) and (III.18b) represent the MSE of the channel estimation based on the number of users in terms of amplitude and delay respectively.



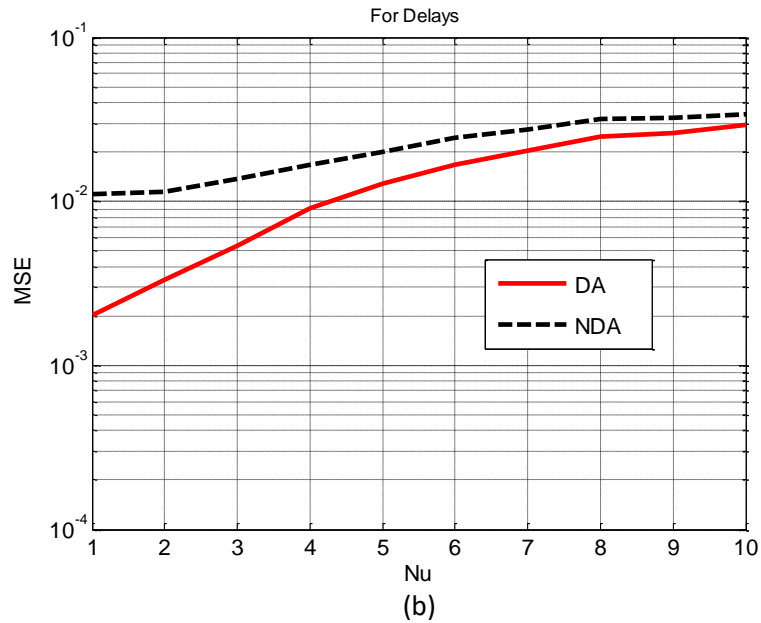
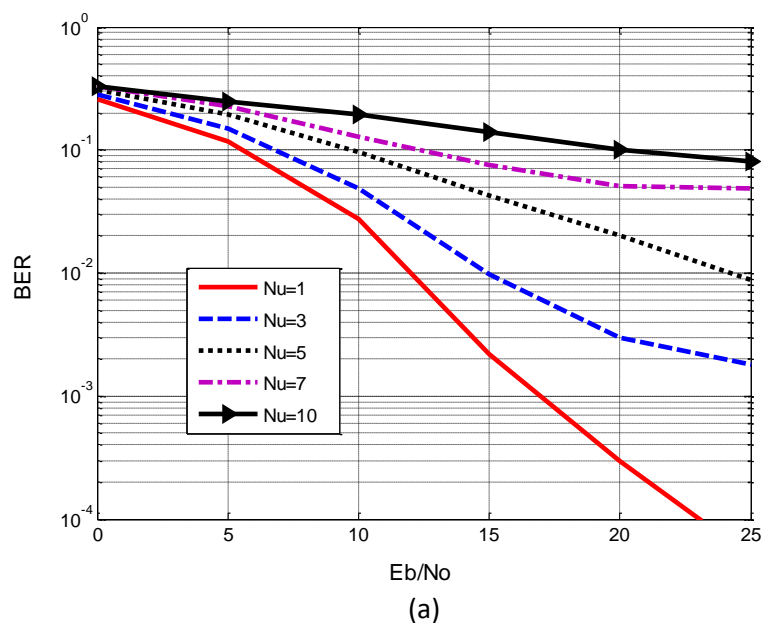


Fig. III.18 MSE of the estimated model CM1 based on the number of users, with SNR = 20dB. a) for amplitudes b) for delays

The figure III.19.a represents the BER evaluation versus SNR for various numbers of users using the DA context. The figure III.19.b represents the BER evaluation versus the number of users Nu using the DA and NDA contexts. It is noted that the BER has been strongly influenced by increasing the number of users in the UWB communication. At the receiver, the number of templates signals that should be used equals the number of existing users during transmission. Each template signal uses the same time hopping codes used at the transmitter, so each user has its correlator.



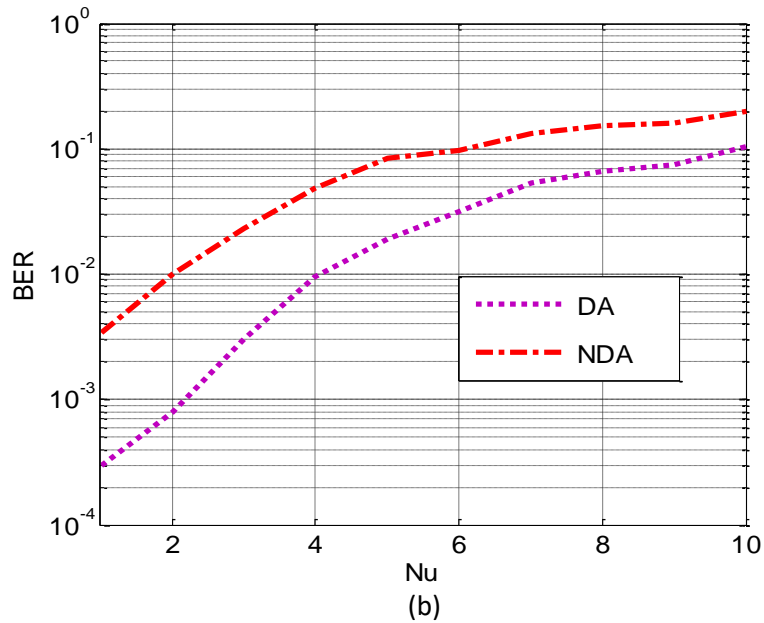


Fig. III. 19 BER evaluations for the model CM1
 a) versus SNR for various numbers of users
 b) versus the number of users Nu, SNR = 20dB

III.7.6 Influence of the estimation sequence length

The length of the estimation sequence is the number of transmitted bits before transmitting information, where this length has a great effect on the BER. It is well seen that from 100 bits we will not have much improvement in the BER; according to [28], they also proved that 100 Mbit is the minimum length needed to make a good estimation.

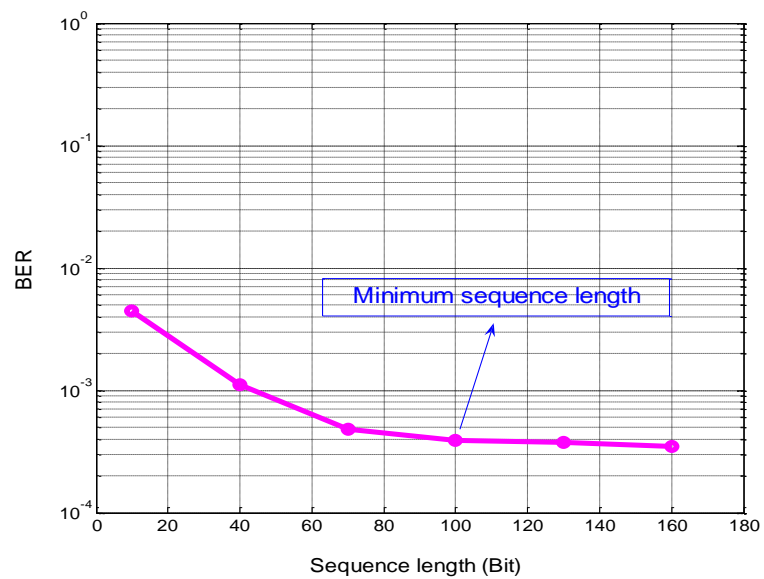


Fig. III.20 BER versus the estimation sequence length,
 SNR = 20dB, for CM1

III.7.7 Influence of the modulation factor

The following figure shows the BER evaluation versus modulation factor δ . It is clear that the factor δ does not affect much on the BER, except for the model CM1 where the BER increases progressively.

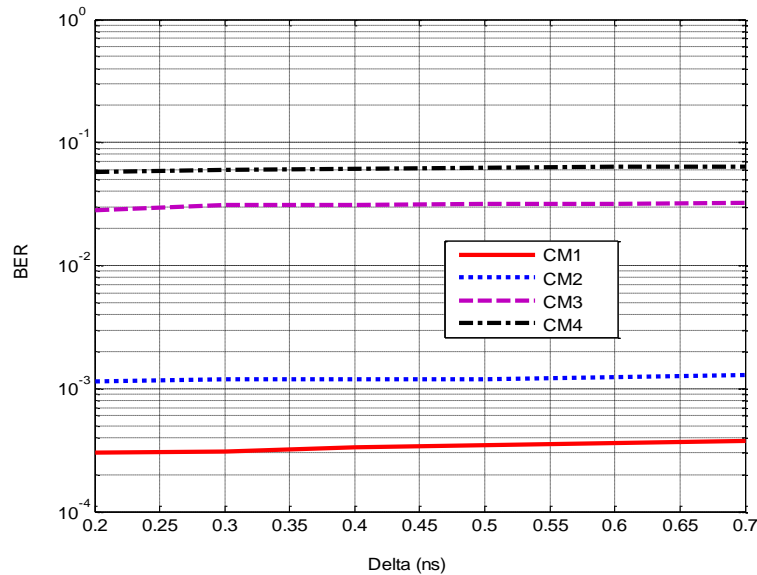


Fig. III.21 BER versus modulation factor δ , SNR = 20dB

III.7.8 Influence of the paths number

The number of paths taken into account plays a key role in the signal reception. The figure III.22.a represents the BER versus SNR for different numbers of paths, using the model CM1. The figure III.22.b represents the BER versus the number of paths for all channel models. It is noted that from 40 paths, there is no significant improvement in the BER.

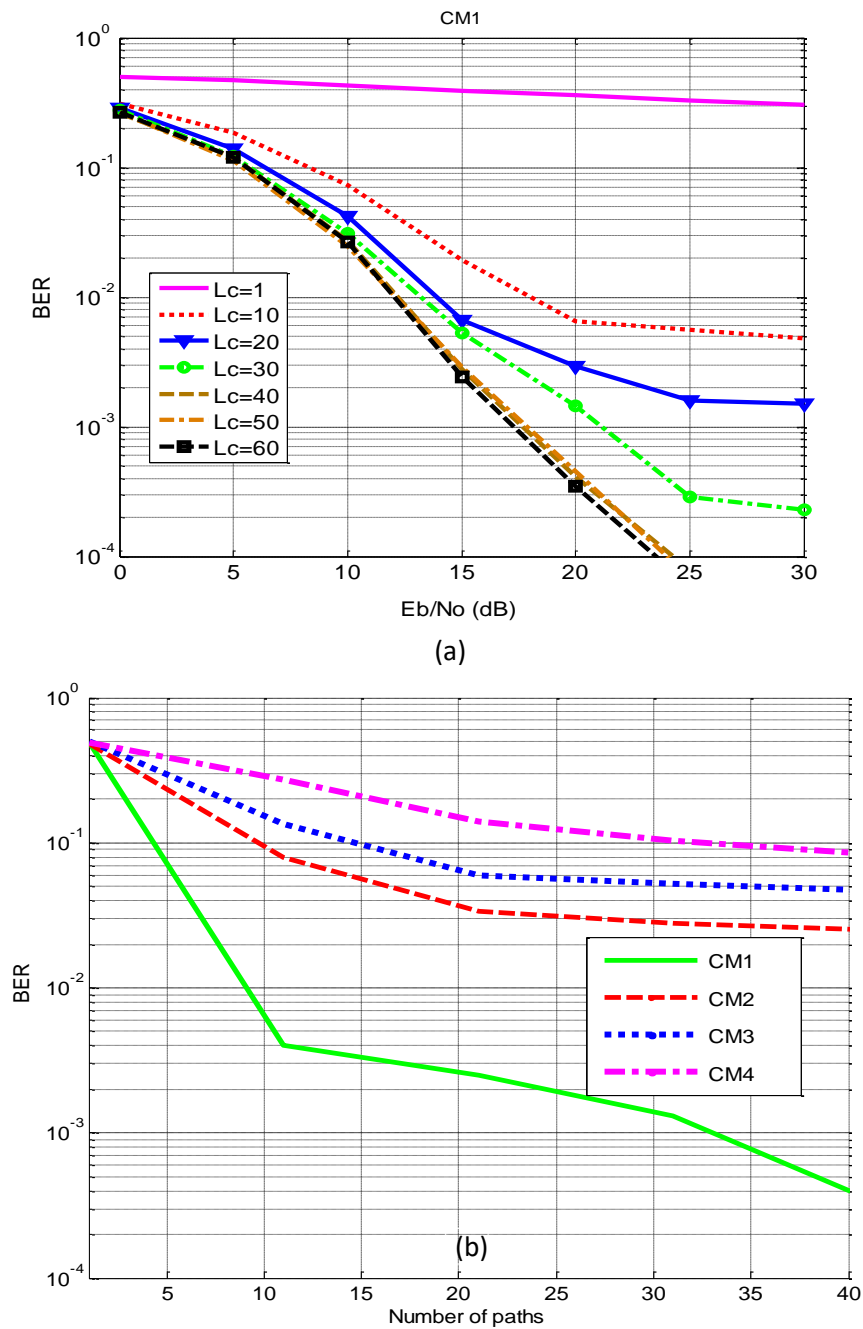


Fig III.22 Influence of the paths number on BER evaluations
 a) BER versus SNR for different numbers of paths
 b) BER versus number of paths, SNR = 20dB

III.7.9 Influence of the receiver type

The following figure shows the BER evaluation for all the following rake receivers: A-Rake, S-Rake and P-Rake. Knowing that the first type is used to pick up all paths arriving at the receiver; the S-Rake type picks up all paths having undergone an attenuation of 10

dB relative to the strongest path, the P-Rake type takes into account only the first paths, the number of paths considered in this case is $L_c=5$. It is shown that the BER performance assessed by the receiver A-Rake is better than other types, yet this receiver type does not exist practically.

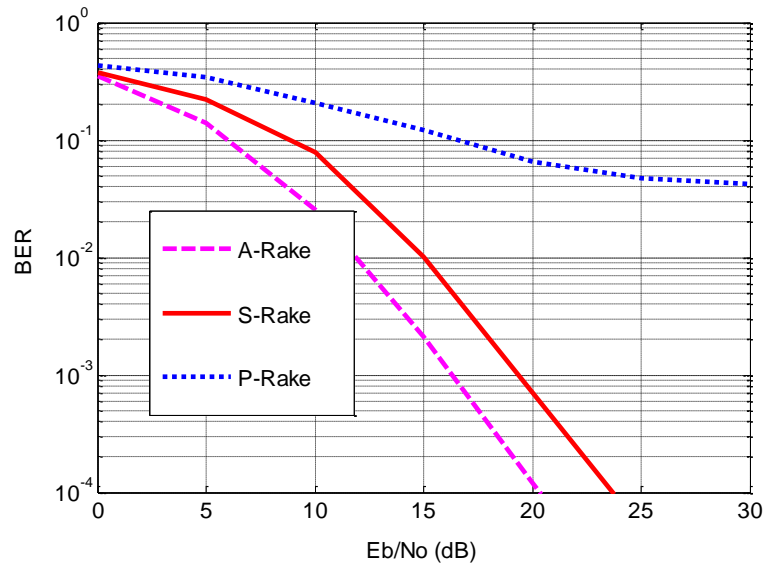


Fig. III.23 BER evaluation versus SNR for A-Rake, S-Rake, and P-Rake

III.8 Summary

In this chapter, we have seen the different sub-blocks associated with the rake receiver, where all UWB communication link based on Time Hopping Code (TH-UWB) has been established. Furthermore, we have seen as well that the received signal is a combination of different replicas of the transmitted signal that have undergone many deformations resulting mainly from the multipath effects as well as the various noises due from coexisting systems signals. Therefore, the need to estimate the UWB channel has become an absolute obligation to compensate the radio channel effects and to correct the incoming signals due to the multi-paths. For this purpose, we have estimated the attenuations and the delays of the multipath phenomenon that must be approximately known at the receiver in order to be used by the template signal, where two estimation contexts Data Aided and Non-Data Aided were considered through the maximum likelihood estimator.

Regarding the results, several parameters (the estimation context, the estimation sequence length, the paths number...and so on) acting on the channel estimation and influencing on the UWB communication link were evaluated. We note that that the effects of the estimation sequence length are usually ignored in the literature.

The results shows that by increasing the model order, the MSE of the UWB channel and the BER is affected brusquely. Also, the DA context seems to be better than the NDA context; the BER has been strongly influenced by increasing the number of users, and the data rate in the UWB communication; 100 Mbits is the minimum length of estimation sequence from which we get a good estimation; the modulation factor has no much effects on the BER; it is noted that from 40 paths taken through rake fingers, there was no significant improvement in the BER; as the rake receiver has three types according to the number and the way of dealing with the multipath, the A-Rake deemed to be better than the others theoretically, but the P-Rake is more practical as it is the most used in the literature.

Finally, it is worth to point out that the results of this chapter have led to two International Publications (please see IP 1-2) and seven International Communications (please see IC 1-7) and one National Communication (please see NC 1); to have a look please see Appendix C. Besides, there are some results that have not yet published like (Figs. III.20 and 21)

Chapter IV

A new strategy for the rapid acquisition of signals

Chapter IV

A new strategy for the rapid acquisition of signals

IV.1 Overview

As shown in the preceding chapter, among the challenges influencing on the UWB systems is the multipath channel as discussed in many other relevant research publications [18, 28, 36-46,]. There have been several techniques proposed to deal with the multipath phenomena in Impulse Radio (IR) domain. Despite the fact that they have different advantages, they are still insufficient for the multipath phenomena because most of them are based on one strategy which assumes a frozen transmission system, i.e., fixed modulation, fixed data rate, restricted receiver and so on. Their assumption remains as negative effect on the system performance when circumstances change. In order to deal with the multipath effects some authors have focused their research in the channel estimation [28, 36, 37, 46], and others were interested in the threshold estimation in detectors [38, 39], where the estimation step has proved its effectiveness as a fundamental process, but presenting some difficulties for a practical implementation. In [40], a diagonally loaded linear minimum mean square error (MMSE) equalization technique is proposed and is incorporated into minimum norm solution to recover the transmitted data sequences caused by the multipath time dispersion. Some works have focused on Time-Reversal (TR) technique based on the space and time at a particular receiver [41- 43], whereas other works have chosen different sides, in [44] a random correlation-based receiver is used to correlate received pilot symbols with the randomly generated base functions according to channel statistics. In [45] a UWB receiver is proposed based on optimally combining multiple MMSE detector outputs which are obtained by applying shifted observation windows, and each MMSE detector uses a smaller number of taps and can be trained separately to make the combined structure suitable for adaptive filter bank implementation.

We aim in this chapter to propose a flexible technique that could deal with the multipath phenomenon when the characteristics of the UWB channel is changing over the time through the movement of users or changes in the indoor environments. Therefore, this research starts from a new strategy that offers a different viewpoint from the other literature works, where it will make some modifications on various UWB communication system blocks, i.e., at the transmitter and the receiver to establish a flexible transmission technique. First, at the transmitter, M-ary PPM Time Hopping scheme is placed, where it is structured in a manner to make the desired user able to transmit data by different modulation levels during the transmission, thus will change the data rate when it is necessary to do that. Secondly at the receiver, a modified rake receiver (named multi-hands rake receiver) is proposed, where this latter is based on a proposed Intelligent Controlling System (ICS) that will play a fundamental role in our strategy.

IV.2 Suggested strategy description

The present strategy aims to establish a flexible transmission technique based on an intelligent controlling system (ICS), which can confront the UWB multipath channel. For that, the ICS ensures an automatic switching between different M-ary PPM modulation levels when the channel model changes during the transmission. For that reason, the philosophy of the scheme is to make the desired user able to transmit data during the transmission by different modulation levels, and this is another trump for our strategy, thus will give a strong capacity to the Medium Access Control (MAC) layer to process separately with multi-users that have different modulation levels.

The Figure (IV.1) shows the proposed global block diagram of the flexible UWB transmission technique for our new strategy, where to facilitate the view one finger is presented at the rake receiver.

Firstly, the UWB signal is generated according to the M-ary PPM Time Hopping scheme, where a shaping filter is chained to designate the impulse shape, and then the signal passes through the UWB multipath channel.

Secondly, at the reception, just like any other rake receiver, an additive white Gaussian noise (AWGN) is intercalated, and the UWB signals are affected by the multipath and accumulated by a constructive or destructive manner, thus causing different attenuations and distortions due to different delay shifts.

Furthermore, the incoming copies of signals will be estimated through the estimation channel block to get the channel parameters and will be multiplied by the generated template signals that have different delay times according to each finger, and then by limited integration, the correlation is set up to correlate the received and template signals. Moreover, the template signals use the same THC employed by the transmitter to detect the temporary position of the transmitted impulses for the desired user. Afterward, a combining operation is done by maximum ratio combining (MRC) to collect all energy resulted from selected paths as in [46]. After that, the received symbols can be distinguished through a threshold detector.

Finally, as a contribution made to the normal rake receiver to reach best performance in the midst of the challenges. Our new strategy proposes an intelligent controlling system to be placed at the receiver; the ICS is based on a Channel Model (CM) Classifier and an Automatic Switching. The CM Classifier classifies the current Channel Model type (from CM1~4) in order to switch the M-ary PPM levels via the Automatic Switching block. Therefore, the switching operation is placed at both of transmitter/receiver.

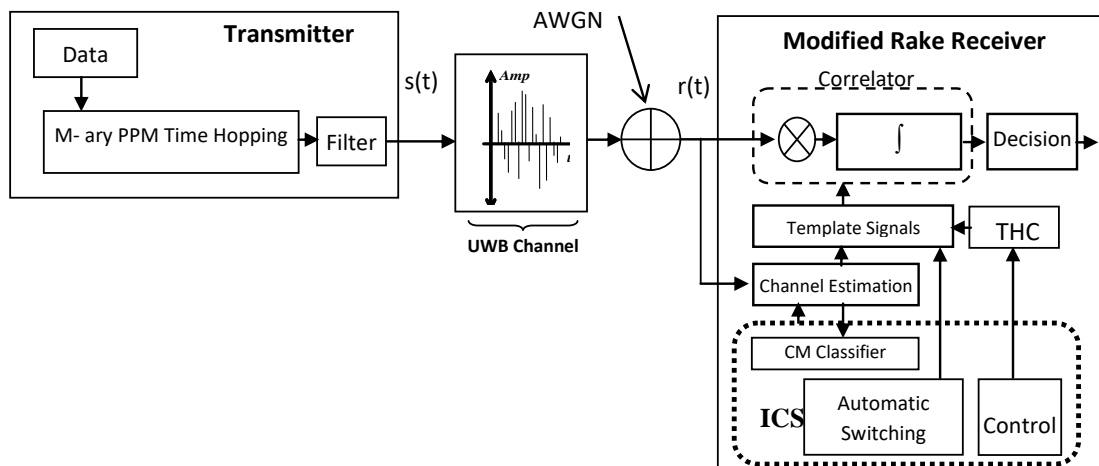


Fig.IV.1 Global block diagram for the flexible UWB transmission technique

IV.3 M-ary PPM time hopping scheme

The UWB signal for the n^{th} user according to the scheme is modulated with M-ary PPM Time Hopping that can be expressed basing on [26, 28] by

$$s^n(t) = \sum_{k=-\infty}^{+\infty} \sum_{j=0}^{N_f-1} \sqrt{E_w^n} w(t - kN_f T_f - jT_f - c_j^n(j)T_c - \delta \cdot (a_k^n)_{10}) \quad (\text{IV.1})$$

where E_w^n is the impulse energy from user n , $w(t)$ is the impulse shape whose energy is normalized to one, Each symbol duration T_s is divided into equally-spaced N_f frames with duration T_f , i.e., $T_s = N_f T_f = 1/R_s$, where R_s is the binary symbol rate. The sequence c_j^n is the Time Hopping Code (THC) associated with the desired user in j^{th} frame and it is between $\{0, N_c - 1\}$; N_c is a number of chips in one frame; the parameter T_c is the duration of the chip, $(a_k^n)_{10}$ is the k^{th} transmitted binary symbol for the desired user n , taken in decimal representation ($0 \leq (a_k^n)_{10} \leq M-1$). An evenly spaced M-PPM scheme is considered, where δ is the time shift difference that represents the modulation factor for M-ary.

We have taken the monocycle shape as the first derivative of a Gaussian impulse. The basic Gaussian waveform is given by [48]

$$w_0(t) = \varepsilon \exp \left[-2\pi \left(\frac{t}{t_p} \right)^2 \right] \quad (\text{IV.2})$$

where t_p is the effective half width of the impulse $w_0(t)$, and ε is introduced to normalize the energy of the impulses.

The q -order monocycle is

$$w_q(t) = \varepsilon_q \frac{d^q}{dt^q} \left[\exp \left(-2\pi \left(\frac{t}{t_p} \right)^2 \right) \right] \quad (\text{IV.3})$$

The autocorrelation function for any q is

$$R_q(\Delta) \triangleq \int_{-\infty}^{+\infty} w_q(t) w_q(t - \Delta) dt = (-1)^q \frac{d^{(2q)}(R_0(\Delta))}{d\Delta^{(2q)}} \quad (\text{IV.4})$$

Thus,

$$R_0(\Delta) = \varepsilon_0^2 \frac{t_p}{2} \exp\left(-\pi \left(\frac{\Delta}{t_p}\right)^2\right)$$

From (IV.2) the Gaussian monocycle $w_I(t)$ in time domain can be defined as

$$w_i(t) = \varepsilon_1 \frac{-4\pi t}{t_p^2} \exp\left[-2\pi \left(\frac{t}{t_p}\right)^2\right] \tag{IV.5}$$

We can derive that the autocorrelation function of the Gaussian monocycle is

$$R_1(\Delta) = \varepsilon_1^2 \frac{\pi}{t_p} \left(1 - 2\pi \left(\frac{\Delta}{t_p}\right)^2\right) \exp\left(-\pi \left(\frac{\Delta}{t_p}\right)^2\right) \tag{IV.6}$$

To normalise the energy of impulse we choose $\varepsilon_1 = \sqrt{t_p / \pi}$.

The figure (IV.2) shows the structure of the M-ary PPM Time Hopping scheme for ($M = 2, 4$) as an example, the transmitted throughput is $\log_2 M_g$, where g is the modulation level, $M_g = 2^{g+1}$ and $g=0, \dots, G$.

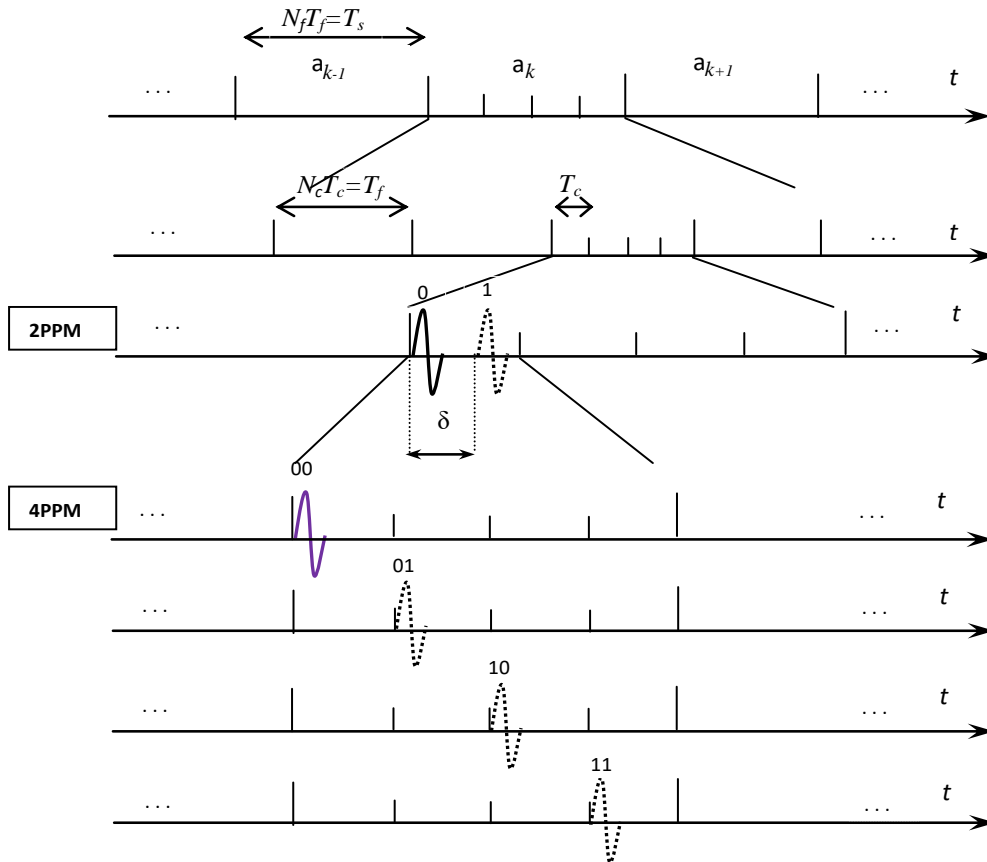


Fig IV.2 Structure of M-ary PPM Time Hopping Scheme

To find out the maximum level G of M-ary PPM modulation that can be involved in the scheme, the following relation must be verified

$$(2)^{G+1} 2t_p \leq T_c \Rightarrow G = \log_2 \left(\frac{T_c}{2t_p} \right) - 1 \quad (\text{IV.7})$$

where $2t_p$ is the time duration of the Gaussian monocycle impulse, and while $T_c = T_f / N_c$

That implies

$$G \leq \log_2 \left(\frac{\rho}{N_c} \right) - 1 \quad (\text{IV.8})$$

where the spreading ratio is expressed as $\rho = T_f / 2t_p$.

IV.4 Proposed multi-hands Rake Receiver

Basing on the new strategy, a modified rake receiver is proposed as depicted in Fig IV 3, where it is named “multi-hands rake receiver”. This name is inspired from the normal rake receiver, where by considering one hand has different fingers allocated for L_c paths; the manner of receiving the signals in our case can be viewed as a rake receiver backed up by a number of hands depending to the number of time slots i pre-assigned for symbols a_k . Furthermore, these hands work simultaneously in parallel making the acquisition of symbols as rapid as possible and getting an UWB system with low latency, where each hand has a template signal $m_i(t)$ allocated for the M-ary PPM modulation level.

Initially, after finishing the channel estimation step and when the communication between the transmitter and the receiver is going to start, the CM classifier seeks the closest model to the real estimated channel (from CM1~ CM4). Thus, when the model is selected, the ICS adapts the suitable modulation level on both of the transmitter/receiver; thereby the Automatic Switcher changes the modulation to the selected level. Accordingly, the ICS will undertake another task, which is the control to keep better performances. Therefore, the controller keeps checking two performance aspects consecutively:

- The first one is to check the conditions in which the system declares an outage. The outage probability P_{out} is the probability that the mean SNR x down-cross the minimum threshold SNR x_0^* corresponding to the maximum allowable probability of bit error P_0^* allocated for the lowest modulation level $g=0$, when the system falls in such case, it would declare an outage and start re-estimating the channel to allocate the adequate modulation level, when x is not sufficient to guarantee the probability of bit error required for the lowest modulation, no bits are transmitted and the communication is in outage until other conditions. In the other hand, if x exceeds or falls below the SNR threshold x_g^* designed for the modulation level g , the throughput may be increased or decreased by increasing or decreasing the modulation level.
- The second aspect is to check the combining performance over each hand through comparing the energy Z_a of time slot a (whose symbol currently received is a_{k-1}) corresponding to the active hand with the energies Z_i of time slots i carried by the other hands, if one of these hands during the transmission gets a higher energy than the active hand, the corresponding symbol a_k of the new time slot would be considered as received.

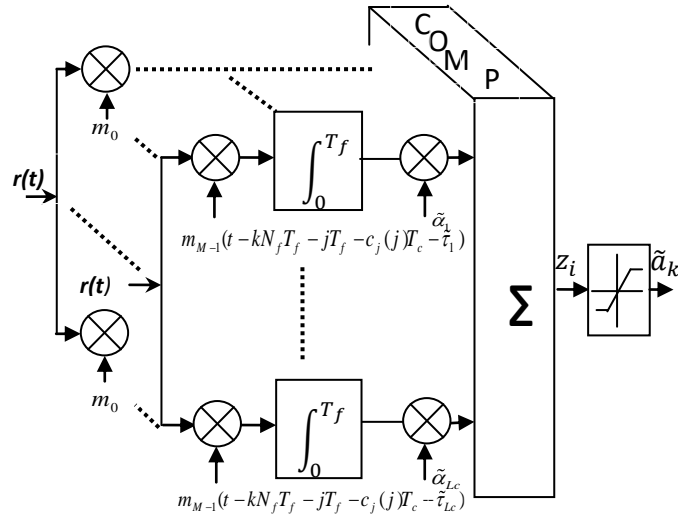


Fig V.3 The proposed multi-hands Rake receiver

In addition, to make the CM classifier able to select channel models from predefined classes, it would be better to subdivide the UWB channel into different models. In this regard, we exploit the existing channel models based on the modified Saleh-Valenzuela model [21] that has been modified and adopted by the IEEE 802.15.3a [19]; taking into account, the clustering phenomena observed in several UWB channel measurements [18]. Therefore, four different channel models are defined namely CM1, CM2, CM3, and CM4, where

CM1: Line-of-Sight (LOS) model for 0-4 m

CM2: Non-LOS (NLOS) model for 0-4 m

CM3: NLOS for 4-10 m

CM4: NLOS for 4-10 m, with an extreme multipath fading channel.

By ignoring the shadowing effect, the channel can be represented as

$$h(t) = \sum_{l=1}^L \alpha_l (t - \tau_l) + n(t) \quad (\text{IV.9})$$

The received signal specified for all users may be written as

$$r^n(t) = \sum_{n=1}^{N_u} \sum_{l=1}^{L_c} \alpha_l^n s^n(t - \tau_l^n) + n(t) \quad (\text{IV.10})$$

L_c characterizes the number of the receiver fingers, which is less than the independent fading paths $L_c < L$.

The parameter α_l^n is the channel attenuation, which follows log-normal distribution [18] and τ_l^n is the relative time delay of the l^{th} path of the received signal associated with user n , and $n(t)$ is zero-mean AWGN with power spectral density $N_0/2$.

The receiver is considered perfectly synchronized to the desired user, so the signal at the receiver can be given by

$$r(t) = \sqrt{E_w} \sum_{k=-\infty}^{+\infty} \sum_{j=0}^{N_f-1} \sum_{l=1}^{L_c} \alpha_l w(t - kN_f T_f - jT_f - c_j(j)T_c - \delta a_k - \tau_l) + n(t) \quad (IV.11)$$

The parameters α_l and τ_l are unknown a priori and must be estimated by a simple and quick method as in [28], where the authors have proposed UWB channel estimation, based on the maximum-likelihood criterion.

Basing on our philosophy, the template signals have this formula

$$m_i(t) = w(t - \delta \cdot i) \quad (i = 0, 1, \dots, M-1) \quad (IV.12)$$

The template signal $m_i(t)$ depends not only on the user's time hopping code but also on $w(t)$. For purposes of analysis, the shape of the monocycle is assumed known.

The decision statistic z_i is the MRC of the correlators outputs specific to the i^{th} slot energy, which is given by the following expression [47]:

$$Z_i = \sum_{l=1}^{L_c} \tilde{\alpha}_l \int_{jT_f}^{(j+1)T_f} r(t) m_i(t - iNT_f - jT_f - c_j(j)T_c - \tilde{\tau}_l) dt \quad (IV.13)$$

The received signal is integrated over a period corresponding to one frame duration. The weighted sum of the correlators is then applied to a detector, which determines the transmitted symbol \tilde{a}_k for the desired user according to PPM modulation level.

IV.5 Performance analysis

To carry out the performance analysis of the new system through a mathematical model, we assume that we have only one desired user. Furthermore, it is interesting to note that only the effects of Inter-Symbol/Frame Interference (*ISFI*) and the AWGN are considered here, and the Multiple Access Interference (*MAI*) effects caused by other users are omitted.

While the UWB channel can be considered as a linear system thus according to the superposition principle, instead of studying the channel effect for a composite signal with several symbols, we are interested in studying the channel effect for one symbol sent by the transmitter. Besides, by applying the same principle for the frames in one symbol, $s(t)$ can be expressed for one frame as

$$s(t) = \sqrt{E_w} w(t - cT_c - \delta \cdot a) \quad (IV.14)$$

where c represents the time code specific to the concerned frame, a is the transmitted binary symbol represented in decimal number.

$$r(t) = \sqrt{E_w} \sum_{l=1}^{Lc} \alpha_l w(t - cT_c - \delta \cdot a - \tau_l) + n(t) \quad (IV.15)$$

$$Z_i = \sum_{l=1}^{Lc} \tilde{\alpha}_l \int_0^{T_f} r(t) m_i(t - cT_c - \tilde{\tau}_l) dt \quad (IV.16)$$

From (IV.12) and (IV.15) we can write

$$\begin{aligned} Z_i = & \sqrt{E_w} \sum_{l=1}^{Lc} \sum_{i=1}^{Lc} \tilde{\alpha}_l \alpha_i \int_0^{T_f} w(t - cT_c - \delta \cdot a - \tau_l) \cdot w(t - cT_c - \delta \cdot i - \tilde{\tau}_l) dt \\ & + \int_0^{T_f} n(t) \left(\sum_{l=1}^{Lc} \tilde{\alpha}_l \cdot w(t - cT_c - \delta \cdot i - \tilde{\tau}_l) \right) dt \end{aligned} \quad (IV.17)$$

$$Z_i = \sqrt{E_w} \sum_{l=1}^{Lc} \sum_{i=1}^{Lc} \tilde{\alpha}_l \alpha_i R_w(\Delta) + N \quad (IV.18)$$

$R_w(\Delta)$ is the correlation function of the Gaussian monocycle $w(t)$, and is given by

$$R_w(\Delta) = \int_0^{T_f} w(t) w(t - \Delta) dt \quad (IV.19)$$

$$\Delta = \delta \cdot (i - a) + (\tilde{\tau}_l - \tau_l) \quad (IV.20.a)$$

Δ is the time difference between the different paths and the different time slots from the a^{th} time slot. Also, It is assumed that Δ is a uniformly distributed RV over the duration T_f .

For the remainder of the study, for analytical convenience and as an attempt to reach simplified, more controllable formulas, the received attenuations α will be considered equal to the estimated attenuations $\tilde{\alpha}$, and in the same time, the estimated delays $\tilde{\tau}$ will be

considered equal to the received delays τ .

Under these assumptions (20a) becomes

$$\Delta = \delta \cdot (i - a) + (\tau_i - \tau_l) \quad (IV.20.b)$$

To get the binary symbol a , Z_i must be maximized by

$$\Delta = 0 \Leftrightarrow (i = a \wedge l = l') \quad (IV.21)$$

Under these assumptions, Z_i can be written as

$$Z_i = \left(\sqrt{E_w} \sum_{l=1}^{Lc} \tilde{\alpha}_l^2 \right) \cdot \delta_{i-a} + ISFI + N \quad (IV.22)$$

where δ_{i-a} is Kronecker delta

$$\delta_{i-a} = \begin{cases} 0, & \text{if } i \neq a \\ 1, & \text{if } i = a \end{cases}$$

For this reason, Z_i is given by

$$Z_i = A \cdot \delta_{i-a} + ISFI + N \quad (IV.23)$$

where A is the desired signal component obtained when $\Delta=0$, and is expressed as

$$A = \sqrt{E_w} \sum_{l=1}^{Lc} \tilde{\alpha}_l^2 \quad (IV.24)$$

$ISFI$ is the self-interference due to the multipath channel

$$ISFI = \sqrt{E_w} \sum_{l'=1}^{Lc} \sum_{l=1}^{Lc} \tilde{\alpha}_{l'} \tilde{\alpha}_l R_w(\Delta) \Big|_{\Delta \neq 0} \quad (IV.25)$$

N is AWGN component at the output receiver and is expressed as

$$N = \int_0^{T_r} n(t) \left(\sum_{l=1}^{Lc} \tilde{\alpha}_l \cdot w(t - cT_c - \delta \cdot i - \tilde{\tau}_l) \right) dt \quad (IV.26)$$

From (6), the normalized autocorrelation function is

$$R_w(\Delta) = \left(1 - 2\pi \left(\frac{\Delta}{t_p}\right)^2\right) \exp\left(-\pi \left(\frac{\Delta}{t_p}\right)^2\right) \quad (\text{IV.27})$$

$R_w(\Delta)$ in particular cases can be expressed as

$$R_w(\Delta) = \begin{cases} 1, & \Delta=0 \\ 0, & |\Delta| \geq T_f \end{cases} \quad (\text{IV.28})$$

The mean of $R_w(\Delta)$ is given by

$$E[R_w(\Delta)] = \int_{-2t_p}^{2t_p} R_w(\Delta) \frac{1}{2T_f} d\Delta \quad (\text{IV.29})$$

The 2nd moment of $R_w(\Delta)$ is given by

$$E[R_w^2(\Delta)] = 2 \int_0^{2t_p} R_w^2(\Delta) \frac{1}{2T_f} d\Delta \quad (\text{IV.30})$$

After some calculus we obtain

$$E[R_w(\Delta)] = \frac{3.4873 \cdot 10^{-6}}{\rho}$$

$$E[R_w^2(\Delta\tau)] = \frac{0.0442}{\rho}$$

where, $\rho = T_f / (2t_p)$

Without loss of generality, and for simplicity we assume that the signals are transmitted in the a^{th} time slot, the decision variables Z_i can be subdivided into two main subsets

$$Z_i = \begin{cases} Z_a: A + ISFI + N, & i=a \\ Z_a^-: ISFI + N, & i=0, \dots, M-1, i \neq a \end{cases} \quad (\text{IV.31})$$

where Z_a represents the desired energy quantity in which the signal is transmitted in the a^{th} time slot, Z_a^- represents the undesired energy quantity.

However, the fact that the UWB multipath channel has a large number of paths, and for analytical reasons, we assume that the *ISFI* follows a Gaussian distribution by calling the

central limit theorem. Hence, the decision variables is as follows

$$\begin{aligned} Z_a &\sim \text{Normal} \left(A + E[ISFI] + E[N], \sigma_{ISFI}^2 + \text{Var}(N) \right) \\ Z_{-a} &\sim \text{Normal} \left(E[ISFI] + E[N], \sigma_{ISFI}^2 + \text{Var}(N) \right) \end{aligned} \quad (\text{IV.32})$$

The $E[N]$ and $\text{Var}(N)$ are 0 and $N_0/2$ respectively.

The (25) can be written as

$$ISFI = \left(\sqrt{E_w} \sum_{l'=1}^{Lc} \sum_{l=1}^{Lc} \tilde{\alpha}_{l'} \tilde{\alpha}_l R_w(\Delta) - A \cdot \delta_{i-a} \right) \quad (\text{IV.33})$$

$$E[ISFI] = \sqrt{E_w} \frac{3.4873 \cdot 10^{-6}}{\rho} \sum_{l'=1}^{Lc} \sum_{l=1}^{Lc} \tilde{\alpha}_{l'} \tilde{\alpha}_l - A \cdot \delta_{i-a} \quad (\text{IV.34})$$

To find out σ_{ISFI}^2 we write $ISFI^2$ as follows

$$\begin{aligned} ISFI^2 &= E_w \cdot \sum_{l'=1}^{Lc} \sum_{l''=1}^{Lc} \sum_{l'=1}^{Lc} \sum_{l=1}^{Lc} \tilde{\alpha}_{l''} \tilde{\alpha}_{l'} \tilde{\alpha}_l \tilde{\alpha}_l R_w(\Delta') \cdot R_w(\Delta) \\ &\quad - 2\sqrt{E_w} A \sum_{l'=1}^{Lc} \sum_{l=1}^{Lc} \tilde{\alpha}_{l'} \tilde{\alpha}_l R_w(\Delta) \cdot \delta_{i-a} \\ &\quad + A^2 \cdot \delta_{i-a} \end{aligned} \quad (\text{IV.35})$$

where, $\Delta = \delta \cdot (i - a) + (\tau_{l'} - \tau_l)$, and $\Delta' = \delta \cdot (i - a) + (\tau_{l''} - \tau_l)$

It is known that $\sigma_{ISFI}^2 = E[ISFI^2] - E[ISFI]^2$ so

$$\begin{aligned} \sigma_{ISFI}^2 &= E_w \cdot \left(\sum_{l''=1}^{Lc} \sum_{l'=1}^{Lc} \sum_{l'=1}^{Lc} \sum_{l=1}^{Lc} \tilde{\alpha}_{l''} \tilde{\alpha}_{l'} \tilde{\alpha}_l \tilde{\alpha}_l \cdot E[R_w(\Delta') \cdot R_w(\Delta)] \right. \\ &\quad \left. - \sum_{l''=1}^{Lc} \sum_{l'=1}^{Lc} \sum_{l'=1}^{Lc} \sum_{l=1}^{Lc} \tilde{\alpha}_{l''} \tilde{\alpha}_{l'} \tilde{\alpha}_l \tilde{\alpha}_l \cdot E[R_w(\Delta)]^2 \right) \end{aligned} \quad (\text{IV.36})$$

Knowing that $E[R_w(\Delta') \cdot R_w(\Delta)] = E[R_w(\Delta)]^2$ if $\Delta \neq \Delta'$, we obtain

$$\begin{aligned}
 \sigma_{ISFI}^2 = E_w \cdot & \left(\frac{12.1613 \cdot 10^{-12}}{\rho^2} \sum_{l^*=1}^{L_c} \sum_{l'=1}^{L_c} \sum_{l=1}^{L_c} \sum_{l=1}^{L_c} \tilde{\alpha}_{l^*} \tilde{\alpha}_{l'} \tilde{\alpha}_l \tilde{\alpha}_l \right)_{\Delta \neq \Delta'} \\
 & + \frac{0.0442}{\rho} \sum_{l^*=1}^{L_c} \sum_{l'=1}^{L_c} \sum_{l=1}^{L_c} \sum_{l=1}^{L_c} \tilde{\alpha}_{l^*} \tilde{\alpha}_{l'} \tilde{\alpha}_l \tilde{\alpha}_l \Big|_{\Delta = \Delta'} \\
 & - \frac{12.1613 \cdot 10^{-12}}{\rho^2} \sum_{l^*=1}^{L_c} \sum_{l'=1}^{L_c} \sum_{l=1}^{L_c} \sum_{l=1}^{L_c} \tilde{\alpha}_{l^*} \tilde{\alpha}_{l'} \tilde{\alpha}_l \tilde{\alpha}_l \Big)
 \end{aligned} \tag{IV.37}$$

The probability density function (pdf) of the desired energy part can be written as

$$P(Z_a) = \frac{1}{\sqrt{2\pi}\sigma} e^{-\frac{(Z_a - \mu_a)^2}{2\sigma^2}} \tag{IV.38}$$

where, $\mu_a = A + E[ISFI]$ and $\sigma = \sqrt{\sigma_{ISFI}^2 + \frac{N_0}{2}}$

The pdf of the undesired energy part can be written as

$$P(Z_a) = \frac{1}{\sqrt{2\pi}\sigma} e^{-\frac{(Z_a - \mu_a)^2}{2\sigma^2}} \tag{IV.39}$$

where, $\mu_a = E[ISFI]$

The conditional probability of correct decision is

$$\begin{aligned}
 P_c = \text{prob}(Z_a > Z_1, \dots, Z_a > Z_i, \\
 \dots, Z_a > Z_M | Z_a, \quad i \neq a)
 \end{aligned} \tag{IV.40}$$

hence,

$$P_c = \int_{-\infty}^{\infty} [\text{prob}(Z_a > Z_i) | Z_a, \quad i \neq a]^{M-1} p(Z_a) dZ_a \tag{IV.41}$$

By substituting (38) and (39) into (41), and after some calculus

$$P_c = \frac{1}{\sqrt{\pi} 2^{M-1}} \int_{-\infty}^{\infty} \left[1 + \text{erf} \left(x + \frac{A}{\sqrt{2}\sigma} \right) \right]^{M-1} e^{-x^2} dx \tag{IV.42}$$

where $x = \frac{Z_a - \mu_a}{\sqrt{2}\sigma}$

The average probability can be found by averaging the conditional probability of correct decision over the $f(\varphi)$, where $\varphi = \sum_{i=1}^{L_c} \tilde{\alpha}_i^2$ is the received energy collected by the L_c fingers of the RAKE receiver and is described as the sum of lognormal random variables (RVs) and follows the pdf $f(\varphi)$ as indicated in [51] for the IEEE 802.15.3a UWB channel.

$$\bar{P}_c = \int_0^{\infty} P_c(\varphi) \cdot f(\varphi) d\varphi \quad (\text{IV.43})$$

To evaluate the performance of M-ary PPM UWB system in UWB multipath channel, we use the probability of bit error given by [50]

$$P_b = \frac{M \cdot P_s}{2(M-1)} = \frac{M(1-\bar{P}_c)}{2(M-1)} \quad (\text{IV.44})$$

Where $P_s = 1 - \bar{P}_c$ is the probability of symbol error, which is computed using the relationship [50]

Taking the case of a slow adaptive modulation towards the channel changes, the minimum SNR threshold x_g^* required for the g^{th} modulation level to guarantee the required probability of bit error P_b^* i.e., $P_b(x_g^*) = P_b^*$. Thus the outage probability P_{out} , which is the probability that the probability of bit error P_b is greater than an allowable probability of bit error P_o^* [52] and it is given by

$$P_{out}(P_o^*) = \mathbb{P}\{P_b(x) > P_o^*\} = F_x(x_g^*) \quad (\text{IV.45})$$

$F_x(\cdot)$ is the cumulative density function (CDF) of the mean SNR parameter x and is expressed as

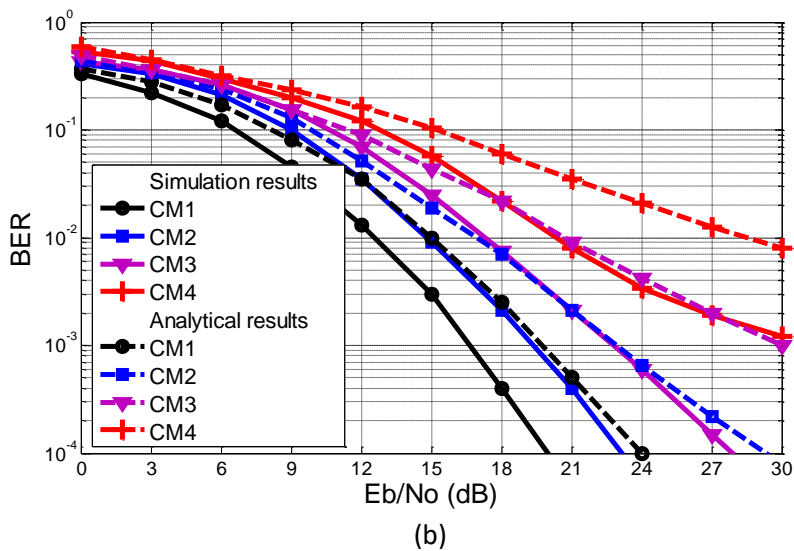
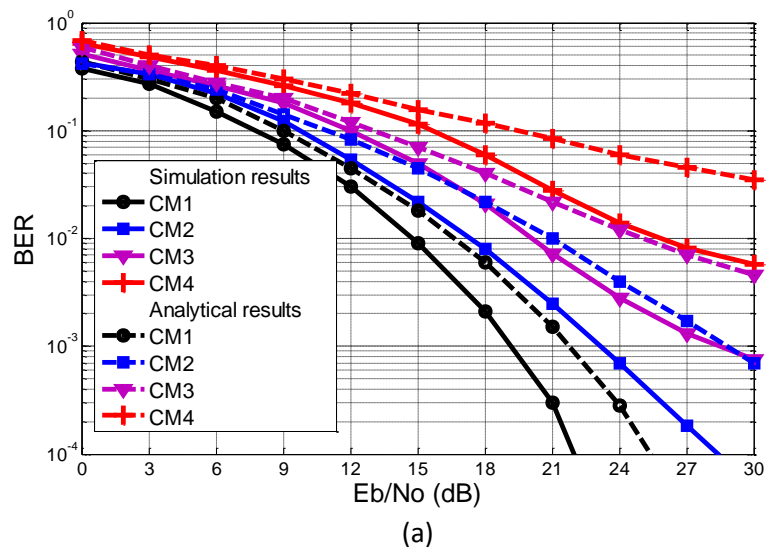
$$F_x(x_g^*) = Q\left(\frac{Z_a - \mu_a}{\sqrt{2}\sigma}\right) \quad (\text{IV.46})$$

Where $Q(\cdot)$ is the Gaussian-Q function.

IV.6 Simulation results

In this part, simulations are performed to show the performance of the flexible transmission technique. All results have been done using Matlab simulations for one user. The sampling frequency is chosen $f_c=30\text{GHz}$; the binary symbol rate $R_s=300\text{Mps}$; the number of frames per symbol and the duration of one frame are respectively $N_f=1$,

$T_f=3.33ns$; where each impulse occupies one frame; the number of chips in one frame and the duration of one chip are respectively $N_c=2$, $T_c=1.66ns$; the time hopping code $c_j = \{1\}$; the modulation factor $\delta=0.1ns$, and the impulse duration $2t_p=0.2ns$, which implies that the spreading ratio $\rho=33.3$ and the maximum modulation level $G=3$, i.e. $M_{max}=16$; the estimation sequence length is 100 and finally the notion of the S-Rake type regarding the manner of capturing the paths is also taken here. A maximum-likelihood criterion with Data Aided context is used to find out the channel estimation. Each UWB channel model is generated by averaging 100 impulse response realizations to reach maximum transparency.



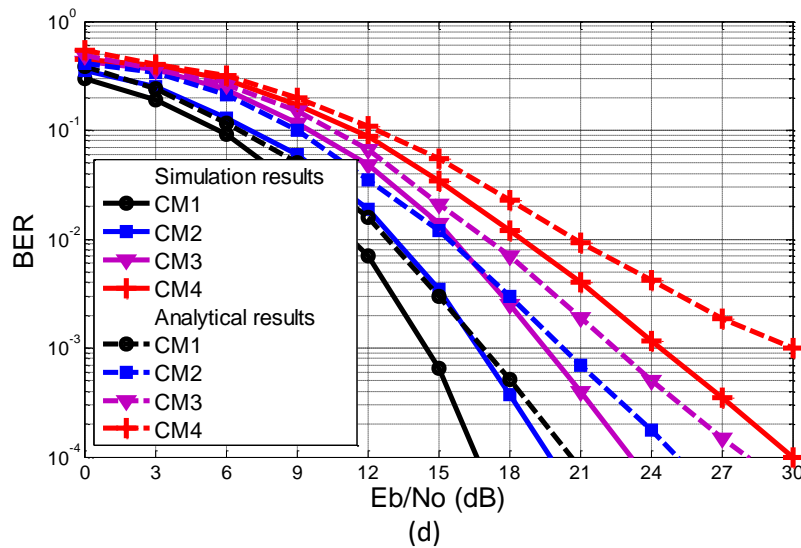
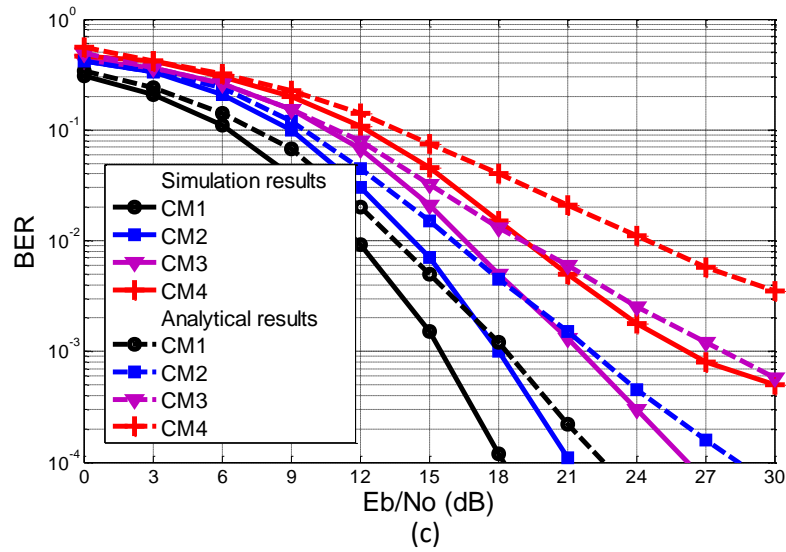


Fig.IV.4 BER evaluation versus E_b/N_0 for the proposed UWB system
 a) 16-ary PPM. b) 8-ary PPM. c) 4-ary PPM. d) 2-ary PPM

The Figure IV.4 (a), (b), (c), (d), presents the performance evaluation of the BER versus E_b/N_0 for channel models (CM1, CM2, CM3, CM4), where the different modulations 2, 4, 8 and 16-ary PPM have been assessed. It is clearly shown that the agreement between simulation and analytical results is excellent where the BER is going higher as we go for higher-level modulation. Furthermore, it is remarked that when the order of the channel model increases, all the curves tend to be diverged and the BER performance performs badly. The analytical results gave less performance than the simulated results by the reason that many suppositions have been taken to reduce the complexity of calculus.

The main objective of these simulations is not only to compare the simulation with the analytical results but also to discuss in what time the ICS should be reacted toward the

multipath phenomena. Hence, as it is discussed in the philosophy of the suggested strategy, it is better for the ICS to switch to the modulation level by looking at the classified model chosen by the CM classifier. First, by taking the required minimum probability of bit error for all modulation levels $P_b^{*} = 10^{-4}$, we can judge that when the estimated channel is classified as CM1; it would be better for the ICS to switch to 16-ary PPM through the Automatic Switcher, this situation corresponds to the Fig. IV.4 (a). Hence we can take $x_3^{*} = 22\text{dB}$ as a SNR threshold for the level $g=3$, if the mean SNR x drops below x_3^{*} , then $g=2$ would be adopted automatically. Secondly, when the estimated channel is classified as CM2; it would be better for the ICS to switch to 8-ary PPM, this situation corresponds to the Fig. IV.4 (b), thereby we can take $x_2^{*} = 23\text{dB}$ as a SNR threshold for the level $g=2$, if the mean SNR x drops below x_2^{*} , then $g=1$ would be adopted automatically. Thirdly, when the estimated channel is classified as CM3; it would be better for the ICS to switch to 4-ary PPM, this situation corresponds to the Fig. IV.4 (c), therefore we can take $x_1^{*} = 26\text{dB}$ as a SNR threshold for the level $g=1$, if the mean SNR x drops below x_1^{*} , then $g=0$ would be adopted automatically. Finally, when the estimated channel is classified as CM4; this latter is characterized by a huge number of paths, it would be better for the ICS to switch to 2-ary PPM or stop the transmission completely until changing other conditions, this situation corresponds to the Fig. IV.4 (d), where we can take $x_0^{*} = 30\text{dB}$ as a minimum threshold SNR allocated for the lowest modulation level $g=0$, if the mean SNR x drops below x_0^{*} , in this case the ICS declares an outage.

IV.7 Summary

This chapter offered a new solution detailed for the first time. The suggested strategy leads the UWB transmission system to have a rapid acquisition of signals using a modified rake receiver named multi-hands rake receiver based on an intelligent controlling system. Furthermore, another benefit that can be drawn from this strategy is to exploit the circumstances when the channel is less complex to switch the transmission to higher data rate through higher M-ary PPM modulation, as can be shown from the results described previously (e.g. M=2,4,8,16):

For CM4 → 2-ary PPM (Symbol of 1bit) → 300Mbps

For CM3 → 4-ary PPM (Symbol of 2bit) → 600Mbps

For CM2 → 8-ary PPM (Symbol of 3bit) → 900Mbps

For CM1 → 16-ary PPM (Symbol of 4bit) → 1.2Gbps

Consequently, when our strategy offers a data rate of the order of Gbps in a flexible transmission, it would be qualified to meet the 5G network requirements and it can be developed to be used in the future technology of Internet of Things (IoT) as it is presented in [53].

Moreover, through a generalized manner, it is interesting to note that the flexible technique could deal with the multiple access case and support different modulation levels from different users while ensuring the time hopping code for each one. Therefore, this matter is considered as a trump for our strategy that gives a strong capacity for the Medium Access Control (MAC) layer to deal separately with different users in a multiple access.

This thesis gave a brief overview of how to take the multipath problem from a new viewpoint; even if the modified rake receiver seems that has some complexities, but it is still a necessity need to deal with the multipath challenge and to transport the wireless personal communication system to the high data rate.

Finally, it is worth to point out that the results of this chapter have led to a work, which is still under submission for an International Publications (please see IP 1), to have a look please see Appendix C.

Conclusions and future works

Conclusions and future works

This thesis falls within the scope of UWB radio communication domain, where the main objective was to seek a solution to deal with the multipath phenomenon to have a rapid acquisition. As we have seen, this challenge was hard to reach by the fact that the duration of the impulse in a UWB signal is of the order of a few nanoseconds, which implies the sensitivity to the various obstacles which have dimensions of the range of millimeters. Therefore, an error of the order of a nanosecond in the time domain may cause an inaccurate channel estimation, the design of the UWB system is very complicated and requires high precision, especially during the channel estimation and equalizing of signals.

To overcome the cited challenge, we have exploited the temporal diversity through the rake receiver, to collect all the energy of the signal transmitted. So instead to consider that the multipath problem as a negative factor on communication, it may become a major benefit for us to increase the signal-to-noise ratio. However, the rake receiver requires a good knowledge about the transmission channel through an estimation step in order to get the attenuations and delays spread of multipath. The channel type assumed in this work follows the standard IEEE 802.15.3a, which is intended for high data rate and short-distance communication.

Under the light of what is above, the transmission channel estimation has become an interesting step to acquire the parameters (amplitudes and delays estimates). In this regard, the entire UWB communications system from the transmitter to the receiver has been assumed and done basing on the technique of the Time-Hopping UWB communications systems, knowing that the multiple access is applied by assigning different codes to different users. Furthermore, the maximum likelihood method was used in two contexts DA and NDA where some evaluations regarding the estimation of four models have been done in terms of the MSE and the BER and all the simulations were assessed using PPM modulation for the desired user.

As we have seen, the results obtained show that the DA context gave better performance than the NDA context because the rake receiver has a pre-information about the estimation sequence.

To show the performances of the system depending on different parameters that might affect the channel estimation and the UWB communication, we have simulated all the UWB transmission link using the conventional rake receiver. Moreover, we have assessed many results to improve the system performances. The results convey to these points:

- The more the order of the model increases, the more the estimation is worse.
- The data rate and the multiple access have a significant influence on the BER and the MSE.
- The length of the estimation sequence can affect the channel estimation, where from 100 bits there will not be much improvement.
- The modulation factor δ has not much influence on the BER except for CM1 where it seems to be affected a little bit.
- From 40 paths, the BER remains without any considered improvement.
- The A-Rake receiver is better than S-Rake and P-Rake, but it remains practically unrealizable, so the S-Rake type remains the most commonly used choice.

After having shown the system performances based on the conventional system. The fourth chapter has offered a new strategy to the Ultra-Wide Band systems that was detailed within the context of this thesis for the first once. The idea aimed to set up a new solution to face the first challenge in UWB communications which is the multipath channel through a flexible transmission. The suggested strategy based on Intelligent Controlling System (ICS) that ensures an automatic switching between the levels of M-ary PPM when the channel changes during the transmission. In view of that, at the transmitter, a frozen scheme was set up that imposes fixed chip duration for all the modulation orders to make the users able to transmit data by different modulations during the transmission. In the other hand, at the receiver, a modified rake receiver named multi-hands rake receiver was proposed to achieve our strategy. Furthermore, a new analytical development is done and assessed conjointly with simulation results to show how our new strategy via ICS should deal to confront the multipath phenomena. The system performance is addressed for M-ary PPM in terms of BER, where the effects of Inter-Symbol/Frame Interference (ISFI) are taken into account.

The results have been verified using computer simulations to discuss the efficacy of this strategy that provides evidence that it is a suitable solution for the multipath phenomena.

CONCLUSIONS AND FUTURE WORKS

The results prove that we can use M-ary PPM positively using the ICS to mitigate the multipath effects and to benefit from the channel state to have a rapid acquisition of signals when is possible.

In fact, this work as it is detailed is very ramified and forked. Therefore, we tried during the study details to confine it to the necessary things, where this research work may open several research topics to investigate many future points. Thus, for the future works relevant to this work, it would be interesting to envisage:

- ✓ Experimental validation of simulation results
- ✓ Adopting more enhancements to the IEEE channel models to be more realistic by assuming the Doppler effect and the angular dispersion
- ✓ Developing of a channel model classifier for the ICS
- ✓ Developing of a synchronization protocol for the ICS

Appendices

Appendices

Appendix A: UWB Technology

A.1 Comparative table of short-range wireless technologies.....98

A.2 Some Applications for UWB and Marketed Products99

Appendix B: IEEE 802.15.3a Channel Standard

B.1 Multipath channel characteristics and modeling parameters.....102

B.2 Illustration of multipath channel characteristics103

Appendix C: Relevant publications and international communications

Appendix A: UWB Technology

A.1 Comparative table of short-range wireless technologies

UWB technology provides opportunities to support short-range, low-power wireless networks such as WPAN. Other wireless access technologies, such as WiFi and Bluetooth, could be used for similar purposes.

Table 1 shows a comparison between UWB technology and other wireless technologies.

Tab. 1 Some Comparisons							
Technologies	R_d	Range (m)	Frequency bands	Power (EIRP)	Modulation	Application	Specification
UWB	>100 Mbit/s	~ 15	3,1–10,6 GHz	$\leq -$ 41,3 dBm/MHz	PPM, etc.	WPAN	IEEE 802.15.3a PAN high data rates
UWB	>500 kbit/s	~ 10	3,1–10,6 GHz	$\leq -$ 41,3 dBm/MHz	PPM, etc.	WPAN	IEEE 802.15.4
Bluetooth	700 kbit/s	~ 15	ISM 2.4 GHz	Class 1 : 20 dBm Class 2 : 0 dBm	GMSK	WPAN	IEEE 802.15.1
WiFi	until 54 Mbit/s	~ 50	5 GHz	Max. 200 mW until 1 W	BPSK, 16-QAM QPSK, 64-QAM	RLAN	IEEE 802.11a
	until 11 Mbit/s	~100	ISM 2.4 GHz	Max. 100 mW until 2 W	CCK	RLAN	IEEE 802.11b
	until 54 Mbit/s	~100	ISM 2.4 GHz	Max. 100 mW until 2 W	BPSK, 16-QAM QPSK, 64-QAM	RLAN	IEEE 802.11g

A.2 Some Applications for UWB and Marketed Products

There are many possible UWB applications. It is unthinkable to draw up an exhaustive list. However, they can be classified roughly into two categories: radar applications and communications applications.

Radar devices that use the UWB can be used to measure distances or positions with greater resolution than existing radar devices or to obtain images of objects buried underground and placed behind surfaces.

In communications, the UWB can enable secure wireless communications for voice and data and allow an important broadband for short distances systems. It could soon be used for broadband Internet, telephony, computer networks.

Some UWB applications are already available on the market. Among them are:

A.2.1 PulsON 200

This is a UWB chipset marketed under the PulsON brand. The first generation is the PulsON 100, followed by the PulsON 200. Time domain was the first company to pass the FCC certification process of a communication product.

The PulsON 200 Kit has a channel capacity of 9.6 Mbps over a 10m range in an unobstructed environment and 7m in an office or residential environment. The parameters of this product are summarized in Table 2 whose appearance is as follows:



Fig. 1 PulseON 200 KIT UWB radios.

Future generations of PulsON are being developed, especially for the ultra wide band devices with low power consumption, intended for wireless multimedia applications.

Tab. 2 Spécifications du PulseON 200 Kit de Time domaine

Paramètres	Valeur
Impulse frequency	9.6 MHz
Channel Capacity	9.6, 4.8, 2.4, 1.2, 0.6, 0.15, 0.075
Central frequency	4.7 GHz
Bandwidth	3.2 GHz
Equivalent isotropically radiated power (EIRP)	-11.5 dBm
Consumed power	12.2 W

A.2.2 UWB Wireless Port Replicator



Fig. 2 Wireless port replicator

Toshiba presents an interesting novelty for mobile workers: a wireless welcoming station. It uses UWB technology to transmit the data, and able to transmit the video signal. Currently, only the R400 is able to use this new welcoming station.

A.2.3 LENOVO Laptop

Other manufacturers are also preparing for the UWB revolution, like Lenovo. The manufacturer has introduced its new laptop named "Thinkpad T61p". It will be the first in the world by integrating the UWB technology.



Fig. 3 LENOVO Laptop

While deliveries of UWB chipsets began at the end of last year, growth forecasts for this technology are particularly optimistic. The firm In-Stat has delivered a total of 289 million UWB chipsets delivered in 2010, including about 125 million PCs with integrated UWB module. In a second step, mobile phones should also adopt this technology.

Appendix B: IEEE 802.15.3a Channel Standard

B1. Multipath channel characteristics and modeling parameters

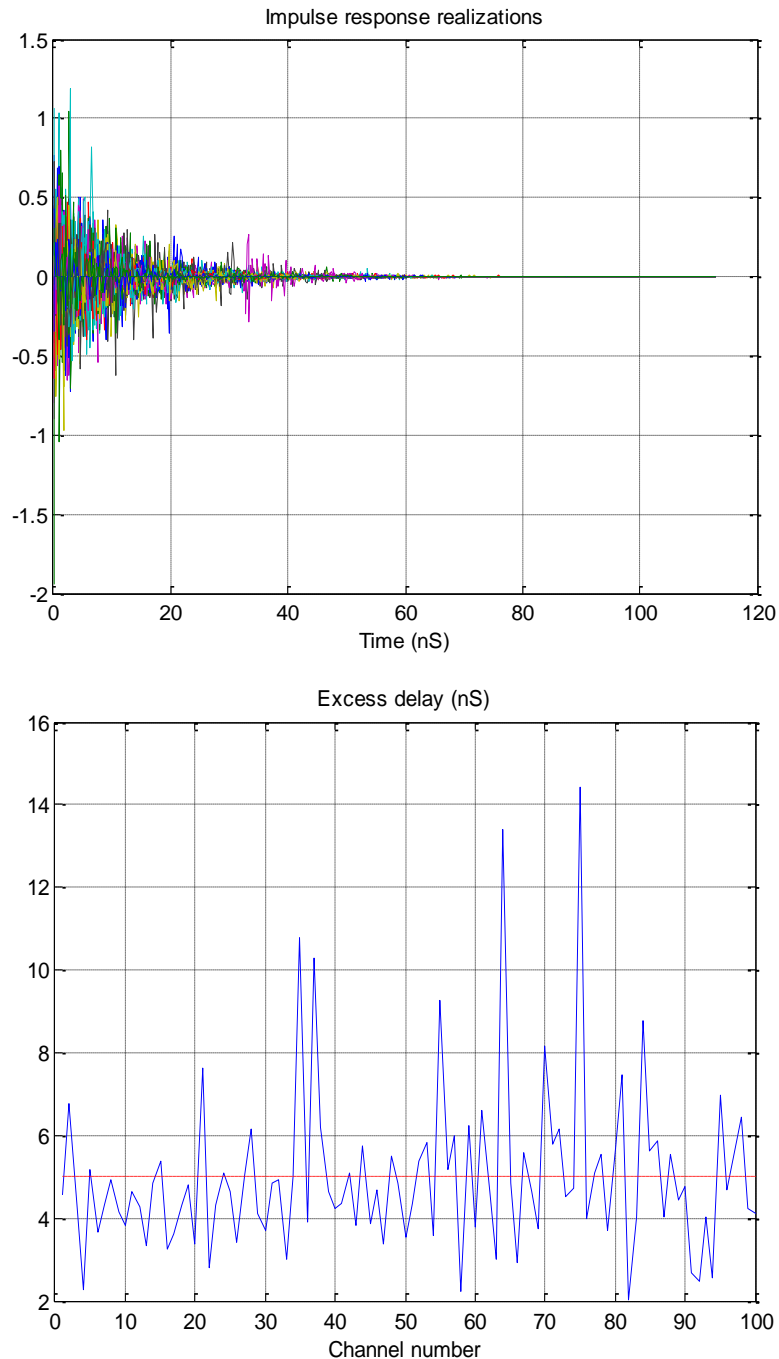
The following table presents the characteristics taken into account by the model 3a, as well as the parameters of the various models and the characteristics of the simulated models which make it possible to compare the measured channels with the modeled channels.

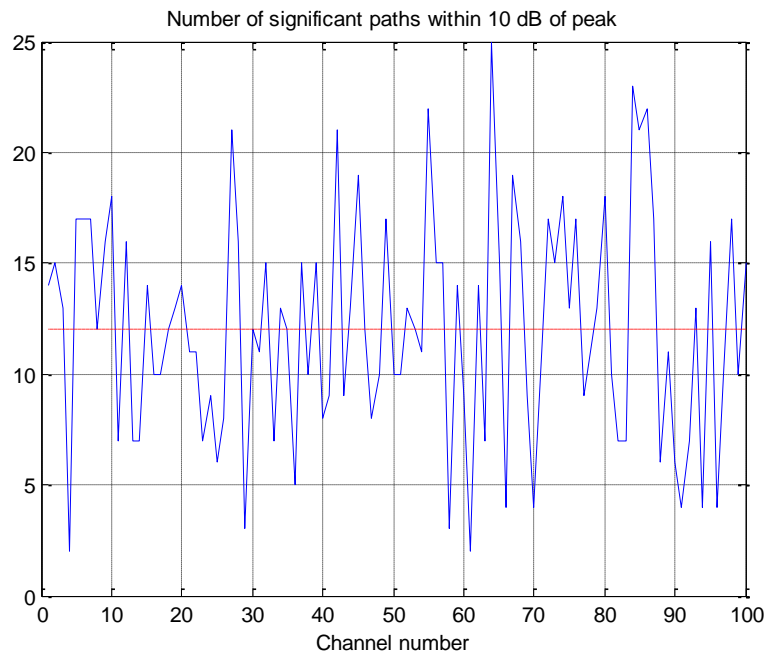
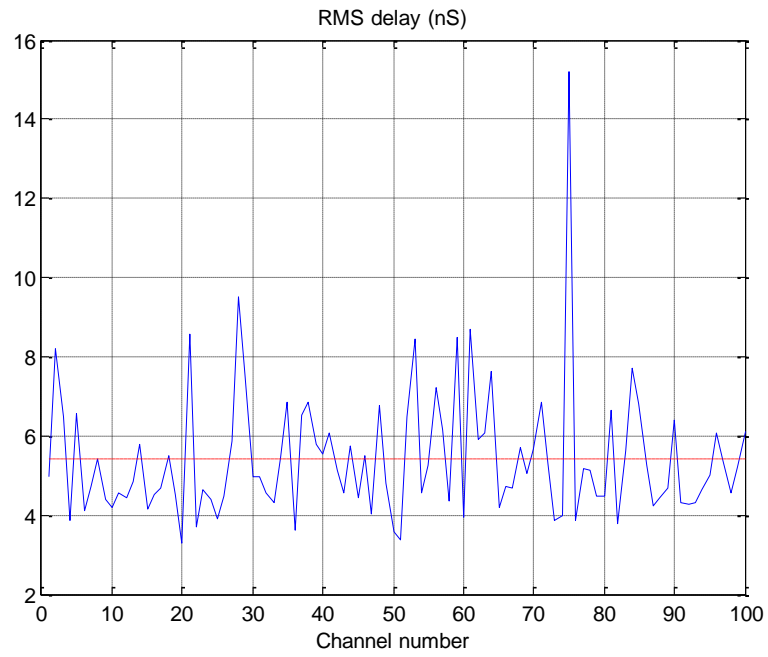
Tab. 3 UWB Multipath channel characteristics and parameters

Targeted channel characteristics ^(e)	CM 1 ^(a)	CM2 ^(b)	CM3 ^(c)	CM4 ^(d)
τ_m [ns] (mean delay)	5,05	10,38	14,18	
τ_{rms} [ns] (Standard deviation of delay)	5,28	8,03	14,28	25
<i>NP10dB</i> (Number of multipath having undergone 10 dB of attenuation compared to the strongest path)	12	15	25	42
<i>NP (85%)</i> (Number of multipath representing 85% of the channel energy)	24	36,1	61,54	
Model's Parameters				
Λ [1/nsec] (arrival rate of a packet)	0,0233	0,4	0,0667	0,0667
λ [1/nsec] (arrival rate of a path)	2,5	0,5	2,1	2,1
Γ (decay factor of a packet)	7,1	5,5	2,1	2,1
γ (decay factor of a path)	4,3	6,7	7,9	12
σ_1 [dB] (standard deviation of a packet)	3,4	3,4	3,4	3,4
σ_2 [dB] (standard deviation of a path)	3,4	3,4	3,4	3,4
σ_x [dB] (standard deviation of the global "shadowing")	3	3	3	3
Caractéristiques du modèle				
τ_m [ns]	5,0	9,9	15,9	30,1
τ_{rms} [ns]	5	8	15	25
<i>NP10dB</i>	12,5	15,3	24,9	41,2
<i>NP(85%)</i>	20,8	33,9	64,7	123,3
Average channel energy (dB)	-0,4	-0,5	0,0	0,3
Standard deviation of. the channel energy (dB)	2,9	3,1	3,1	2,7

B2. Illustration of multipath channel characteristics

The following figures are taken from the simulation program of the IEEE 802.15.3a channel. They illustrate the characteristics of the model CM1 (LOS for a distance of 0 to 4 m) and obtained by averaging the results over 100 realizations.





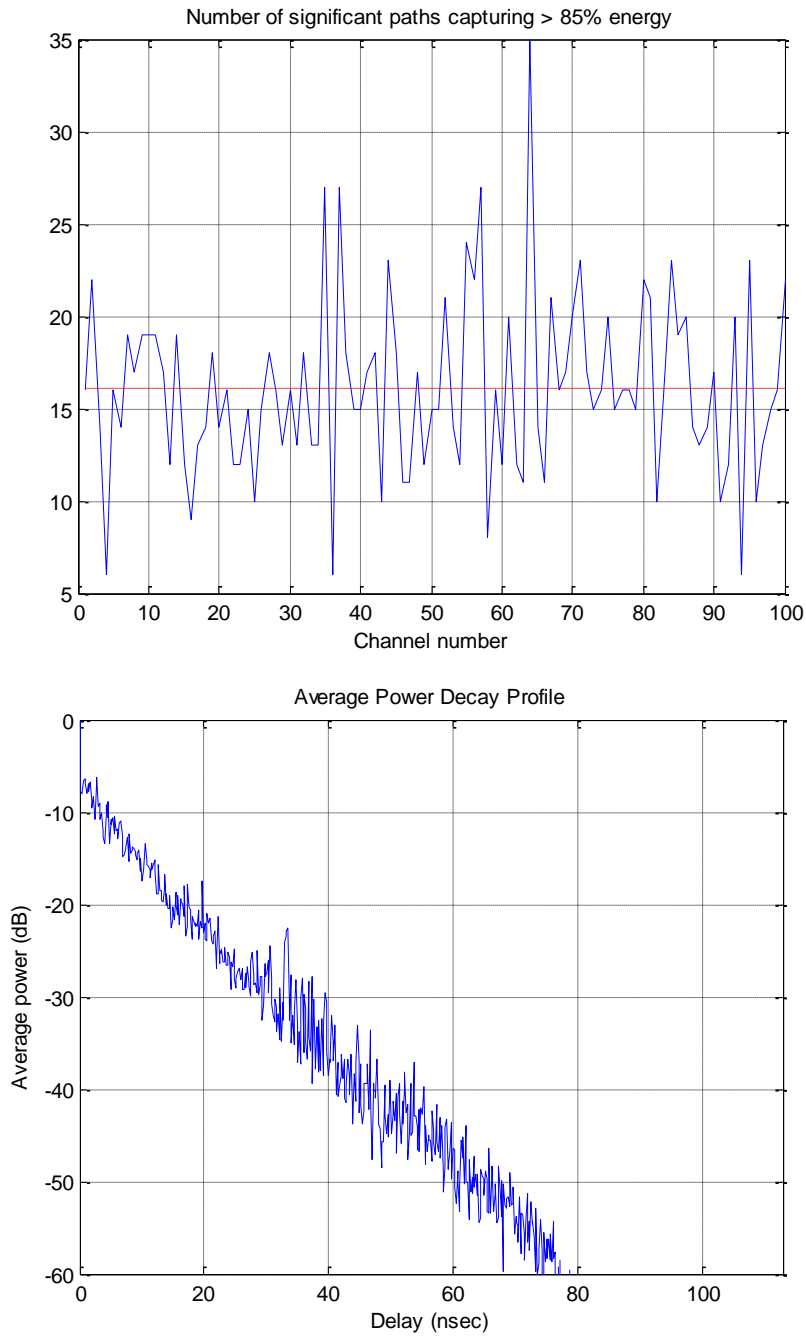


Fig. 4 the UWB multipath channel characteristics

Appendix C: Relevant International Publications and International Communications

International Publications:

1. S. Ghendir, S. Sbaa, R. Ajgou, A. Chemsas, A. Taleb-Ahmed, "Performance Evaluation of Time Hopping UWB Transmission using S-Rake Receiver", *WSEAS Transactions on communication*, vol.14, pp. 74-81, 2015
2. GHENDIR, S., SBAA, S., AL-SHERBAZ, A., AJGOU, R., et CHEMSA, A. " Performance Assessment of UWB Multipath Channel using Rake Receiver Types" *Courrier du Savoir*, V 24, oct 2017
3. S. Ghendir, S., SBAA, et al. "Towards 5G: Design and Performance Analysis of UWB System using Multi-hands Rake Receiver over Indoor Multipath Channels." in *IEEE Transactions on Communications* (Under Submission).

International Communications:

1. Said. Ghendir, Salim. Sbaa, Riadh. Ajgou, Abdelmalik. Taleb-Ahmed and Ali. Chemsas, " High Bit Rate UWB Communication in Dense Multipath Channels. In Proc. 18th International Conference on Communications (part of CSCC'14), Santorini Island, Greece, pp. 74-79, 2014
2. Said GHENDIR, Salim SBAA, Riadh AJGOU, Ali CHEMSA and A. TALEB-AHMED, "Novel M-ary PPM Time Hopping Scheme for UWB Communications", *Proceedings of the International Conference on Circuits, Systems, Signal Processing, Communications and Computers (CSSCC 2015)*, Vienna, Austria, pp. 156-160, 2015
3. S. Ghendir, S. Sbaa, R. Ajgou, A. Chemsas, A. Taleb-Ahmed , "Caractérisation des Communications Ultra-large Bande en Utilisant les Récepteurs RAKE, " *International Conference on Embedded Systems in Telecommunications and Instrumentation*, Annaba, Algeria, Novembre 05-07, 2012
4. Said GHENDIR, " Rake receiver type effects on the received UWB signals", In the fifth International Conference SETIT 2009, Hammamet, Tunisia, March 22- 26, 2009

5. Said. Ghendir, Messaoud. Bensebti, " Comparative study of channel evaluation for UWB system performance enhancement", International Conference on Systems and Information Processing ICSIP'09 May 2-4, Guelma, 2009
6. S. Ghendir, S. Sbaa, R. Ajgou, A. Chemsas, A. Taleb-Ahmed , "Radio Channel Estimation for UWB Communications Using Maximum-Likelihood Criterion, " Image and Signal processing their Applications, ISPA'2012, Mostaganem, Algeria, Décembre 2-3 & 4,2012
7. S. Ghendir, R. Ajgou, S. Sbaa and A. Al-Sherbaz, "Evaluation of multi-user effects on the channel in the TH-UWB communication systems," *2017 5th International Conference on Electrical Engineering - Boumerdes (ICEE-B)*, Boumerdes, Algeria, 2017, pp. 1-6. doi: 10.1109/ICEE-B.2017.8192105

National Communication:

1. S. Ghendir, S. Sbaa, R. Ajgou, A. Chemsas, A. Taleb-Ahmed, "Radio Channel Estimation for UWB Communications, " Première Conférence Nationale sur les Télécommunications, CNT'2012, Guelma, Algérie, Octobre 11&12, 2012

Bibliography

Bibliography

- [1] J. R. Pierce and A. L. Hopper, "Non synchronous Time Division with Holding and wit Random Sampling," *Proc. of the IRE*, vol. 40, pp. 1079-1088, Sept. 1952.
- [2] G. F. Ross, "Transmission and Reception System for Generating and Receiving Baseband Duration Pulse Signals for Short Base-band Pulse Communication System," U.S. Patent 3,728,025 dated July 31, 1973.
- [3] M. K. Simon, B. K. Levitt, R. A. Scholtz and J. K. Omura, "Spread Spectrum Communcations Handbook," Mac Graw Hill, 1994.
- [4] M. Win, F. Ramirez-Mireles, R. A. Scholtz and M. A. Barnes, "Ultra-Wide Bandwidth (UWB) Signal Propagation for Outdoor Wireless Communications," *Proc. of the 47th Vehicular Technology. Conference VTC 1997*, Phoenix, AZ, USA, pp. 251-255, May 1997.
- [5] P. II. Withington and L. Fullerton, "An Impulse Radio Communications System," in Proc.of the International.Conference.on Ultra-Wide Band, Short Pulse Electromagnetics,Brooklyn NY, USA, pp113-120, Oct. 1992.
- [6] R. A. Scholtz, "Multiple Access with Time-Hopping Impulse Radio," *Proc. of the IE Milcom Conference*, Boston, MA, USA, pp 447-450, Oct. 1993.
- [7] M. Z.Win, R.A. Scholtz and L. W. Fullerton,"Time-Hopping SSMA Techniques for Pulse Radio with an Analog Modulated Data Subcarrier," *proc. IEEE Vehicular Technoogy Conference VTC1997*, May 1997.
- [8] Docket No. 98-153, "Revision of Part 15 of the Comission's Rules Regarding Ultra Wideband Transmission Systems, Federal Communications Commission," Adopted Febrary 14, 2002, Released April 22, 2002.
- [9] C. J. Martret and G. B. Giannakis, "All-digital Impulse Radio For Wireless Cellular System," *IEEE Trans. On Communications*, vol. 50, p.1440–1450, sept. 2002.
- [10] S.Lasaulce, J.Dumont and S.Hassanaly, "Signaux à Bande Ultra Large: Caractéristiques et Performances,".
- [11] MBOA-SIG White Paper, September 1, 2004.
- [12] I. Oppermann, H.Matti and I. Jari, "UWB Theory and Applications," John Wiley & Sons, Inc. 250 p, 2004.
- [13] A. Deleuze, "Contributions à l'Étude des Systèmes Ultra Large Bande par Impulsions," PhD Thesis, the superior national school of Telecommunications Paris, 2006.
- [14] Y. Duroc, "Contribution Au Développement De Modèles Orients Système Pour Les Antennes des Communication Ultra Large Bande," PhD thesis, National Polytechnic Institute of Grenoble, 2007 .

- [15] M. Ghavami, B. Michael and R. Kohno, "Ultra Wideband Signals and Systems in Communication Engineering," Second Edition, John Wiley & Sons Ltd, 2007.
- [16] J. Zhang, "Short-Range High-Speed Ultra wideband Communications," A Thesis of Doctorate, the Australian National University, 2004.
- [17] M. Win and R.A. Scholtz, "Impulse Radio," Invited Paper, In Proc. IEEE International Symposium on Personal, Indoor and Mobile Radio Communications, Helsinki, Finland, 1997, pp. 245-257.
- [18] A.F Molisch, J. Foerster, "Channel Models for Ultrawideband Personal Area Networks," IEEE Wireless Communications, Vol. 10, No. 6, pp. 14-21, December 2003.
- [19] A.F Molisch, "UWB Wireless Channels – Propagation Aspects and Interplay with System Design," in Proc. 34th European Microwave Conference, Amsterdam, Nederland, October 2004, Vol. 2, pp. 1101-1104.
- [20] A.F. Molisch, "Ultrawideband Propagation Channels – Theory, Measurement and Modeling," Invited Paper, IEEE Transactions on Vehicular Technology Special Issue on UWB, Vol. 54, No. 5, pp. 1528-1545, September 2005.
- [21] A. Saleh and R. Valenzuela, "A Statistical Model for Indoor Multipath Propagation," *IEEE J. Select. Areas Commun*, vol. SAC-5, no. 2, pp. 128–137, Feb. 1987.
- [22] B.H. Fleury, M. Tschudin, R. Heddergott, D. Dalhaus and I.K. Pedersen, "Channel Parameter Estimation in Mobile Radio Environments Using the SAGE Algorithm," IEEE Journal Selected Areas Communications, Vol. 17, No. 3, pp. 434-450, March 1999.
- [23] K. Haneda, J.I. Takada and K. Kobayashi, "Experimental Evaluation of a SAGE Algorithm for Ultra Wideband Channel Sounding in an Anechoic Chamber," in Proc. International Workshop on Ultra Wideband Systems Joint with Conference on Ultra Wideband Systems and Technologies, Kyoto, Japan, May 2004, pp. 66-70.
- [24] J.M. Cramer, R. Scholtz and W. Win, "Evaluation of an Ultra Wideband Propagation Channel," IEEE Transactions on Antenna and Propagation, Vol. 5, No. 5, pp. 561-570, May 2002
- [25] R. D. Wilson and R. A. Scholtz, "On the Dependence of UWB Impulse Radio Link Performance on Channels Statistics," in Proc. IEEE International Conference on Communications, Paris, France, June 2004, Vol. 6, pp. 3566-3570.
- [26] M.Z. Win and R.A. Scholtz, "Ultra-Wide Bandwidth Time-Hopping Spread-Spectrum Impulse Radio for Wireless Multiple-Access Communications," IEEE Trans. Commun, vol. 48, pp. 679–691, Apr. 2000.
- [27] M.Z. Win and R.A. Scholtz, "Impulse Radio: How it Works," *IEEE Commun. Lett.*, vol. 2, pp. 10–12, Jan. 1998.
- [28] V. Lottici, A. D'Andrea and U. Mengali, "Channel Estimation for Ultrawideband Communications," IEEE J. Select. Area. Commun, vol. 20, no. 9, pp. 1638-1645, Dec. 2002.

- [29] F. Ramirez-Mireles and R. A. Scholtz, "Multiple Access Performance Limits with Time-Hopping And Pulse-Position Modulation," International Conference on Acoustics, Speech, and Signal Processing (ICASSP), 1998, pp. 529-533.
- [30] M. Z. Win and R. A. Scholtz, "On the Energy Capture of Ultrawide Bandwidth Signals on Dense Multipath Environments," IEEE Communications Letters, vol. 2, no. 9, p 245-247, Sep. 1998.
- [31] I. Maravic and M. Vetterli, "Low-Complexity Subspace Methods for Channel Estimation and Synchronization in Ultra-Wide Band Systems," International Workshop on Ultra-Wide Band (IWUWB), May 2003.
- [32] C. J. L. Martret and G. B. Giannakis, "All digital PPM impulse radio for multiple-access through frequency-selective multipath," in Proceedings IEEE Sensor Array and Multichannel Sig. Proc., March 2000, pp. 22-26.
- [33] R. A. Scholtz, "Multiple access with time hopping impulse modulation," in Proc. MILCOM, Bedford, MA, Oct. 11-13, 1993
- [34] Wan Q, Wang Q, Zheng Z. "Design and analysis of a 3.1-10.6 GHz UWB low noise amplifier with forward body bias technique". AEU-International Journal of Electronics and Communications 2015;69(1):119-125.
- [35] Wu WC. "Multiuser detection of time-hopping PPM UWB system in the presence of multipath fading". AEU-International Journal of Electronics and Communications 2007;61(1):22-29.
- [36] Dong K, Yan S, Meng X, Wang D. "UWB channel estimation based on compressed sensing using dual-kernel dictionaries". In: Signal Processing, Communications and Computing, IEEE International Conference on. 2015. p. 1-5.
- [37] Cheng X, Wang M, Guan YL. "Ultrawideband Channel Estimation: A Bayesian Compressive Sensing Strategy Based on Statistical Sparsity. In Vehicular Technology", IEEE Transactions on 2015;64(5):1819-1832.
- [38] Ranjay H, Tyagi A. "Bit error rate performance of IR-UWB ED-PPM system using cooperative dual-hop AF strategy". In IET Communications 2016;10(1):34-43.
- [39] Lee JY, Yoo S. "Large error performance of UWB ranging in multipath and multiuser environments", IEEE Transactions on Microwave Theory and Techniques 2006;54(4):1887-1895.
- [40] Zhiwei L, Premkumar AB, Madhukumar AS, Chin F. "Diagonally Loaded Linear MMSE Equalization for UWB Multipath Channel Under Limited Training Sample Support". In: Vehicular Technology Conference (VTC), vol. 5. 2006. p. 2359-2363.

- [41] Strohmer T, Emami M, Hansen J, Papanicolaou G, Paulraj AJ. "Application of time-reversal with MMSE equalizer to UWB communications". In: Proceeding 2004 IEEE Global Telecommunications Conference, vol. 5. 2004. P. 3123-3127.
- [42] Monsef F, Cozza A, Abboud L. "Effectiveness of Time-Reversal technique for UWB wireless communications in standard indoor environments". In: ICECom, 2010 Conference Proceedings. 2010. p. 1-4.
- [43] Liu XF, Wang BZ, Xiao SQ, Deng JH. "Performance of impulse radio UWB communications based on time reversal technique". Progress In Electromagnetics Research 2008;79:401-413.
- [44] Zhang Q, Qin J. "Random Correlation-Based Receiver for Impulse Radio Communications in UWB Channels". Wireless Personal Communications 2014;79(1):21-30.
- [45] Abou-Rjeily C. "A Symbol-by-Symbol Cooperative Diversity Scheme for Relay-Assisted UWB Communications with PPM". IEEE Journal on Selected Areas in Communication 2013;31(8):1436-1445.
- [46] Sheng H, Haimovich AM. "Impact of channel estimation on ultra-wideband system design". IEEE Journal of Selected Topics in Signal Processing 2007;1(3):498-507.
- [47] Turin GL. "Introduction to Spread-Spectrum anti Multipath Techniques and Their Application to Urban Digital Radio". In: Proc. IEEE, vol. 68. 1980. p. 328-353.
- [48] Zhang T, Abhayapala TD, Kennedy RA. "Performance of ultra-wideband correlator receiver using Gaussian monocycles". In: Proceedings of the IEEE International Conference on Communications, vol. 3. 2003. p. 2192-2196.
- [49] Kunish J, Pamp J. "Measurement results and modelling aspects for the UWB radio channel". In: Proc. IEEE Conf. Ultra Wideband Syst. Technol., Baltimore, MD. 2002. p. 19-23.
- [50] Proakis JG. "Digital Communications". 3rd edition: McGraw-Hill; 1995.
- [51] Wang L, Liu W. "Bit error rate analysis in IEEE 802.15. 3a UWB channels". IEEE Transactions on Wireless Communications 2010;9(5):1537-1542.
- [52] A. Conti, M. Z. Win, M. Chiani and J. H. Winters, "Bit error outage for diversity reception in shadowing environment," in *IEEE Communications Letters*, vol. 7, no. 1, pp. 15-17, Jan. 2003.
- [53] KUMAR, Sanjay, GUPTA, Gagan, et SINGH, Kunwar Rajat. "5G: Revolution of future communication technology. In : Green Computing and Internet of Things (ICGCIoT)", 2015 International Conference on. IEEE, 2015. p. 143-147.